Kinetic assessment by *in vitro* approaches - A contribution to reduce animals in toxicity testing

Dissertation

zur Erlangung des naturwissenschaftlichen Doktorgrades

der Julius-Maximilians-Universität Würzburg

vorgelegt von

Patricia Bellwon

aus Würzburg

Würzburg 2015

Eingereicht am: .....

Mitglieder der Promotionskommission:

Vorsitzender: .....

Gutachter : .....

Gutachter: .....

Tag des Promotionskolloquiums: .....

Doktorurkunde ausgehändigt am: .....

Parts of this thesis have already been published or submitted for publication:

Published

Bellwon P., Culot M., Wilmes A., Schmidt T., Zurich M.G., Schultz L., Schmal O., Gramowski-Voss A., Weiss D.G., Jennings P., Bal-Price A., Testai E., Dekant W. (2015).
Cyclosporine A kinetics in brain cell culture and its potential of crossing the blood-brain barrier. Toxicology in Vitro. doi: 10.1016/j.tiv.2015.01.003

Crean D., Bellwon P., Aschauer L., Limonciel A., Moenks K., Hewitt P., Schmidt T., Herrgen K., Dekant W., Lukas A., Bois F., Wilmes A., Jennings P., Leonard M. (2014).
Development of an in vitro renal epithelial disease state model for xenobiotic toxicity testing. Toxicology in Vitro. doi: 10.1016/j.tiv.2014.11.015

Wilmes A., Bielow C., Ranninger C., Bellwon P., Aschauer L., Limonciel A., Chassaigne H., Kristl T., Aiche S., Huber C.G., Guillou C., Hewitt P., Leonard M., Dekant W., Bois F., Jennings P. (2014)
Mechanism of cisplatinum proximal tubule toxicity revealed by integrating transcriptomics, proteomics, metabolomics and biokinetics. Toxicology in Vitro. doi: 10.1016/j.tiv.2014.10.006

Submitted

Bellwon P., Truisi G., Bois F., Wilmes A., Schmidt T., Savary C., Parmentier C., Hewitt P., Schmal O., Josse R., Richert L., Mueller S.O., Jennings P., Testai E., Dekant W.
Kinetics and dynamics of Cyclosporine A in three hepatic cell culture systems.

Poster-presentation

Bellwon, P., Schmidt T., Truisi G.L., Savary C., Parmentier C., Mueller S.O., Dekant W. (2014). Cyclosporine A biokinetics in hepatic *in vitro* systems. Poster presentation at SOT 53rd Annual Meeting, Phoenix, Arizona, March 23-27. 2014

Table of contents

Summary

The adoption of directives and regulations by the EU requires the development of alternative testing strategies as opposed to animal testing for risk assessment of xenobiotics. Additionally, high attrition rates of drugs late in the discovery phase demand improvement of current test batteries applied in the preclinical phase within the pharmaceutical area. These issues were taken up by the EU founded 7th Framework Program "Predict-IV"; with the overall goal to improve the predictability of safety of an investigational product, after repeated exposure, by integration of "omics" technologies applied on well-established *in vitro* approaches. Three major target organs for drug-induced toxicity were in focus: liver, kidney and central nervous system. To relate obtained dynamic data with the *in vivo* situation, kinetics of the test compounds have to be evaluated and extrapolated by physiologically-based pharmacokinetic modeling.

This thesis assessed *in vitro* kinetics of the selected test compounds (cyclosporine A, adefovir dipivoxil and cisplatinum) regarding their reliability and relevance to respective *in vivo* pharmacokinetics. Cells were exposed daily or every other day to the test compounds at two concentration levels (toxic and non-toxic) for up to 14 days. Concentrations of the test compounds or their major biotransformation products were determined by LC-MS/MS or ICP-MS in vehicle, media, cells and plastic adsorption samples generated at five different time-points on the first and the last treatment day.

Cyclosporine A bioaccumulation was evident in primary rat hepatocytes (PRH) at the high concentration, while efficient biotransformation mediated by CYP3A4 and CYP3A5 was determined in primary human hepatocytes (PHH) and HepaRG cells. The lower biotransformation in PRH is in accordance with observation made *in vivo* with the rat being a poor model for CYP3A biotransformation. Further, inter-assay variability was noticed in PHH caused by biological variability in CYP3A4 and CYP3A5 activity in human donors. The inter-assay variability observed for PRH and HepaRG cells was a result of differences between vehicles regarding their cyclosporine A content. Cyclosporine A biotransformation was more prominent in HepaRG cells due to stable and high CYP3A4 and CYP3A5 activity. In addition, *in vitro* clearances were calculated and scaled to *in vivo*. All scaled *in vitro* clearances were overestimated (PRH: 10-fold, PHH: 2-fold, HepaRG cells: 2-fold). These results should be proven by physiologically-based pharmacokinetic modeling and additional experiments, in order to verify that these

overestimations are constant for each system and subsequently can be diminished by implementation of further scaling factors.

Brain cell cultures, primary neuronal culture of mouse cortex cells and primary aggregating rat brain cells, revealed fast achieved steady state levels of cyclosporine A. This indicates a chemical distribution of cyclosporine A between the aqueous and organic phases and only minor involvement of biological processes such as active transport and biotransformation. Hence, cyclosporine A uptake into cells is presumably transport-mediated, supported by findings of transporter experiments performed on a parallel artificial membrane and Caco-2 cells. Plastic adsorption of cyclosporine A was significant, but different for each model, and should be considered by physiologically-based pharmacokinetic modeling.

Kinetics of adefovir dipivoxil highlights the limits of *in vitro* approaches. Active transporters are required for adefovir uptake, but were not functional in RPTECT/TERT1. Therefore, adefovir uptake was limited to passive diffusion of adefovir dipivoxil, which itself degrades time-dependently under culture conditions.

Cisplatinum kinetics, studied in RPTEC/TERT1 cells, indicated intracellular enrichment of platinum, while significant bioaccumulation was not noted. This could be due to cisplatinum not reaching steady state levels within 14 days repeated exposure. As shown *in vivo*, active transport occurred from the basolateral to apical side, but with lower velocity. Hence, obtained data need to be modeled to estimate cellular processes, which can be scaled and compared to *in vivo*.

Repeated daily exposure to two different drug concentrations makes it possible to account for bioaccumulation at toxic concentrations or biotransformation/extrusion at non-toxic concentrations. Potential errors leading to misinterpretation of data were reduced by analyses of the vehicles as the applied drug concentrations do not necessarily correspond to the nominal concentrations. Finally, analyses of separate compartments (medium, cells, plastic) give insights into a compound's distribution, reduce misprediction of cellular processes, e.g. biotransformation, and help to interpret kinetic data. On the other hand, the limits of *in vitro* approaches have also been pointed out. For correct extrapolation to *in vivo*, it is essential that the studied *in vitro* system exhibits the functionality of proteins, which play a key role in the specific drug-induced toxicity. Considering the benefits and limitations, it is worth to validate this long-term

treatment experimental set-up and expand it on co-culture systems and on organs-on-chips with regard to alternative toxicity testing strategies for repeated dose toxicity studies.

Zusammenfassung

Die Erlassung von Richtlinien und Verordnungen durch die EU führte zu der Entwicklung von alternativen Testmethoden als Ersatz von Tierversuchen zur Risikobewertung von Xenobiotika. Des Weiteren weisen hohe Ausfallraten von Arzneimitteln in der späten Entwicklungsphase auf die Notwendigkeit hin, die bisher verwendeten Testmethoden der präklinischen Phase zu verbessern. Diese Punkte wurden in dem im siebten Rahmenprogramm der EU finanzierten Projekt „Predict-IV“ aufgegriffen. Ziel des Projektes war es, die Vorhersage der Arzneimittelsicherheit durch integrierte „omics“-Technologien, angewendet an etablierten *in vitro* Ansätzen, zu verbessern. Dabei standen drei Zielorgane bzgl. Arzneimittel-induzierter Organtoxizität im Mittelpunkt: Leber, Niere und zentrales Nervensystem, die jeweils durch Zelllinien oder primäre Zellen vertreten waren. Um die *in vitro* generierten Dynamik-Daten mit der *in vivo* Situation in Korrelation zu bringen, muss die Kinetik der Testsubstanz berücksichtigt und die Ergebnisse mit Hilfe von physiologisch-basierter pharmakokinetischer Modellierung extrapoliert werden.

Ziel der vorliegenden Arbeit war es, Kinetik-Daten der gewählten Testsubstanzen (Cyclosporin A, Adefovir dipivoxil und Cisplatin) *in vitro* zu erheben und bzgl. ihrer Zuverlässigkeit sowie ihrer Relevanz verglichen mit *in vivo* Daten zu beurteilen. Hierfür wurden kultivierte Zellen täglich bzw. jeden zweiten Tag für zwei Wochen mit zwei verschiedenen Konzentrationen (toxisch und nicht-toxisch) des Arzneimittels behandelt. Der Gehalt des applizierten Arzneimittels oder die Hauptmetaboliten wurden mittels LC-MS/MS oder ICP-MS in Vehikel, Medium und Zellen sowie die vom Plastik adsorbierte Menge in Proben bestimmt, die am ersten und letzten Behandlungstag zu fünf unterschiedlichen Zeitpunkten gewonnen wurden.

Eine eindeutige Bioakkumulation von Cyclosporin A wurde in primären Rattenhepatozyten nach Behandlung mit der hohen Konzentration festgestellt. Eine effiziente CYP3A4- und CYP3A5-vermittelte Biotransformation von Cyclosporin A wurde für primäre humane Hepatozyten sowie HepaRG Zellen beobachtet. Diese Ergebnisse stimmten mit der *in vivo* Situation überein. Ratten sind aufgrund ihrer geringen CYP3A Aktivität schlechte Tiermodelle für CYP3A-Biotransformationsstudien. Des Weiteren wurden Interassay-Schwankungen bei primären human Hepatozyten bemerkt, die auf die biologische Variabilität der CYP3A4- sowie CYP3A5-Aktivität zwischen den

menschlichen Spendern zurückzuführen sind. Rattenhepatozyten und HepaRG Zellen hingegen wiesen Interassay-Schwankungen auf, die durch unterschiedliche Cyclosporin A Behandlungskonzentrationen zwischen den Replikaten verursacht wurden. Die Cyclosporin A Biotransformation war in HepaRG Zellen am stärksten ausgeprägt, was durch stabile und wesentlich höhere CYP3A4- und CYP3A5-Aktivität in HepaRG Zellen zu erklären ist. Zusätzlich wurden die *in vitro* Clearance-Werte bestimmt und auf *in vivo* Clearance-Werte extrapoliert. Alle extrapolierten Werte waren zu hoch geschätzt (primäre Rattenhepatozyten: 10fach, primäre human Hepatpzyten: 2fach, HepaRG Zellen: 2fach). Diese Ergebnisse sollten mittels physiologisch-basierter pharmakokinetischer Modellierung sowie durch weitere Experimente überprüft werden, um zu ermitteln, ob diese hohen Schätzungen für jedes System konstant sind und somit durch die Einführung von weiteren Skalierungsfaktoren verringert werden können.

Kultivierte Gehirnzellen, primäre Nervenzellkulturen der Kortex von Mäusen und primäre Hirnzellaggregate der Ratte, zeigten schnell erreichte Cyclosporin A Gleichgewichtskonzentrationen. Diese Ergebnisse deuteten auf eine Verteilung von Cyclosporin A zwischen der wässrigen und organischen Phase hin, wobei biologische Prozesse nur eine untergeordnete Rolle spielen. Daher scheint die intrazelluläre Cyclosporin A Aufnahme Transporter-vermittelt zu sein. Ergebnisse der Transporter-Experimente, die an einer künstlichen Membran und Caco-2 Zellen durchgeführt wurden, unterstützten diese Hypothese. Messungen der Plastikbindung von Cyclosporin A zeigten signifikante, aber für jedes Zellsystem unterschiedliche, Adsorptionsraten, die mittels physiologisch-basierter pharmakokinetischer Modellierung berücksichtigt werden sollten.

Die Kinetik von Adefovir dipivoxil machte auf die Nachteile von *in vitro* Versuchen aufmerksam. Für die intrazelluläre Aufnahme von Adefovir sind aktive Transportproteine nötig, die jedoch in der Nierenzelllinie RPTEC/TERT1 nicht funktionell vorhanden sind. Daher war die Aufnahme von Adefovir auf die passive Diffusion von Adefovir dipivoxil beschränkt, das aber auch zeitabhängig unter den experimentellen Konditionen zerfiel.

Die an RPTEC/TERT1 Zellen untersuchte Kinetik von Cisplatin deutete auf eine intrazelluläre Platin-Anreicherung hin, die jedoch nicht in einer signifikanten

Bioakkumulation resultierte. Möglicherweise sind innerhalb von 14 Tagen die Gleichgewichtskonzentrationen von Cisplatin noch nicht erreicht. Die Kinetikprofile von Cisplatin in Medium ließen einen aktiven, von der basolateralen zur apikalen Seite gerichteten Cisplatin Transport erkennen, wie schon *in vivo* beschrieben, wobei die Geschwindigkeit dieser Transportprozesse *in vitro* langsamer zu sein scheint als in der intakte Niere. Daher müssen die generierten Daten zur Schätzung von zellulären Prozessen modelliert werden, um durch anschließende Extrapolation mit *in vivo* Daten verglichen werden zu können.

Abschließend bleibt zu sagen, dass das experimentelle Design vorteilhaft war. Wiederholte tägliche Administration von zwei unterschiedlichen Konzentrationen eines Medikaments ermöglichte die Erfassung von Bioakkumulation bei toxischen Konzentrationen sowie Biotransformation/Export bei nicht-toxischen Konzentrationen. Potenzielle Fehler, die zu einer Fehlinterpretation führen könnten, wurden durch die exakte Bestimmung der tatsächlich applizierten Arzneimittelmenge reduziert, da nicht immer die applizierte Konzentration mit der Nominalkonzentration übereinstimmt. Darüber hinaus erwies es sich als Vorteil, die Arzneimittelkonzentrationen in den einzelnen Kompartimenten (Medium, Zellen und Plastik) zu bestimmen. Somit konnten zum einen Erkenntnisse über die Verteilung der Substanz gewonnen werden und zum anderen Fehleinschätzungen von zellulären Prozessen, z.B. Biotransformation, verhindert werden, was letzten Endes bei die Interpretation von Kinetik-Daten behilflich ist. Jedoch, wurden auch die Grenzen von *in vitro* Ansätzen deutlich. Für eine korrekte Extrapolation ist es unverzichtbar, dass die untersuchten *in vitro* Systeme funktionierende Proteine aufweisen, die bei der untersuchten Arzneimittel-induzierten Toxizität eine Schlüsselrolle übernehmen. Abschließend kann festgehalten werden, dass es, unter Berücksichtigung der Vor- und Nachteile, von Nutzen sein kann diesen Versuchsansatz der Langzeitbehandlung zu validieren und darüber hinaus auf Co-Kultursysteme sowie Organ-Chips anzuwenden hinsichtlich der Entwicklung von Alternativmethoden für Toxizitätsstudien bei wiederholter Gabe.

Acknowledgments

Die vorliegende Arbeit wurde am Lehrstuhl für Toxikologie der Julius-Maximilians-Universität Würzburg durchgeführt. Herzlichen Dank an meinen Betreuer Prof. Dr. Dr. Wolfgang Dekant für die Bereitstellung des interessanten Themas, das entgegengebrachte Vertrauen, die Hilfestellungen und Denkanstöße, die Einführung in die Toxikologie und schließlich für die erfolgreiche Zusammenarbeit.

Vielen Dank an Prof. Dr. Dr. Martin Müller als Vertreter der Fakultät für Biologie. Ich danke Ihnen für die Übernahme der Betreuung meiner Arbeit sowie für Ihre überaus freundliche und hilfreiche Unterstützung.

Die Arbeit war Teil des Projektes „Predict-IV“ innerhalb des siebten Rahmenprogramms der EU. Ich danke allen Projektpartnern für die erfolgreiche Kooperation. Vor allem möchte ich mich an dieser Stelle bei Dr. Emanuela Testai für Ihre schnellen und förderlichen Ratschläge bedanken. Ebenfalls danke ich Nils Opel von der Firma Müller-BBM GmbH für die Platin-Messungen.

Ich möchte mich von ganzen Herzen beim dritten Stock des Lehrstuhls für Toxikologie bedanken. Vielen Dank für Eure tatkräftige Unterstützung. PD Dr. Angela Mally möchte ich für die stets offene Tür und Hilfe während meiner Promotion danken. Hannelore Popa-Henning, herzlichen Dank für Deine Antworten auf alle meine Fragen (ob fachlich oder privat), Deine Kritik sowie Lob und den gemeinsamen Spaß. Nataly Bittner, danke für die Einführung in die hohe Kunst der Analytik mittels LC-MS/MS, die liebevolle Betreuung und Wartung der Geräte sowie für Deine stets rücksichtsvollen und aufmunternden Worte. Heike Keim-Heusler, vielen Dank für Deine Hilfe bei den tausenden von Proben, Dein Wissen zum Thema Chemikalien und vor allem für Deine Geduld. Elisabeth Rüb-Spiegel, Michaela Bekteshi, Ursula Tatsch und Marion Friedewald, bei Euch möchte ich mich ebenfalls für die Unterstützung im Labor bedanken. Dr. Susanne Ramm, Dr. Melanie Adler, Dr. Elisabeth Limbeck, Karin Herrgen und Olga Schmal, ich danke Euch für die Beratung zu sämtlichen Themen, die wir in der (leider) kurzen Zeit diskutieren durften. Dr. Tobias Schmidt, ich bin Dir dankbar für die vielen, kritischen Verbesserungsvorschläge, die offenen und ehrlichen Diskussionen und selbstverständlich auch für das viele Lachen. Ich würde mir immer wieder gerne ein

Büro mit Dir teilen! Ihr alle macht durch Eure fachlichen und vor allem persönlichen Kompetenzen unsere Oase zu dem was sie ist.

Vielen Dank an meine Familie, meine Freunde und meinen Schnuffel, die mich durch alle Lebenslagen begleitet, unterstützt und darüber hinaus ertragen haben. Ihr seid die Wichtigsten und ich danke Euch, dass ich Euch habe. Nur mit Euch konnte ich so weit und jetzt auch die nächste Schritte gehen.

Abbreviations

AB	Apical to basolateral
ADME	Absorption, distribution, metabolism, excretion
ADV	Adefovir
ADVd	Adefovir dipivoxil
ADV – d_4	Deuterium labeled adefovir
AUC	Area under the curve
BA	Basolateral to apical
BBB	Blood-brain barrier
BSEP	Bile salt export pump
CAD	Collisionally activated dissociation
CE	Collision energy
Cl	Clearance
CNS	Central nervous system
COX	Cyclooxygenase
CsA	Cyclosporine A
CsA-d_{12}	Deuterium labeled cyclosporine A
CTR	Copper transporter
CXP	Cell exit potential
CYP	Cytochrome P450-dependent monooxygenase
DMEM	Dulbecco's modified eagle medium
DMSO	Dimethyl sulfoxide
DOPC	1,2-dioleoyl-*sn*-glycero-3-phosphocholine
DP	Declustering potential
EDTA	Ethylenediaminetetraacetic acid
EP	Entrance potential
$\mathbf{F}_{(cum)}$	Cumulative, transported fraction
FCS	Fetal calf serum
FMO	Flavin-dependent monooxygenase

FP	Focusing potential
GST	Glutathione S-transfereases
HMM	Human hepatocyte maintenance medium
hOAT	Human organic anion transporter
hOCT	Human organic cation transporter
HPLC	High performance liquid chromatography
ICH	International Conference on Harmonization
ICP-MS	Inductively coupled plasma mass spectrometry
ITS	Insulin-transferrin-selenium
LC	Liquid chromatography
LOD	Limit of detection
LOQ	Limit of quantification
MAO	Monoamine oxidase
MAPK	Mitogen-activated protein-kinase
MATE1	Multidrug and toxin extrusion protein 1
MRP2	Multidrug resistance-associated protein 2
MRP3	Multidrug resistance associated protein 3
MRM	Multiple reaction monitoring mode
MS	Mass spectrometry
NAT	N-acetyltransferases
OECD	Organization for Economic Co-operation and Development
$\mathbf{P}_{app}$	Apparent permeability coefficients
PAMPA	Parallel artificial membrane permeability assay
PBS	Phosphate-buffered saline
Pgp	Permeability glycoprotein
PHH	Primary human hepatocytes
PNB	Primary neurobasal medium
PRH	Primary rat hepatocytes
$\mathbf{R^2}$	Coefficient of determination
RT	Retention time

S	Fraction of sample remaining in the wells
SULT	Sulfotransferases
TC_{10}	10% cytotoxic concentration
TNF α	tumor necrosis factor alpha
UGT	Uridine 5'-diphospho-glucuronosyltransferases

1. Introduction

Safety assessment of chemicals, drugs, pesticides or ingredients of personal care products is time-consuming and costly, since a large number of animal testing has to be performed for toxicity studies (Soldatow *et al.*, 2013). In addition to these economic issues, ethical concerns have also been mentioned regarding animal welfare. Therefore, according to the "3R principles", regulatory changes forced the development of alternative methods for toxicity testing, which are now widely accepted to study mechanisms and predict adverse effects in humans after single exposure (Russell and Burch, 1959; Lilienblum *et al.*, 2008). Since humans are repeatedly exposed to a particular drug during therapy, repeated dose toxicity studies performed on animals are required to emulate this condition, despite the fact that repeated exposure is not considered by alternative methods (Adler *et al.*, 2011).

The EU project "Predict-IV" has taken up the repeated daily exposure of well-established *in vitro* systems. The overall aim was to improve risk assessment in the early stage of drug development by applying "omics" technologies, kinetics and modeling. Pharmacokinetics plays a key role for extrapolation of dynamic data from animal to human and is now recognized to be essential for the harmonization of *in vitro* data with *in vivo*. In addition, kinetic evaluation *in vitro* is crucial for the understanding and correct interpretation of dynamic data (Coecke *et al.*, 2013). Many factors often ignored have a deep impact on the dynamic outcome. The concentration of a compound reaching cells is often different from the nominal concentration added due to evaporation, plastic adsorption and protein binding (Blaauboer, 2010; Coecke *et al.*, 2013). Further, *in vitro*, a compound might not reach its molecular target due to missing transporter activity (Coecke *et al.*, 2013). The focus of this thesis is the assessment of kinetics *in vitro* as an essential part of interpreting dynamic outcomes and assessing the feasibility with regard to human subjects.

1.1. Definition of Pharmacokinetics

Pharmacokinetics is defined as the time-course of **A**bsorption, **D**istribution, biotransformation (**M**etabolism) and **E**xcretion (**ADME**) of xenobiotics in the whole organism (Renwick, 2001).

Absorption is the uptake of xenobiotics into the circulatory system and is dependent on the application route, e.g. intravenous, oral, inhalation, and on the compound's cellular uptake. The pharmacokinetic parameter describing absorption is bioavailability, which represents the fraction of the applied drug reaching the systemic circulation and takes into account absorption and first pass biotransformation, i.e. pre-systemic biotransformation in the gastro-intestinal tract and/or liver after per oral exposure (Pond and Tozer, 1984; Dekant and Vamvakas, 2005; Bessems and Geraets, 2013).

A bioavailable compound is distributed subsequently in three major disposition spaces, namely the intravascular, interstitial and intracellular space. The pharmacokinetic parameter for disposition is the apparent volume of distribution, which represents a fictive volume that is needed to dissolve the initial dose of a compound to reach the determined plasma concentration (Fichtl *et al.*, 1999). The apparent volume of distribution is dependent on the physicochemical characteristics of a compound and on its capability of protein and tissue binding and its numerical values can exceed that of the physiological distribution space (approx. 0.6 L/kg). For cyclosporine A, the apparent volume of distribution at steady state (the equilibrium of input and output during repeated dosing) was determined as 3.5 L/kg body weight in humans, which is 6-fold higher than the physiological distribution space and can be explained by the lipophilic character of cyclosporine A (Follath *et al.*, 1983). The drug is distributed to lipophilic in organs and tissue such as fat, liver and kidneys and reaches higher concentrations there as compared to plasma (Bernareggi and Rowland, 1991; Lensmeyer *et al.*, 1991). Thus, the apparent volume of distribution holds the information on a compound's localization in the body and is used to calculate the initial dose that is needed to reach a specific plasma concentration (Fichtl *et al.*, 1999).

Metabolism describes the transformation of an endogenous or exogenous substance from its chemical form to another, whereas biotransformation specifically describes the conversion of xenobiotics from a non-excretable, lipophilic and nonpolar form to a water-soluble structure (Ito, 2014). Biotransformation is divided in two phases (Dekant

and Vamvakas, 2005). Phase I is the functionalization of xenobiotics and major involved enzymes are oxidoreductases as cytochrome P450-dependent monooxygenase (CYP), flavin-dependent monooxygenase (FMO), monoamine oxidase (MAO), cyclooxygenase (COX) and hydrolases such as esterases and epoxide hydrolases (Dekant and Vamvakas, 2005). Products of the functionalization phase are either nucleophiles (alcohols, acids, amines) or electrophiles (epoxides), whereas epoxides can be converted by epoxide hydrolases to nucleophiles. Phase I reactions lead to detoxification, toxification or activation of xenobiotics (Parke, 1987; Guengerich, 2001). The second step, phase II, is the conjugation of these products by transferases, for instance, uridine 5'-diphospho-glucuronosyltransferases (UGT), sulfotransferases (SULT), glutathione S-transfereases (GST) and N-acetyltransferases (NAT) (Dekant and Vamvakas, 2005). Occasionally, a third phase is listed, namely phase III, which accounts for the transport of xenobiotic conjugates out of the cell/organism (Xu *et al.*, 2005; Nakata *et al.*, 2006; Shen and Kong, 2009). The pharmacokinetic parameter describing biotransformation is the metabolic clearance, which is defined by the ratio of v_{max} and K_m. V_{max} is the maximal rate of turnover at saturating substrate concentrations and K_m is the Michealis constant, i.e. the substrate concentration at which the reaction is half of v_{max} (Fichtl *et al.*, 1999).

Elimination is defined as the excretion through the kidney and bile or exhalation through the lung. The pharmacokinetic parameter describing the elimination is the total clearance and includes both the elimination out of the body and the biotransformation of a xenobiotic, although its biotransformation products are still present (Fichtl *et al.*, 1999).

1.2. Pharmacokinetics used for risk assessment and evaluation of relevant pharmacokinetic parameters

Pharmacokinetic data enhance the understanding of mechanisms of action and/or toxicity induced by xenobiotics and help to assess the risk and safety of xenobiotics in humans and provide the basis for dosing of drugs (ICH S3A Guideline; OECD Test Guideline No. 417). Pharmacokinetic evaluations are necessary to describe the systemic exposure and its relationship to observed (adverse) effects. Further, conclusions can be made regarding species and gender differences, influence of the life-stage and the biological variability (Baldrick, 2003). This knowledge is crucial for the design of further

studies (pre-clinical repeated-dose or clinical studies) and for the estimation of margins of safety (Baldrick, 2003; Bessems and Geraets, 2013).

Usually, the concentration of a xenobiotic is determined in body fluid (plasma, serum or whole blood) at several time-points after administration of the xenobiotic, while the choice of sampling time-points has to be carefully considered as too late sampling might miss essential information and too short intervals may stress animals and cause hypovolemic shock (Diehl *et al.*, 2001). The determined xenobiotic concentrations are plotted versus time and an example of a resulting graph after per oral exposure is given in Figure 1.

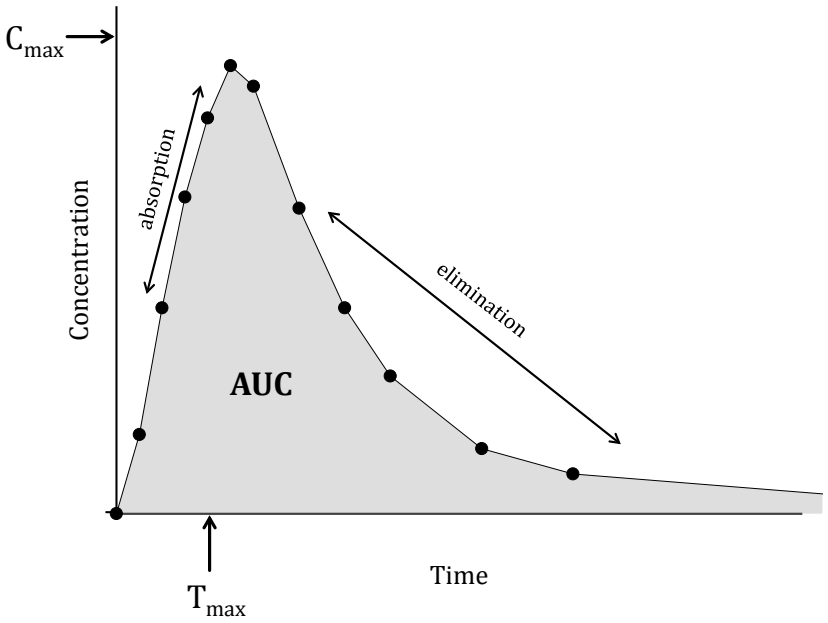

Figure 1. *Concentration-time curve for a xenobiotic after oral administration. Determined concentrations of a xenobiotic in body fluid samples are plotted versus time. The peak concentration (C_{max}) and the time to reach C_{max} (T_{max}) can be read from the resulting graph. The ascending branch (until C_{max}) illustrates the absorption of the xenobiotic and the descending branch (beyond C_{max}) contains the distribution, biotransformation and elimination of a xenobiotic. The grey colored area illustrates the "area under the curve" (AUC).*

C_{max}, the maximum or peak concentration of the substance, and the time to reach C_{max} (T_{max}) can be read out directly from the graph without any further calculations. In the case of intravenous administration, the initial dose corresponds to C_{max}. The area under the resulting concentration-time curve (AUC, area under the curve) can be calculated manually by the trapezoidal method separating the curve into squares, of which the area is calculated by either using the linear (Eq. 1) or the logarithmic method (Eq. 2) (Bailer and Piegorsch, 1990; Matthews *et al.*, 1990; Purves, 1992). Often a combination of both

is used, where the linear method is applied for increasing concentrations up to C_{max} ("absorption phase") and the logarithmic method is utilized for decreasing concentrations after C_{max} ("elimination phase") (Yeh and Kwan, 1978; Fracasso *et al.*, 2004; Fok *et al.*, 2013; Hu *et al.*, 2013; Fossler *et al.*, 2014).

$$AUC_{t_0-t_{max}} = \sum \frac{1}{2}(C_0 + C_1)(t_1 - t_0) \ldots \frac{1}{2}(C_{max-1} + C_{max})(t_{max} - t_{max-1}) \quad \text{(Eq. 1)}$$

$$AUC_{t_{max}-t_{last}} = \sum \frac{C_{max} - C_{max+1}}{\ln(C_{max}) - \ln(C_{max+1})}(t_{max+1} - t_{max}) \ldots \frac{C_{last-1} - C_{last}}{\ln(C_{last-1}) - \ln(C_{last})}(t_{last} - t_{last-1}) \quad \text{(Eq. 2)}$$

C_0 is the measured concentration at the first sampling time-point t_0 and C_{last} is the determined concentration at the last sampling time-point t_{last}. It is possible that a xenobiotic might still be present in the body after t_{last}. Therefore, AUC is extrapolated from t_{last} to infinity (t_∞) (Martinez and Jackson, 1991):

$$AUC_{t_{last}-t_\infty} = \frac{C_{last}}{k_{el}} \quad \text{(Eq. 3)}$$

The terminal elimination rate (k_{el}) is estimated as the negative slope of the elimination phase of the concentration-time curve plotting the concentration on the natural logarithmic scale. To verify the reliability of extrapolated AUC, its fraction of the total AUC (to infinity) is calculated and should be <20%.

The sum of all AUCs including the extrapolation to infinity gives the total AUC.

$$AUC = AUC_{t_0-t_{max}} + AUC_{t_{max}-t_{last}} + AUC_{t_{last}-t_\infty} \quad \text{(Eq. 4)}$$

Once AUC is determined, other relevant pharmacokinetic parameters can be calculated like bioavailability and total clearance (Baldrick, 2003; Ploemen *et al.*, 2007). The bioavailability needs to be considered when a compound is not administered intravenously and is represented as the ratio of AUC obtained after any application route such as oral and AUC after intravenous administration. It is assumed that 100% of the given compound is bioavailable after intravenous administration, although for some compounds pulmonary first-pass elimination plays an important role (Iwamoto *et al.*, 1987; Kuipers *et al.*, 1999; Aoki *et al.*, 2010). The total clearance is the ratio of dose and AUC multiplied with the bioavailability, where bioavailability is 1 after intravenous application. Renal clearance can be similarly obtained by measuring the unchanged

compound in urine, plotting the determined concentration versus time and calculating AUC. Subtraction of the renal clearance from the total clearance leads to the non-renal clearance.

1.3. Why *in vitro* approaches?

In 1959, Russell and Burch pointed out the ethical aspects of animal testing and proposed to *Reduce* the number of animals, *Replace* animal testing whenever feasible alternative methods are available and *Refine* animal husbandry; known as the "3R principle" (Russell and Burch, 1959). Following this, the European Directive 86/609/EEC was established in 1986 in order to "protect animals used for experimental and other scientific purposes"(Directive, 1986). Due to disparities between member states the Directive was recently updated in the Directive 2010/63/EU (European Commission, 2010). Simultaneously, the total ban of animal testing in the safety assessment of cosmetic products and ingredients was manifested in the Regulation (EU) 1223/2009 (European Commission, 2009). Moreover, the Registration, Evaluation, Authorization and Restriction of Chemicals (REACH) came into force in 2007 to protect human health and the environment, while shifting the responsibility of providing data and performing risk assessment to the industry (European Commission, 2006). As all chemicals in the European Union have to be registered until 2018, this leads to a large number of animal testing for data generation. Therefore, it is enshrined by the Regulation (EU) 1907/2006 that the use of vertebrate animals should be avoided and replaced by feasible alternative methods including *in vitro* approaches, in silico methods and read across strategies (European Commission, 2006). Furthermore, the European Commission should ensure the promotion of alternative test methods within its future Research Framework Programs (Regulation (EU) 1907/2006, article 40 (European Commission, 2006)).

To date, several *in vitro* methods are validated and recommended by the Organization for Economic Co-operation and Development (OECD), which should be applied in advance of animal trials for the testing of chemicals. Cell viability assays are utilized to estimate starting doses for acute oral systemic toxicity tests using normal human keratinocyte and/or mouse fibroblasts (OECD No. 129, 2010). Skin absorption, corrosion and irritation is tested *in vitro* or *ex vivo* using human or animal skin (OECD Test No. 428; OECD Test No. 430; OECD Test No. 431; OECD Test No. 435; OECD Test No. 439). Genotoxicity and phototoxicity are evaluated by *in vitro* approaches (OECD Test

No. 432; OECD Test No. 471; OECD Test No. 473; OECD Test No. 476). On the other hand, also non-standard *in vitro* methods are applied for acute and repeated dose testing focusing on the discovery of organ-specific toxicity mechanisms and biomarker evaluation (Adler *et al.*, 2011). While *in vitro* approaches are representing only a fraction of an organ, they cannot provide information on interactions between organs, systemic effects and are technically limited, but may be useful for hazard identification and for obtaining mechanistic information (Kandárová and Letašiová, 2011; Worth *et al.*, 2014). A lot of data have been generated *in vitro*, but less was known about harmonizing the observations made *in vitro* with the *in vivo* situation. The importance of kinetics has now been recognized and plays a key role in the interpretation of data generated *in vitro* and the *in vitro* to *in vivo* extrapolation by physiologically-based pharmacokinetic modeling (Adler *et al.*, 2011; Blaauboer *et al.*, 2012; Coecke *et al.*, 2013).

1.4. Kinetics in *in vitro* approaches

Browsing through the literature one may find many terms regarding pharmacokinetics such as toxicokinetics, biokinetics and kinetics (Filov, 1973; Kato *et al.*, 1993; Bouvier *et al.*, 2007). In this thesis the terms pharmacokinetics and kinetics are used for *in vivo* and *in vitro*, respectively.

Evaluation of kinetics *in vitro* may aim for two goals: (i) to predict a compound's ADME *in vivo* or (ii) to help to interpret evaluated dynamic data *in vitro* and their relevance *in vivo*.

It is obvious that ADME cannot be determined by a single *in vitro* approach, but is split in its four categories: absorption, distribution, biotransformation and excretion. The model approach to test the absorption of a compound has to be chosen dependent on its application route and on the model's capacity of reconstructing the *in vivo* situation (Worth *et al.*, 2014). The estimation of a compound's distribution in whole body by an *in vitro* approach seems challenging, but it was successfully done by utilizing two parameters determined *in vitro*, the substance's lipophilicity and its plasma protein binding (Poulin and Theil, 2002). A major disadvantage was that only compounds undergoing passive diffusion revealed predictions with good *in vitro*/*in vivo* correlation (Poulin and Theil, 2002). Therefore, determining active transport processes *in vitro* is crucial for the correct prediction of the apparent volume of distribution at steady state considering the high abundance of influx and efflux transporters, especially at the

blood-brain barrier and blood-placenta barrier (Worth *et al.*, 2014). The liver is the predominant organ for biotransformation, whereas biotransformation may also occur in the skin, gastro-intestinal tract and lung (Li, 2001; Worth *et al.*, 2014). S9-mix, microsomes, primary hepatocytes, liver slices and hepatic cell cultures are used for biotransformation studies *in vitro* with each system having advantages and disadvantages. While human derived primary cells or tissues are in limited supply, this aspect can be avoided using immortalized cell lines of human origin, e.g. HepG2, HepaRG. Disadvantages of using cell cultures are the missing biological variability, often low enzyme activity, limited reproducibility of results across laboratories and passage numbers (Zanelli *et al.*, 2012). Excretion may take place in the kidney, bile or lung. *In vitro* approaches for renal elimination are not developed yet, but may be predicted by in silico methods (Coecke *et al.*, 2013). Biliary clearance can be determined by studies on primary hepatocytes under sandwich culture conditions and pulmonary excretion can be estimated by blood/air coefficients (Coecke *et al.*, 2013; Bessems *et al.*, 2014; Worth *et al.*, 2014).

Although it has been accepted that kinetic evaluation *in vitro* is essential for the interpretation of generated dynamic data, many crucial factors were not considered. Often the nominal concentration, i.e. the administered amount per mL volume of cell culture medium, was assumed to be the free available concentration for cells (Blaauboer, 2010). In fact, protein binding, adsorption to plastic devices (well walls, inserts, Eppendorf-caps), evaporation and the compound's stability have a deep impact on the actual concentration applied to cells (Blaauboer, 2010; Coecke *et al.*, 2013). Therefore, prior to conducting *in vitro* tests, specificity and relevance to *in vivo* scenarios have to be evaluated. Further, when using *in vitro* approaches, it has to be considered that cells may lose time-dependently expression of transport or enzyme activities (Coecke *et al.*, 2013). Hence, the test system has to be well characterized or at least one should be aware of possible pitfalls for correct data interpretation.

1.5. EU project – Predict-IV

"Predict-IV" was a collaborative large-scale integrating project consisting of 21 participants from academia, industry and SMEs (small and medium-sized enterprises) and was supported by the 7th Framework Program of the European Commission. The overall aim of "PredictIV" was to improve risk assessment in the early stage of drug development by data generation on the basis of well-established *in vitro* systems in

combination with cell biology, mechanistic toxicology and in silico modeling. Reason for the focus on drugs is the productivity crisis in the pharmaceutical industry for the past two decades (Kola and Landis, 2004; Pammolli *et al.*, 2011; Watkins, 2011). Drug development is becoming more expensive and simultaneously attrition rates in clinical trials are increasing (DiMasi *et al.*, 2010). Drug failures in phase II trials and beyond are more often due to lack of efficacy (56% between 2011 and 2012) and occurring safety issues (28% between 2011 and 2012), indicating the need of better prediction models and strategies in the preclinical phase (Arrowsmith and Miller, 2013). Besides cardiovascular toxicity (22%), hepatotoxicity (22%) and neurotoxicity (22%) are the most prominent adverse drug effects leading to termination of drug development in phase I-III (Watkins, 2011). Therefore, the liver, the central nervous system (CNS) and the kidney were the chosen target organs within "Predict-IV", represented by primary cell cultures or established cell lines, for evaluation of potential toxicities by an integrated testing strategy of "omics" technologies (transcriptomics, proteomics and metabolomics), kinetics and physiologically-based pharmacokinetic modeling.

The liver was represented by the human derived HepaRG cell line, primary rat (PRH) and human hepatocytes (PHH). Primary cells were cultured as sandwich cultures, which prolongs the duration of cell viability and enzyme function and improves the hepatocyte morphology, such as formation of functional bile canaliculi (LeCluyse *et al.*, 2012; Soldatow *et al.*, 2013). Rodent derived primary cells, i.e. primary neuronal culture of mouse cortex (2D model) and primary aggregating rat brain cells (3D model), were utilized as respective brain cell culture models. Although species differences exist and human models would be preferable, rodent tissues were the only models at start of the project, which could be routinely used in *in vitro* studies of the CNS. Throughout the thesis both systems will be described as brain cell culture models, despite not possessing a blood-brain barrier. A separate blood-brain barrier model based on co-culture of bovine brain capillary endothelial cells and rat astrocytes was included into the CNS section of "Predict-IV". Human derived renal proximal tubules epithelial cells immortalized by Telomerase Reverse Transcriptase 1 (TERT1), RPTEC/TERT1 cells, were chosen as *in vitro* model for nephrotoxicity evaluation.

1.6. Test compounds

Major criteria for selection of the test compounds were: induction of nephro-, hepato- and/or neurotoxicity and knowledge of well-defined systemic toxicological *in vivo* data

and pharmacokinetic *in vivo* data. The selected test compounds were applied to the respective *in vitro* models based on known drug-induced toxicity *in vivo*. Hence, not all *in vitro* systems were exposed to all test compounds. The test compounds used for analysis of drug-induced changes on the transcriptome, proteome and metabolome level and their kinetic behavior are listed in Table 1.

Table 1. *List of selected test compounds.*

Hepatotoxic	Neurotoxic	Nephrotoxic
Chlorpromazine	Chlorpromazine	Cisplatinum
Ibuprofen	Diazepam	Adefovir dipivoxil
Amiodarone	Amiodarone	
Cyclosporine A	Cyclosporine A	Cyclosporine A

Central to this thesis are the kinetics of cyclosporine A in the hepatic and brain cell culture models, along with adefovir dipivoxil and cisplatinum kinetics in the kidney *in vitro* model.

1.6.1. Cyclosporine A

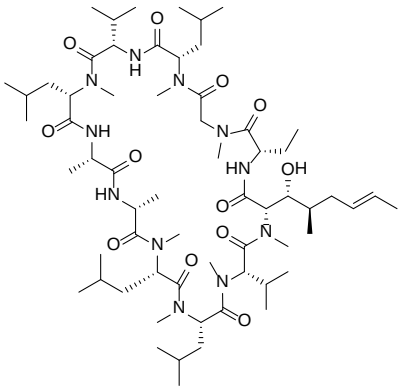

Figure 2. *Chemical structure of cyclosporine A (molecular weight = 1202.61 g/mol)*

Cyclosporine A (CsA) is a cyclic peptide consisting of 11 amino acids (Figure 2). It was initially isolated from the fungus *Tolypocladium inflatum* and is used as immunosuppressant to prevent graft rejection after transplantation (Christians and Sewing, 1993; Fahr, 1993). The immunosuppressive effect is assumed to occur by suppression of T-cell production due to inhibition of the phosphatase calcineurin (Fearon *et al.*, 2011) by the complex of CsA and cyclophilins. Cyclophilins are ubiquitously distributed proteins possessing peptidyl-prolyl cis-trans isomerase activity

(Fearon *et al.*, 2011). Especially cyclophilin A and B are involved in the complex formation, while only cyclophilin B secretion is induced by CsA (Price *et al.*, 1994; Fearon *et al.*, 2011; Wilmes *et al.*, 2013). Cyclophilin B is constrained to the endoplasmic reticulum by a specific amino-terminal sequence and its CsA-induced release might be used as an indicator for intracellular CsA uptake (Wang and Heitman, 2005; Wilmes *et al.*, 2013). However, cyclophilin B secretion was also observed *in vitro* and *in vivo* at very low levels in the absence of CsA (Spik *et al.*, 1991; Mariller *et al.*, 1996; De Ceuninck *et al.*, 2003; Fearon *et al.*, 2011).

Besides its role as an immunosuppressant, CsA was shown to induce hepato-, neuro- and nephrotoxicity (Calne *et al.*, 1979; Klintmalm *et al.*, 1981; Atkinson *et al.*, 1983; Bennett and Pulliam, 1983; Palestine *et al.*, 1984; Klintmalm *et al.*, 1985; Gijtenbeek *et al.*, 1999). Due to the narrow therapeutic window and low bioavailability of CsA, drug monitoring is essential (Serkova *et al.*, 2004). CsA is assumed to enter the cells by passive diffusion (Ziegler *et al.*, 1988; Fricker and Fahr, 1997). CsA biotransformation is catalyzed by CYP3A4 and CYP3A5 (CYP3A4/5) to at least 30 metabolites (Combalbert *et al.*, 1989; Christians and Sewing, 1993; Fahr, 1993; Kelly and Kahan, 2002). Further, CsA is a known substrate of the permeability glycoprotein (Pgp) efflux pump (Fricker and Fahr, 1997). Besides its function as substrate for both the CYP3A4/5 and Pgp, strong inhibitory effects of CsA on CYP3A4/5 and transporters, including Pgp, are described, presumably due to reversible competitive inhibition by CsA (Saeki *et al.*, 1993; Giacomini *et al.*, 2010; Amundsen *et al.*, 2012; Englund *et al.*, 2014). Systemically available CsA is almost completely eliminated by hepatic biotransformation (Ducharme *et al.*, 1995). Although CsA is a well-studied compound, the exact mechanism of toxicity is not clear. Both nephro- and hepatotoxicity might be caused by production of reactive oxygen species since antioxidants could reduce the CsA-induced toxicity (Rezzani, 2006; de Arriba *et al.*, 2013; Sharanek *et al.*, 2014). Furthermore, hepatotoxicity was shown to be related to impairment of transporters leading to cholestasis, this might be conceivable for transport systems in the kidney as well (Sharanek *et al.*, 2014). No clear evidence regarding CsA-induced neurotoxicity is available. Neurotoxicity is reversible by termination of CsA administration (Gijtenbeek *et al.*, 1999). Whereas nephro- and hepatotoxicity are linked to elevated blood levels, well above therapeutic levels, neurotoxicity was also observed in patients with CsA plasma levels within the normal therapeutic range (Serkova *et al.*, 2004). Significant CsA brain tissue concentrations are

missing and data lack describing both together, CsA tissue concentrations and neurotoxicity in human. No significant CsA concentrations were detected in mice, while neurotoxicity occurred (Boland *et al.*, 1984).

1.6.2. Adefovir dipivoxil

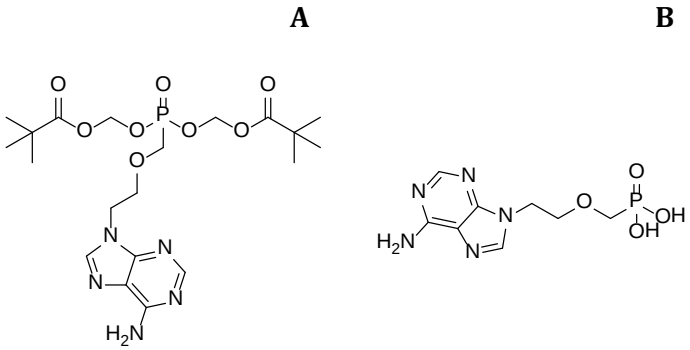

Figure 3. *Chemical structures of adefovir dipivoxil (molecular weight = 501.47 g/mol;* ***A****) and adefovir (molecular weight = 273.19 g/mol;* ***B****).*

Adefovir dipivoxil (ADVd) is the diester prodrug of the acyclic nucleotide analog adefovir (ADV) and is given orally for treatment of chronic infection with hepatitis B virus (Danta and Dusheiko, 2004). After oral administration, ADVd is hydrolyzed completely to ADV in the intestine and approximately 60% ADV of the given ADVd dose is bioavailable (Danta and Dusheiko, 2004). ADV intracellular uptake is mediated by active transporter systems, namely human organic anion transporter 1 and 3 (hOAT1/3) (Cihlar *et al.*, 1999; Ho *et al.*, 2000; Izzedine *et al.*, 2005; Uwai *et al.*, 2007). Inside the cells, ADV is converted to its active form ADV diphosphate by phosphorylation (Qaqish *et al.*, 2003; Law *et al.*, 2012). ADV diphosphate is incorporated into viral DNA and terminates viral DNA elongation by inhibiting the viral DNA-polymerase and reverse transcriptase (Law *et al.*, 2012). ADV diphosphate has a low affinity to human DNA-polymerase γ and ADV toxicity is limited to the kidneys, particularly to the proximal tubular system (Danta and Dusheiko, 2004). ADV bioaccumulation in kidneys seems to play a role in ADV-induced nephrotoxicity (Hitchcock and Lacy, 1994). Although the mechanism of toxicity is not clear, it might be related to inhibition of transporters and human DNA-polymerase γ in the renal mitochondria due to increased intracellular concentration caused by bioaccumulation (Tanji *et al.*, 2001; Izzedine *et al.*, 2005).

1.6.3. Cisplatinum

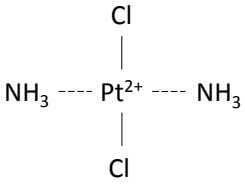

Figure 4. *Chemical structure of cisplatinum (molecular weight = 300.05 g/mol)*

Cisplatinum was accidently discovered by Rosenberg *et al.* (1965) and is now widely used as an anti-cancer drug for treatment of solid tumors (Prestayko *et al.*, 1979; Pabla and Dong, 2008). Cisplatinum is applied intravenously and is taken up by cells via active transporters, human organic transporter 2 (hOCT2) and copper transporter 1 (CTR1), both predominantly present at basolateral side of proximal tubule cells (Ciarimboli *et al.*, 2005; Pabla *et al.*, 2009). The mechanism of action is similar to alkylating antineoplastic agents by binding to DNA, leading to DNA inter- and intrastrand crosslinks, which results in DNA damage and triggers apoptosis, specifically in tumor cells (Siddik, 2003; Wang and Lippard, 2005; Pabla and Dong, 2008). Notably, products of cisplatinum hydration are highly reactive to cellular targets (Long and Repta, 1981; Wang and Lippard, 2005). Further, cisplatinum-glutathione conjugates are formed (Miller *et al.*, 2010). Intracellular cisplatinum and its glutathione conjugates are actively exported by multidrug and toxin extrusion protein 1 (MATE1) and multidrug resistance-associated protein 2 (MRP2) to the apical surface of proximal tubule cells (Nakamura *et al.*, 2010; Wen *et al.*, 2014). Cisplatinum-glutathione conjugates are activated in the kidney to cysteinyl-glycine conjugates and cysteine conjugates by gamma glutamyl transpeptidase and aminodipeptidase, respectively, at the extracellular, apical surface of proximal tubule cells (Townsend *et al.*, 2003). Cysteine conjugates might be transported back into the proximal tubule cells and be converted to reactive thiols (Miller *et al.*, 2010).

Cisplatinum treatment is limited by acquired resistance to cisplatinum and organ toxicity, in particular nephrotoxicity (Arany and Safirstein, 2003; Siddik, 2003; Wang and Lippard, 2005; Pabla and Dong, 2008). Nephrotoxicity is related to cisplatinum bioaccumulation within the kidneys (Stewart *et al.*, 1985; Pabla and Dong, 2008; Miller *et al.*, 2010). Renal tubular cell death might be triggered by tumor necrosis factor alpha (TNF α) production and/or by activation of cell death inducing signaling pathways, e.g. reactive oxygen species, mitogen-activated protein-kinase (MAPK), p53 (Pabla and Dong, 2008).

1.7. Objectives

Due to ethical and economic issues, there is an urgent need to develop alternative toxicity testing methods. The implication of *in vitro* approaches has been accepted for elucidation of pharmacological and/or toxicological mechanisms induced by xenobiotics. In addition, the necessity of *in vitro* kinetics data has been recognized in order to relate the *in vitro* results to *in vivo*. While most *in vitro* data were gained after single administration of a compound, "Predict-IV" intended to get a step closer to the real world scenario by repeated daily exposure. In most cases humans are exposed repeatedly to xenobiotics either accidently or intentionally. Particularly in therapy, long-term treatment with a drug is applied and rarely adverse effects occur after single administration. In some cases drug-induced toxicity is related to bioaccumulation of the parent compound or its metabolite(s) in the target organ, an outcome that cannot be kept *in vitro* after single exposure.

The aim of this thesis was the assessment of kinetics obtained *in vitro* with respect to their relevance *in vivo*. Cells were exposed to a toxic and non-toxic concentration for one and 14 consecutive days to obtain indications regarding a compound's biotransformation and bioaccumulation. Due to known hepato- and neurotoxicity, CsA was administered to *in vitro* models representing the liver and the CNS. In addition, RPTEC/TERT1 cells were treated with the nephrotoxins ADVd and cisplatinum. Therefore, analytical methods were adapted for determination of drug concentrations in vehicle, medium, cells and plastic adsorption samples. Experiments were performed in the "Predict-IV" project and analyses were conducted in-house, if not indicated specifically. Obtained kinetic data were compared across models for one organ, across organs and finally with respective *in vivo* data.

In addition, intracellular CsA uptake mechanism was studied, albeit it is reported to occur by simple passive diffusion. As the purpose of these experiments was not to identify a transport system, by which CsA is actively transported, but to demonstrate whether CsA enters the cells by passive diffusion, transport experiments were performed on a parallel artificial membrane and the human intestinal cell line Caco-2.

2. Material and methods

In experiments performed by project partners (indicated as lab 1 – 7), samples were shipped to the Department of Toxicology at the University of Wuerzburg, where samples were analyzed by mass spectrometry coupled with liquid chromatography (LC-MS/MS).

2.1. Chemicals

Dulbecco's modified eagle medium/nutrient mixture F-12 (DMEM/F12), GlutaMAX™, Williams' E medium, sodium pyruvate, insulin-transferrin-selenium (ITS), gentamycin, Geltrex™, glutamine, phosphate-buffered saline (PBS) and trypsin/ethylenediaminetetraacetic acid (EDTA) were purchased from Life technologies (Darmstadt, Germany; Saint-Aubin and Illkirch, France). Collagenase, insulin, penicillin/streptomycin, dexamethasone, bovine serum albumin, dimethyl sulfoxide (DMSO), Percoll®, 1,2-dioleoyl-*sn*-glycero-3-phosphocholine (DOPC), dodecane, lucifer yellow, adefovir dipivoxil, adefovir, cisplatinum and sodium hydroxid were obtained from Sigma-Aldrich (Taufkirchen and Munich, Germany; St. Quentin-Fallavier, France; Zwijndrecht, Netherlands). Primary neurobasal medium (PNB) and human hepatocyte maintenance medium (HMM) were purchased from Lonza (Verviers, Belgium) and HepaRG Williams' E medium from Laboratories Eurobio (Les Ulis, France). Fetal calf serum (FCS) was from Hyclone® UK Ltd (Cramlington, UK) or Perbio (Brebières, France) and hydrocortisone hemisuccinate was obtained from Upjohn Pharmacia (Guyancourt, France). DNase I and papain were purchased from Roche (Mannheim, Germany).

CsA was obtained from Calbiochem (Darmstadt, Germany), deuterium-labeled CsA (CsA-d_{12}) from Analytical Services International Ltd (London, United Kingdom) and deuterium-labeled adefovir from Toronto Research Chemicals Inc. (Toronto, Canada). For the mobile phase preparation ammonium acetate, formic acid, methanol (HPLC grade), acetonitrile (HPLC grade), water (HPLC grade) and hydrochloric acid (25%) were purchased from Carl Roth (Karlsruhe, Germany).

For Caco-2 cells, DMEM was purchased from PAN Biotech (Aidenbach, Germany) and all other cell culture reagents from PAA (Coelbe, Germany).

For the isolation of primary rat hepatocytes, the liver perfusion, liver digest and hepatocyte wash buffer were prepared in-house using chemicals purchased from Merck,

Applichem (Darmstadt, Germany), Roche (Mannheim, Germany) and Sigma (Steinheim, Germany).

For the isolation of the primary human hepatocytes (PHH), liver perfusion and liver digestion buffer were prepared in-house with chemicals from Sigma (St. Quentin-Fallavier, France). Wash buffer was HBSS supplemented with 10% FCS purchased from Life technologies (Illkirch, France).

2.2. *In vitro* systems and cell culture

2.2.1. Primary rat hepatocytes (samples derived from lab 1)

Using a two-step liver perfusion method according to Seglen (1976) primary rat hepatocytes were isolated from 12-16 weeks old male Wistar rats (280-330 g) and were cultured in a collagen/collagen sandwich configuration using rat tail collagen type I (Tuschl *et al.*, 2009). Cells were seeded at a density of 0.25 x 10^6 cells/well in 24-well plates for concentration-range experiments and at a density of 1.5 x 10^6 cells/well in 6-well plates for kinetic experiments. The cell seeding medium consisted of DMEM/F12 supplemented with 10% FCS, 100 units/mL penicillin, 100 µg/mL streptomycin, 1 mM sodium pyruvate and 5 µg/mL human recombinant insulin. The cell culture medium consisted of DMEM/F12 GlutaMAX™ with 100 units penicillin, 100 µg/mL streptomycin, 1mM sodium pyruvate, 17.2 mM insulin, 0.7 mM transferrin, 0.4 µM sodium selenite, 100 nM dexamethasone and 0.44 mg/mL bovine serum albumin. Experiments were performed three days after cell seeding.

2.2.2. Primary human hepatocytes (samples derived from lab 2)

With the permission of the national ethics committees and regulatory authorities, primary human hepatocytes were extracted from human liver tissue obtained from liver resections of patients for therapy of hepatic tumors. 20-100 g liver tissue from the safety margin near the tumor was removed and a two-step liver perfusion method according to Alexandre and LeCluyse (2010) was applied for isolation of hepatocytes. Information on patients and determined CYP activities are summarized in Table 2. Preparations with more than 70% viability were used for further experiments. Cells were seeded into collagen I coated (Biocoat®, Dutscher, France) 6-well plates at a density of 2 x 10^6 cells/well in Williams' E medium supplemented with 10% FCS, 4 µg/mL insulin, 1 µM dexamethasone and antibiotics (penicillin/streptomycin or gentamycin). The monolayer was cultured overnight, covered afterwards with 350 µg/mL Geltrex™ in

seeding medium without FCS and cultured for further 24 h. The culture medium consisted of Hepatocyte Maintenance Medium (HMM) supplemented with 1% ITS, 100 nM dexamethasone and antibiotics. A new overlay with Geltrex™ (350 µg/mL) was performed every three to four days and cell culture medium was refreshed every day. Experiments started two days after seeding.

Table 2. *Characteristics of human donors used for isolation of primary hepatocytes (gender, age, pathology). CYP activities were determined in Geltrex™ coated PHH by adding substrates as cocktail for determination of CYP2B6 (100 µM bupropion), CYP2C9 (10 µM diclofenac), CYP2D6 (10 µM bufuralol) and CYP3A4/5 (3 µM midazolam) activity. Specific metabolites were quantified by LC-MS/MS (hydroxy-bupropion for CYP2B6, 4-hydroxy-diclofenac for CYP2C9, hydroxyl-bufuralol for CYP2D6 and 1'-hydroxymidazolam for CYP3A4/5) (Alexandre et al., 2012).*

Donor	Gender	Age	Pathology	CYP activities [a]			
				2B6	2C9	2D6	3A4/5
PHH I	Male	42	Alveolar hydatid disease	Low	Low	Low	Low
PHH II	Male	75	Hepatic Tumor	High	High	Low	High
PHH III	Male	63	Hydatic cyst	High	High	Medium	Low

[a] *Enzyme activity was determined by project participant and categorized in "low", "medium" and "high" enzyme activity based on historical in-house data (number of previously tested donors: n = 64 for CYP2B6, CYP2C9 and CYP3A4/5; n = 38 for CYP2D6).*

2.2.3. HepaRG cells (samples derived from lab 3)

The human hepatoma cell line HepaRG was cultured in Williams' E medium supplemented with 10% FCS, 2 mM glutamine, 100 units/mL penicillin, 100 µg/mL streptomycin and 50 µM hydrocortisone hemisuccinate (Josse *et al.*, 2008). HepaRG cells were passaged every second week by trypsinization. Cells were seeded in 6-well plates at a density of 2.5×10^5 cells/well and medium was refreshed twice a week. After 14 days of culture, 2% DMSO was added to the cell culture medium to initiate cell differentiation, where cultures contained hepatocyte-like and primitive biliary cells in a ratio 1:1 after two weeks. Two days before start of experiments, cell culture medium was refreshed containing 2% FBS and 1% DMSO. Experiments started four weeks after seeding.

2.2.4. Primary neuronal mouse cells (samples derived from lab 4)

Primary frontal cortex cultures were derived from dissociated embryonic frontal cortex tissue from NMRI mice (Charles River, Sulzfeld, Germany) on day 16. The culture was processed according to Ransom et al (1977). The method was modified by the usage of

DNase I (8000 units/mL) and papain (10 U/mL) for enzymatic tissue dissociation (Huettner and Baughman, 1986). Cells were seeded at a density of 1 x 10^6 cells/well in primary neurobasal medium (PNB) and incubated under defined conditions (37°C, 5% CO_2; Binder, Tuttlingen Germany). The cell culture networks, formed from a mixture of different types of neurons and glial cells, can be cultured for several months due to their stability by co-cultivation (Gramowski *et al.*, 2006). Glial cells were allowed to proliferate for 3 to 5 days after seeding. After reaching 80% confluency, growth of glial cells was stopped by 5 fluoro-2´-deoxyuridine (25 µM). Serum-free cell culture medium was refreshed three times a week. Experiments started 28 days after seeding.

2.2.5. Primary aggregating rat brain cell cultures (samples derived from lab 5)

The aggregating rat brain cultures were prepared from 16-day old Sprague-Dawley rat embryos (Janvier, St Berthevin, France) as described by Honegger *et al.* (2011). Brains of embryos were dissected and dissociated to single cell suspension by sequential passage through nylon sieves of 200 µm and 100 µm pore sizes (Sefar, Heiden, Switzerland). Cells were washed by centrifugation, re-suspended in cold serum-free culture medium (modified DMEM) and incubated in culture flasks (modified Erlenmeyer flasks). The spontaneously generated three-dimensional cultures were maintained as suspension culture under constant gyratory agitation (80 rpm) at 37°C in an atmosphere of 10% CO_2 and 90% humidified air. Culture medium was replenished with fresh medium every third day for two weeks by exchanging 5 mL (of a total of 8 mL per flask). After 14 days culture medium was replenished every second day. The repeated exposure experiments started 18 days after seeding.

2.2.6. Renal proximal tubule epithelial cell (RPTEC/TERT1) (samples derived from lab 6 and lab 7)

Renal proximal tubules epithelial cells (RPTEC) immortalized by Telomerase Reverse Transcriptase 1 (TERT1) transfection were obtained from Evercyte GmbH, Vienna, and cultured in DMEM/Ham's F-12 (1:1) nutrient mix supplemented with 2 mM glutamax, 5 µg/mL insulin, 5 µg/mL transferrin and 5 ng/mL sodium selenite, 100 U/ml penicillin and 100 µg/mL streptomycin, 10 ng/mL epithelial growth factor and 36 ng/mL hydrocortisone. Cell culture medium was refreshed every second day and cells were split 1:4 near or at confluency by trypsinization. For experiments, RPTEC/TERT1 cells were seeded at a density of 1 x 10^6 cells/well into 0.2 µm pore size, 25 mm diameter

aluminum oxide 6-well filters (apical) (Nunc) and blank cell culture medium was added to the bottom well (basolateral). Experiments started ten days after reaching confluency.

2.2.7. Human intestinal cell line (Caco-2 cells)

The human intestinal cell line Caco-2 was cultured in DMEM supplemented with 2 mM L-glutamine, 1 x nonessential amino acids, 1 mM sodium pyruvate, 100 U/mL penicillin, 100 µg/mL streptomycin and 10% FCS. Cell culture medium was refreshed twice a week and Caco-2 cells were split 1:5 by trypsinization after reaching 70 to 85% confluency. For transport experiments cells were seeded at a density of 3×10^5 cells/well into 12-well polyethylene terephthalate filter inserts (apical) (Thinserts, 0.4 µm pore size, translucent; Greiner Bio-One) and blank cell culture medium was added to the bottom well (basolateral). After 2 weeks of cell culture FCS was reduced from 10% to 5% and after three weeks to 0% FCS. Experiments started 21 days after seeding.

2.3. Experimental design

2.3.1. Kinetic experiments

In order to investigate the kinetic profile of a drug at a toxic and non-toxic concentration and to study the kinetic behavior after repeated exposure, cells were treated daily with a high and low drug concentration for 14 days. In concentration-range experiments conducted previously, the 10% cytotoxic concentration (TC_{10}) and a non-toxic concentration were determined specifically for each *in vitro* system and drug. Due to its lipophilic character, CsA was dissolved in DMSO and diluted in cell culture medium. The determined CsA treatment concentrations and DMSO contents are listed in Table 3.

Table 3. *Specific treatment volumes, final DMSO content and CsA treatment concentrations in specific media for the investigated in vitro models*

***In vitro* system**	**Treatment volumes [mL]**	**DMSO content [%]**	**CsA low concentration [µM]**	**CsA high concentration [µM]**
PRH	1.5	0.2	0.25	2.5
PHH	2	0.2	0.7	7
HepaRG	2	1	0.5	5
3D model	8	0.05	0.2	1
2D model	3	1	0.1	2

Due to the hydrophilic character of ADVd, the substance was dissolved in water containing 0.1 M sodium hydroxide reaching a final concentration of 9.9 mM and was further diluted in RPTECT/TERT1 medium. Prior to cell exposure, vehicle solutions were adjusted to the pH of 7.5. Cells were treated with 2.5 µM (low concentration) and 8 µM (high concentration) ADVd by adding 1 mL and 2 mL to the apical and basolateral side, respectively.

Cisplatinum was dissolved in RPTEC/TERT1 medium reaching a final concentration of 1 mM. Prior to treatment the stock solution was diluted in medium. Cells were treated with 0.5 µM (low concentration) and 2 µM (high concentration) cisplatinum, where 1 mL was added to the apical and 2 mL was applied from the basolateral side.

Samples from the stock and vehicle solutions were taken, in order to determine the actual amount of the drug given to cells. The determined treatment concentrations were used for further calculations.

Hepatic and RPTEC/TERT1 cells were treated daily for 14 days and samples from the drug containing cell culture media and cell lysates were generated at five different time points (Table 4) on the first day (day 0) and the last treatment day (day 13). Brain cell cultures were treated every second day for up to 13 days (primary aggregating rat brain cells) or 14 days (primary neuronal mouse cells). Simultaneously, plastic adsorption samples were taken in order to determine the drug amount adsorbed to plastic of the well walls.

Table 4. *Chosen sampling time points on the first and last treatment day and number of performed biological replicates for the in vitro models.*

***In vitro* system**	**Sampling time points [hrs]**	**Biological replicates**
PRH	1, 2, 4, 8, 24	1
	0.03, 0.5, 1, 3, 24	2
PHH	0.03, 0.5, 1, 3, 24	3
HepaRG	1, 2, 4, 8, 24	3
2D	0.5, 1, 3, 6, 24	4
3D	0.5, 1, 3, 6, 24	3
RPTEC/TERT1	0.5, 1, 3, 6, 24	3

In addition, medium samples were collected after treatment for 24 h on day 2, 4, 6 and 9.

Samples were generated by transferring the cell culture medium quantitatively to LoBind tubes (Eppendorf, Hamburg, Germany). For experiments on RPTEC/TERT1 cells, the medium was collected separately from the apical and basolateral compartment. The remaining cells were washed 2 to 3 times with PBS.

The sandwich cultures, PRH and PHH, were scraped and transferred into LoBind tubes. After washing the wells with 0.25 mL of methanol and transferring the methanol quantitatively to the same tube, samples were in-probe sonicated and filled to 1 mL with methanol. HepaRG cells were scraped in 0.2 mL of PBS and transferred into a glass vial containing 0.6 mL methanol. Wells were washed with another 0.2 mL of PBS, which was also transferred to the same glass vial and sonicated. Cells from the 2D model were scraped in 0.25 mL of methanol, transferred to a glass vial and rinsed with further 0.1 mL of methanol, while to cells of the floating 3D model 1 mL of methanol was added and subsequently transferred to LoBind tubes. RPTEC/TERT1 cells were scraped in 1 mL of methanol from the filters, transferred to LoBind tubes and in-probe sonicated. The aluminum oxide filter was removed and the plastic structure was put back into the original well.

For plastic adsorption sampling, wells were washed twice with PBS. Subsequently 2 mL of methanol were added to each well for PHH, HepaRG and RPTECT/TERT1 cells, 1.5 mL for PRH and the 2D model. The methanol concentrations were chosen based on the volume of medium during experiments, in order to reach the same filling level. Plates were incubated under gentle shaking at room temperature for 2 h and afterwards samples were transferred to LoBind tubes. No plastic adsorption samples were generated for the 3D model as cells were cultured in glass flasks.

In order to investigate the potential of CsA trapping to the sandwich layers, so-called blank studies were performed for PRH and PHH. Therefore, blank wells and wells coated with the specific sandwich layers without cells were incubated with CsA. CsA containing medium was refreshed every day for 14 days. The low (025 µM) and high (2.5 µM) CsA concentration were used for PRH and only the high (7 µM) CsA concentration for PHH. Samples were taken as described above after 2 min and 24 h on the first (day 0) and the last (day 13) treatment day.

All samples were stored at -80°C until completion of the biological replicates. For PRH, HepaRG cells and the 3D model, three biological replicates were performed consisting of

two technical replicates per biological replicate. For PHH and RPTEC/TERT1 cells three biological replicates were performed consisting of one technical replicate. Further, the biological replicates for RPTEC/TERT1 cells were performed in two different laboratories. Four biological replicates were performed for the 2D model each consisting of one technical replicate.

2.3.2. Cyclosporine A - Transport experiments (performed in-house)

Experiments were performed in triplicates and for each experiment corresponding controls were generated by using medium containing 0.1% DMSO.

Caco-2 cells

The test substance CsA was dissolved in DMSO (1 mM and 10 mM) and diluted in medium to final concentrations of 1 µM and 10 µM with 0.1 % DMSO content in vehicles.

The transport of CsA was tested in both directions apical-to-basolateral (AB) and basolateral-to-apical (BA). Therefore, CsA treatment solutions were added either to the apical (0.5 mL) or to the basolateral side (1.5 mL), i.e. donor well, while the corresponding opposite sides were filled with medium containing 0.1% DMSO, i.e. acceptor well. An aliquot of the treatment solutions was taken for determination of the actual CsA amount given to cells.

Aliquots (50% of total volume) were taken from the acceptor well and were replaced by medium containing 0.1% DMSO after 30 min and 60 min of incubation and the incubation was terminated after 3 h. Cell culture medium was collected separately from both donor and acceptor wells into glass vials.

In order to investigate the cell integrity of the cell monolayer after exposure to CsA a marker, lucifer yellow, was used prior to cell lysis. Hereto, cells were washed with PBS and cell integrity was determined as described by Broeders *et al.* (2012). 0.5 mL lucifer yellow dissolved in medium (0.2 mM) was added to each well from the apical side and blank medium from the basolateral side. After 1 h, aliquots (0.1 mL) were taken from the basolateral compartments, transferred into a 96-well plate and fluorescence was measured at 485 nm (excitation) and 535 nm (emission) using the Mithras LB 940 Multimode microplate Reader (Berthold Technologies, Bad Wildbad, Germany). Medium was set as blank reference and 0.2 mM lucifer yellow treatment solution in medium as 100%.

In order to study the CsA distribution and biotransformation, the CsA content was determined in cells and adsorbed to the plastic of the well walls. For this purpose, after removal of the cell culture medium, cells were washed with PBS and 0.1 mL trypsin was added to each well for cell harvesting. Samples were transferred to glass vials. Wells were washed with 0.4 mL methanol and added to the same vials. Afterwards, 0.5 mL and 1.5 mL methanol were added to the apical and basolateral side, respectively. Plates were covered with parafilm and shaken gently at room temperature. After 1 h, samples from the apical and basolateral compartment of one well were pooled. All samples were stored at -20°C until LC-MS/MS quantification.

The apparent permeability coefficient (P_{app}) was calculated according to Broeders *et al.* (2012):

$$P_{app} = \frac{\Delta F_{(cum)}}{\Delta t} \times \mathrm{A}^{-1} \times V_D \qquad \text{(Eq. 5)}$$

$\Delta F_{(cum)}/ \Delta t$ is the slope of the graphs representing the cumulative CsA fraction transported over time determined by GraphPad Prism 6.01, A [cm^2] is the filter insert area (i.e. 1.131 cm^2) and V_D is the CsA solution volume [cm^3] filled into the donor well (apical: 0.5 cm^3; basolateral: 1.5 cm^3).

$F_{(cum)}$ is the cumulative fraction transported [$pmol/cm^3$] and was determined as:

$$F_{(cum)} = \sum \frac{\left\lfloor C_{A(TPx)} - f \times C_{A(TPx-1)} \right\rfloor \times V_A}{C_D \times V_D} \qquad \text{(Eq. 6)}$$

C_D and C_A are the measured CsA concentrations [$pmol/cm^3$] at each time point (TP_X) in the donor and acceptor well, respectively; V_A is the volume [cm^3] of medium in the acceptor well and f is the replacement factor and was calculated as:

$$f = 1 - \frac{V_S}{V_A} \qquad \text{(Eq. 7)}$$

V_S is the volume of the taken sample.

<u>Parallel artificial membrane permeability assay (PAMPA)</u>

1,2-dioleoyl-*sn*-glycero-3-phosphocholine (DOPC) was dissolved in dodecan to reach a final concentration of 1 mg/mL. After adding 0.05 mL of the 0.1% DOPC solution to the

filter inserts, plates were shaken for 5 min at room temperature. Passive diffusion was tested from the apical to basolateral side. Therefore, CsA treatment solutions were added to the apical and blank medium containing 0.1% DMSO to the basolateral compartments. Aliquots (0.75 mL) were taken from the acceptor well and replaced by fresh medium containing 0.1% DMSO after 30 min incubation. The incubation was terminated after 3 h and samples were taken separately from the donor and acceptor well. Inserts were washed with PBS. The integrity of the parallel artificial membrane was tested by lucifer yellow and plastic adsorption samples were taken as described above.

In order to investigate the effect of the polyethylene terephthalate filter insert on CsA diffusion, the same experiment was performed without DOPC layer.

As the experiments were not performed under sink conditions and also the effect of mass loss has to be considered, P_{app} was calculated with the modified "two-way flux" equation according to Liu et al. (2003):

$$P_{app} = -2.303 \times \frac{V_A V_D}{V_A + V_D \times A \times t} \times \log_{10}\left(1 - \frac{V_A + V_D}{V_D \times S} \times \frac{C_{A(t)}}{C_{D(0)}}\right) \quad \text{(Eq. 8)}$$

S (fraction of sample remaining in the wells) was determined as:

$$S = \frac{V_A}{V_D} \times \frac{C_{A(t)}}{C_{D(0)}} + \frac{C_{D(t)}}{C_{D(0)}} \quad \text{(Eq. 9)}$$

2.3.3. Adefovir dipivoxil stability

For stability tests, ADVd was dissolved in water (0.5 mM). Further, ADVd was diluted in RPTEC/TERT1 cell culture medium yielding the low (2.5 µM) and high (8 µM) treatment concentration. ADVd solutions were incubated without cells at 37°C for 24 h and aliquots were taken after 30 min, 1 h, 3 h and 24 h for LC-MS/MS analyses.

2.4. Sample preparation

2.4.1. Cyclosporine A

Stock solutions of the reference substance CsA and the internal standard CsA-d_{12} were prepared yielding 0.1 mM and 0.823 µM, respectively, in methanol. CsA was further diluted in methanol for calibration curve standards (Table 5). The working solution of the internal standard CsA-d_{12} contained 25 nM in methanol. Three independent calibration curves were prepared per analysis batch.

For CsA quantification in the specific culture media, 0.05 mL aliquots of the calibration curve standards were evaporated at room temperature using the Heraeus Instruments vacuum centrifuge (Osterode, Germany) and were dissolved in 0.05 mL of the corresponding medium. 0.05 mL of the sample was placed in a 1.5 mL LoBind tube. After adding 0.15 mL of the 25 nM CsA-d_{12} working solution, samples were vortexed for 30 seconds and centrifuged at 21,380 x *g* and 4 °C for 15 min. Aliquots (0.1 mL) of the clear supernatant were transferred to 2 mL auto sampler vials with 0.3 mL limited volume inserts and closed with silicone/polytetrafluoroethylene septa caps (Brown Chromatography Supplies, Wertheim, Germany).

Table 5. *Calibration standard concentrations used for the quantification of CsA.*

Calibration standard	Cyclosporine A concentration	
	[nM]	[µg/L]
1	0	0
2	10	12
3	13	15
4	25	30
5	50	60
6	100	120
7	250	301
8	500	601
9	1,000	1,203
10	1,500	1,804
11	2,000	2,405
12	2,500	3,007

2.4.2. Adefovir dipivoxil and adefovir in medium

The reference substances ADVd and ADV were dissolved in water yielding final concentrations of 0.5 mM and 1 mM, respectively. Working solutions (0.1, 0.01 and 0.001 mM) of ADVd and ADV were prepared in water prior to analysis. The internal standard acyclovir was dissolved in water (0.5 mM) and stored at -20°C. Working solutions were prepared prior to analysis. The acyclovir stock solution was diluted to 1 µM acyclovir in water containing 0.1% formic acid for determination of ADVd and ADV in medium.

For calibrations curves working solutions of ADVd and ADV were diluted in medium (Table 6). Three independent calibration curves were prepared per analysis batch.

Sample preparation was performed by placing 0.05 mL of the sample in an Eppendorf tube and 0.05 mL of 1 µM acyclovir solution was added and vortexed briefly. Medium samples were centrifuged at 21,380 x *g* and 20 °C for 10 min and transferred quantitatively to auto sampler vials with 0.3 mL limited volume inserts and closed with silicone/ polytetrafluoroethylene septa caps.

Table 6. *Calibration standard concentrations used for the quantification of adefovir dipivoxil and adefovir.*

Calibration standard	Adefovir dipivoxil concentration		Adefovir concentration	
	[nM]	[µg/L]	[nM]	[µg/L]
1	0	0	0	0
2	20	10	20	3
3	40	20	40	4
4	60	30	60	8
5	80	40	80	11
6	100	50	100	14
7	200	100	200	27
8	400	201	400	55
9	-	-	800	110
10	-	-	1,000	137
11	-	-	2,000	274

2.4.3. Adefovir dipivoxil hydrolysis to adefovir and quantification of adefovir

Three independent calibration curves were prepared for ADV quantification. Hence, working solutions of ADV in water were diluted in cell culture medium or methanol for calibrations standards (Table 7).

Cell culture medium

Acyclovir was used as internal standard for ADV quantification in medium. The acyclovir stock solution (0.5 mM in water) was diluted freshly in 0.5 M sodium hydroxid solution to a working concentration of 0.02 mM.

Aliquots (5 µL) of the samples were placed in an Eppendorf tube, 5 µL of 0.02 mM acyclovir was added and incubated at 60°C for 10 min in order to catalyze ADVd hydrolysis. 0.09 mL water (HPLC grade) was added after incubation at room temperature for 5 min. Samples were vortexed, centrifuged at 21,380 x *g* and 22 °C for 10 min, subsequently transferred to auto sampler vials with 0.3 mL limited volume inserts and closed with silicone/polytetrafluoroethylene septa caps.

In order to protect the analytical column against overload, high concentration samples were diluted in a ratio 1:1 with medium as a first sample preparation step.

Cell lysate and plastic adsorption samples (methanol)

Deuterium labeled adefovir (ADV-d_4), the internal standard for ADV quantification in cell lysate and plastic adsorption samples, was dissolved in water (0.05 mM) and stored at -20°C. Prior to measurements, working solutions were prepared containing 1 µM ADV-d_4 in methanol.

Aliquots (0.1 mL) of the samples were placed in Eppendorf tubes. After adding the internal standard (0.05 mL), samples were vortexed and subsequently evaporated to dryness using a vacuum centrifuge at room temperature. Samples were reconstituted in 0.05 mL water containing 0.1% formic acid, vortexed and after centrifugation (21,380 x *g*, 20 °C, 10 min) transferred to auto sampler vials with 0.3 mL limited volume inserts and closed with silicone/polytetrafluoroethylene septa caps.

Table 7. *Calibration standard concentrations used for the quantification of ADV in cell culture medium and methanol.*

Calibration standard	Adefovir concentration in cell culture medium		Adefovir concentration in methanol	
	[µM]	[mg/L]	[nM]	[µg/L]
1	0	0	0	0
2	0.4	0.1	20	5.5
3	0.8	0.2	40	10.9
4	1.2	0.3	60	16.4
5	1.6	0.4	80	21.9
6	2	0.6	100	27.3
7	2.4	0.7	120	32.8
8	2.8	0.8	140	38.3
9	4	1.1	200	54.6
10	8	2.2	400	109.3
11	10	2.7	800	218.6

2.4.4. Cisplatinum

Quantitative analysis was performed by inductively coupled plasma mass spectrometry (ICP-MS) at the contract laboratory Mueller-BBM GmbH (Zirndorf, Germany).

Quantification by ICP-MS leads to partial element breakdown of organic structures and inorganic compounds are detected afterwards. In order to release quantitatively platinum from binding to organic structures, aqua regia was added to all samples. Aqua regia is the mixture of hydrochloric acid and nitric acid in the ratio 3:1. Cell lysate and plastic adsorption samples were decomposed additionally by microwave heating at the contract laboratory. Due to shipment regulations in Germany, it is not allowed to send aqua regia albeit at limited quantities. Therefore, three parts hydrochloride acid were added to the samples prior to shipment.

For determination of the cisplatinum amount in medium, 200 µL of the samples were placed in Eppendorf tubes and 600 µL hydrochloric acid were added. For cell lysate and plastic adsorption samples, methanol was evaporated quantitatively in a vacuum centrifuge at 40°C. Samples were re-dissolved in 200 µL water (bidest), 600 µl

concentrated hydrochloric acid were added and samples were shipped for measurement.

Further sample preparation (adding of 200 µL nitric acid, microwave heating) and measurements were conducted at the contract laboratory according to DIN EN ISO 17294-2.

The limit of quantification (LOQ) was 5 nM for medium samples and 10 nM for cell lysate and plastic adsorption samples. As cisplatinum contains one platinum atom per molecule, the given concentration of cisplatinum [µM] corresponds to the measured concentration of platinum [µM].

2.5. Quantification by mass spectrometry coupled with liquid chromatography

Device control, data acquisition and analyses were accomplished by the Analyst™ 1.4.1 Software (AB Sciex, Darmstadt, Germany).

2.5.1. Cyclosporine A

A triple stage quadrupole mass spectrometer equipped with a Turbolon®Spray source (API 3000, AB Sciex, Darmstadt, Germany) was used for analyses. The mass spectrometer was coupled to an Agilent 1100 HPLC system consisting of a binary pump system, a vacuum degasser and an autosampler (Waldbrunn, Germany). Chromatographic separation was performed at room temperature on a SymmetryShield™ RP_8 column (2.1 mm x 50 mm, 3.5 µm, 100 Å; Waters GmbH, Eschborn, Germany) coupled to a Sentry™ guard column (2.1 mm x 10 mm, 3.5 µm) using a binary step gradient at a flow rate of 0.3 mL/min with the following gradient: 0 min 30% A, 2 min 30% A, 4 min 0% A, 8 min 0% A, 10 min 30% A and 15 min 30% A. Mobile phases consisted of water containing 0.1% formic acid and 4 mM ammonium acetate (A) and methanol containing 0.1% formic acid (B). The injection volume was set to 0.01 mL and the total analysis time was 15 min. Analytes, CsA and CsA-d_{12}, were detected in positive ion mode at a vaporizer temperature of 400 °C and a Turbolon®Spray voltage of 4 kV using N_2 as nebulizer gas. Spectral data were recorded with N_2 as collision gas (CAD = 4). Data acquisition was performed in the sensitive multiple reaction monitoring mode (MRM) detecting two transitions per analyte. Specific MS parameters are given in Table 8.

Table 8. *LC-MS/MS parameters for MRM detection of CsA and CsA-d_{12}; focusing potential (FP), declustering potential (DP), entrance potential (EP), collision energy (CE), cell exit potential (CXP).*

Compound	Transition [m/z]	FP [V]	DP [V]	EP [V]	CE [V]	CXP [V]	RT [min]
Cyclosporine A	1,220 → 1,203 1,220 → 199	180	36	10	27 103	38 18	6.9
Deuterium-labeled Cyclosporine A	1,232 → 1,215 1,232 → 100	310	66	10	33 12	38 16	6.9

CsA was quantified on the base of calibration curves consisting of known CsA concentrations in the correspondent matrix. The method was linear with coefficient of determination (R^2) values ranging from 0.98 to 0.99. The LOQ and the limit of detection (LOD) were calculated according to DIN 32645 using DINTEST (Institut für Rechtsmedizin und Verkehrsmedizin, Universität Heidelberg, Version 2004 DE) and the accuracy of measured analytical quality controls was determined by Analyst™ 1.4.1 Software (Table 9).

Table 9. *Determined limits of detection (LOD), limits of quantification (LOQ) and accuracy of analytical quality controls for CsA dissolved in the specific cell culture media and methanol.*

Matrix	LOD [nM]	LOQ [nM]	Accuracy of quality controls [%]
Cell culture medium PRH	0.63 ± 0.05	1.93 ± 0.14	83 ± 14
Cell culture medium PHH	0.21 ± 0.00	0.72 ± 0.01	96 ± 11
Cell culture medium HepaRG	0.17 ± 0.00	0.60 ± 0.02	97 ± 10
Cell culture medium 2D	0.16 ± 0.01	0.56 ± 0.06	102 ± 3
Cell culture medium 3D	0.19 ± 0.01	0.65 ± 0.02	109 ± 14
Methanol	0.20 ± 0.01	0.68 ± 0.02	100 ± 10

2.5.2. Adefovir dipivoxil and adefovir

Analyses were performed by a triple stage quadrupole mass spectrometer equipped with a Turbolon®Spray source (API 2000/QTrap, AB Sciex, Darmstadt, Germany) and coupled to an Agilent 1100 HPLC system consisting of a binary pump system, a vacuum degasser and an autosampler (Waldbrunn, Germany). Chromatographic separation was

carried out on a Gemini 5µ C18 110A 150 x 2.0 mm (Phenomenex) with a Gemini C18 guard column (4 x 2mm) at room temperature and a flow rate of 0.240 mL/min by a binary step gradient elution described in the following: 0 min 97% A, 3.8 min 40% A, 6 min 40% A, 7 min 97% A and 12 min 97% A, where mobile phases consisted of 0.1% formic acid in water (A) and 0.1% formic acid in acetonitrile (B). The total analysis time was 12 min and the injection volume was set to 0.01 mL. Acyclovir, ADVd and ADV were detected in positive ion mode at a vaporizer temperature of 400 °C and a Turbolon®Spray voltage of 4 kV using N_2 as nebulizer gas. Spectral data were recorded with N_2 as collision gas (CAD = 4). Data acquisition was performed in the sensitive MRM mode detecting two transitions per analyte. Specific MS parameters are given in Table 10.

Table 10. *LC-MS/MS parameters for MRM detection of ADVd, ADV, ADV-d_4 and acyclovir; declustering potential (DP), entrance potential (EP), collision energy (CE), cell exit potential (CXP).*

Compound	Transition [m/z]	DP [V]	EP [V]	CE [V]	CXP [V]	Retention time [min]
Adefovir dipivoxil	502 → 256	46	9.5	37	6	8.5
	502 → 162			75	4	
Adefovir	274 → 162	66	11	37	4	2.2
	274 → 136			31	4	
Deuterium labeled adefovir	278 → 136	86	8.5	39	4	2.2
	278 → 136			31	4	
Acyclovir	226 → 152	31	9	17	4	2.5
	226 → 135			35		

ADVd and ADV were quantified on the base of calibration curves consisting of known concentrations as a mixture in medium. The method was linear with R^2 values ranging from 0.994 to 0.999 and from 0.996 to 0.999 for ADVd and ADV, respectively. The determined LOD was 7.2 ± 2.4 nM for ADVd and 5.0 ± 3.3 nM for ADV. The determined LOQ was 24.5 ± 7.5 nM for ADVd and 14.9 ± 9.5 nM for ADV. The accuracy of analytical quality controls was 104 ± 11% for ADVd and 103 ± 7% for ADV.

2.5.3. Adefovir dipivoxil hydrolysis to adefovir and quantification of adefovir

Analysis was performed as described in section 2.5.2.

ADV was quantified on the base of calibration curves consisting of known concentrations in medium or methanol. The method was linear with R^2 values ranging from 0.992 to 0.997 for ADV in medium and from 0.993 to 0.996 in methanol. The LOD was 0.16 ± 0.04 µM and the LOQ was 0.53 ± 0.11 µM in medium and determined LOD and LOQ were 5.8 ± 2.1 nM and 19.8 ± 6.8 nM , respectively, in methanol. The accuracy of analytical quality controls was 103 ± 11% in medium and 103 ± 11% in methanol.

2.6. Calculation of kinetic parameters

2.6.1. Mass balance

A mass balance is the sum of a compound recovered in medium, cells and the amount adsorbed to plastic related to the administered compound's amount.

$$mass\ balance = \frac{C_M \times V_M}{C_0 \times V_M} + \frac{C_C \times V_C}{C_0 \times V_M} + \frac{C_P \times V_P}{C_0 \times V_M} \quad \text{(Eq. 10)}$$

C_0, C_M, C_C and C_P are the determined concentrations of a substance in vehicle, medium, cells and plastic adsorption samples, respectively, and V_M, V_C and V_P is the volume of vehicle/medium, cell harvest and plastic adsorption samples, respectively.

2.6.2. Area under the curve and clearance

AUCs for CsA in cells were obtained by GraphPad Prism 5, where the measured CsA concentrations [µM] were plotted versus time. Hence the dimension for AUC is [µM/h]. Clearances were calculated as described in the following:

$$Cl_{in\ vitro} = \frac{C_0 \times V_0}{AUC \times N_{cell}}$$

C_0 is the determined CsA concentration in vehicle [nmol/mL] and V_0 the treatment volume [mL]. N_{cell} represents the seeded cell number and was utilized for $Cl_{in\ vitro}$ calculations on day 0 and day 13 for low concentration treatment as well as on day 0 for high concentration samples. As the high concentration was chosen on the base of causing 10% cytotoxicity after 14 days, the seeded cell number was assumed to be decreased by 10% on day 13.

2.6.3. Scaling to *in vivo*

The clearances determined *in vitro* [mL/h per 10^6 cells] were recalculated to the unit of [L/h] by multiplying with the hepatocellularity (117.5 x 10^6 cells and 108 x 10^6 cells per

g liver for human and rat, respectively) and the liver size (1730 g and 9 g, for human and rat, respectively) (Jamei *et al.*, 2014). The obtained i*n vitro* clearances were scaled to *in vivo* whole-body equivalent as described by Jamei *et al.* (2014)

$$scaled\ \ Cl_{in\ vitro} = \frac{Q_H \times fu_B \times Cl_{in\ vitro}}{Q_H + Cl_{in\ vitro} \times fu_B} \qquad \text{(Eq. 11)}$$

Q_H is the liver portal blood flow being 90 L/h for human and 1.452 L/h for rat. Fu_b (27.21) is the fraction unbound to blood and was calculated by dividing the product of the fraction unbound in plasma (0.037) and the ratio of cells to unbound plasma concentration (1000) by the blood to plasma ratio (1.36). Although these numerical values were estimated for humans, they were assumed to be equal for rats.

3. Results

3.1. Cyclosporine A in hepatic *in vitro* models

Cells of three different hepatic *in vitro* models were exposed to two different CsA concentrations. Treatment concentrations were determined specifically for each system with the tested high concentrations corresponding to TC_{10} and the low, non-toxic concentrations corresponding to $1/10^{th}$ of TC_{10}. Cells were treated daily for up to 14 days. Samples were generated at five different time-points on day 0 and day 13. The determined CsA concentrations in vehicle, media and cells were used to assess the kinetic profile of CsA and to obtain indications regarding CsA biotransformation and bioaccumulation in the different hepatic *in vitro* models. Additionally, in order to investigate the potential CsA trapping to sandwich layers, so-called blank studies were performed for collagen and Geltrex™.

3.1.1. Primary rat hepatocytes (PRH)

CsA concentrations were 0.56 ± 0.01 µM in vehicles for treatment with 0.25 µM CsA in one of three replicates and 0.16 ± 0.01 µM in two of three replicates on day 0. Similar aberrations from the nominal concentrations were observed for 0.25 µM CsA vehicles on day 13, while determined CsA concentrations in vehicles for treatment with 2.5 µM CsA were comparable to the nominal concentration (2.44 µM ± 0.10 µM on day 0 and 2.17 ± 0.07 µM on day 13).

CsA concentrations in medium slowly decreased to 0.18 ± 0.24 µM (day 0) and 0.23 ± 0.27 µM (day 13) after low concentration treatment within 24 h (Figure 5 A and B). Treatment with 2.5 µM CsA also resulted in a CsA decrease in medium within 24 h (0.97 ± 0.45 µM) on day 0 (Figure 5 C), while stable CsA concentrations were quantified ranging from 1.9 to 2.4 µM on day 13 (Figure 5 D). Determination of the CsA contents in cells revealed for both 0.25 µM and 2.5 µM CsA treatment apparent stable CsA levels after 2 min on day 0 (Figure 5 A and C). While no increased CsA levels were determined after repeated exposure to 0.25 µM (Figure 5 B), CsA levels were 4- to 6-fold increased after treatment with 2.5 µM CsA for 14 days (Figure 5 D), suggesting no significant CsA biotransformation in PRH and resulting in CsA bioaccumulation.

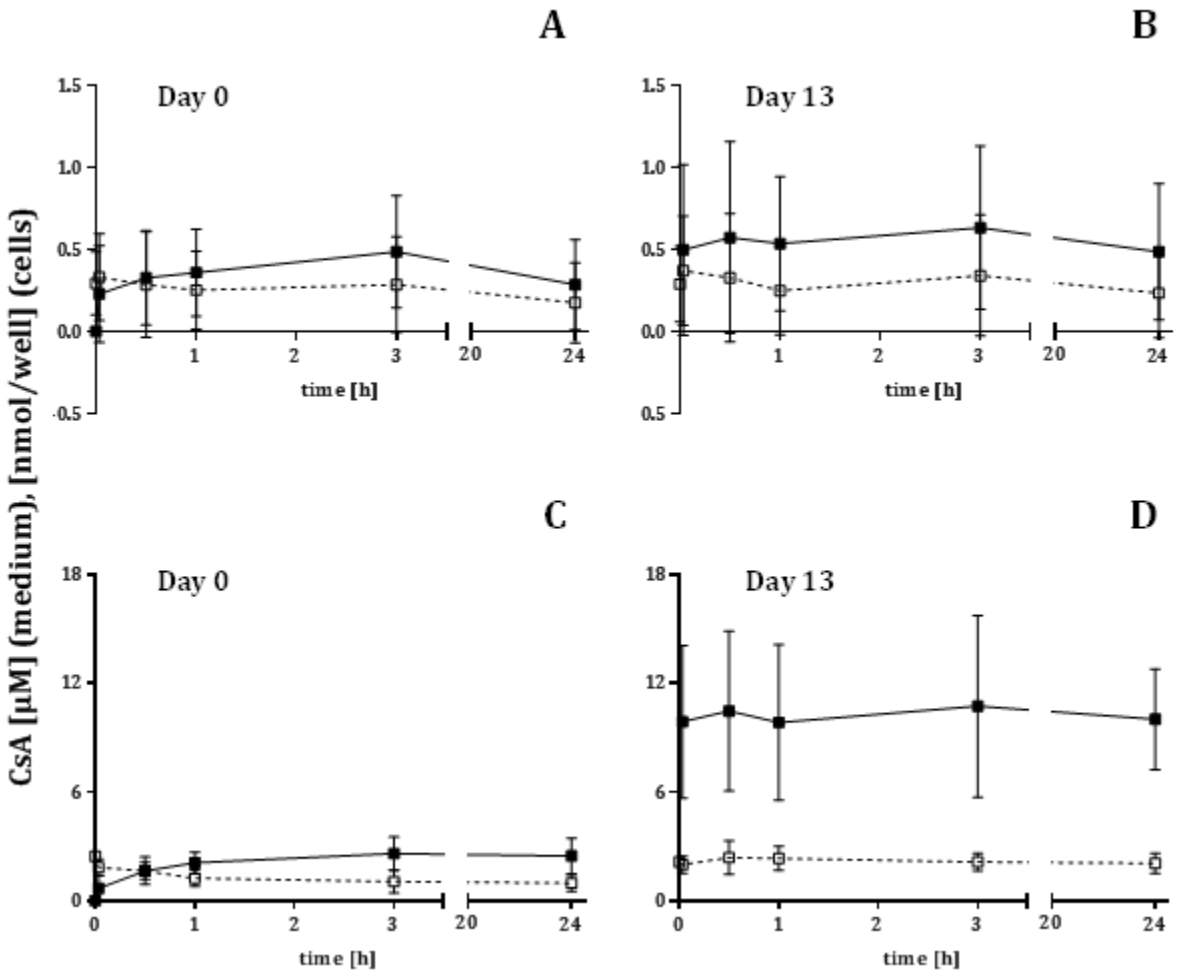

Figure 5. *Extra- and intracellular cyclosporine A concentration-time curves in primary rat hepatocytes. PRH derived from male Wistar rats as described in the method section (2.2.1). CsA concentrations were measured by LC-MS/MS (2.4.1 and 2.5.1) in vehicle (time point 0 min □), medium (□) and cells (■) of PRH after treatment with 0.25 µM (A,B) and 2.5 µM CsA (C,D). Samples were generated after 2 min, 30 min, 1 h, 3 h and 24 h on day 0 (A,C) and day 13 (B,D). Mean (± SD) of two biological replicates is shown for the first (2 min), the second (30 min) and the fourth sampling time point (3 h) after both 0.25 µM and 2.5 µM CsA treatment on day 0 and day 13. Mean (± SD) of three biological replicates is illustrated for remaining sampling time-points.*

The total CsA recovery in medium, cells and the amount adsorbed to plastic after treatment with 0.25 µM CsA shows no statistical significant difference (p value = 0.58; unpaired, two-tailed Student's *t*-test) between day 1 (120.8 ± 140.6%) and day 14 (205.3 ± 200.2%) (Figure 6 A and B). By contrast, 2.5 µM CsA treatment led to significant accumulation (p value = 0.01; unpaired, two-tailed Student's *t*-test) in PRH after 14 days (105.9 ± 42.6% on day 1 and 420.1 ± 109.8% on day 14), with 311.4 ± 86.7% being recovered in cells (Figure 6 C and D).

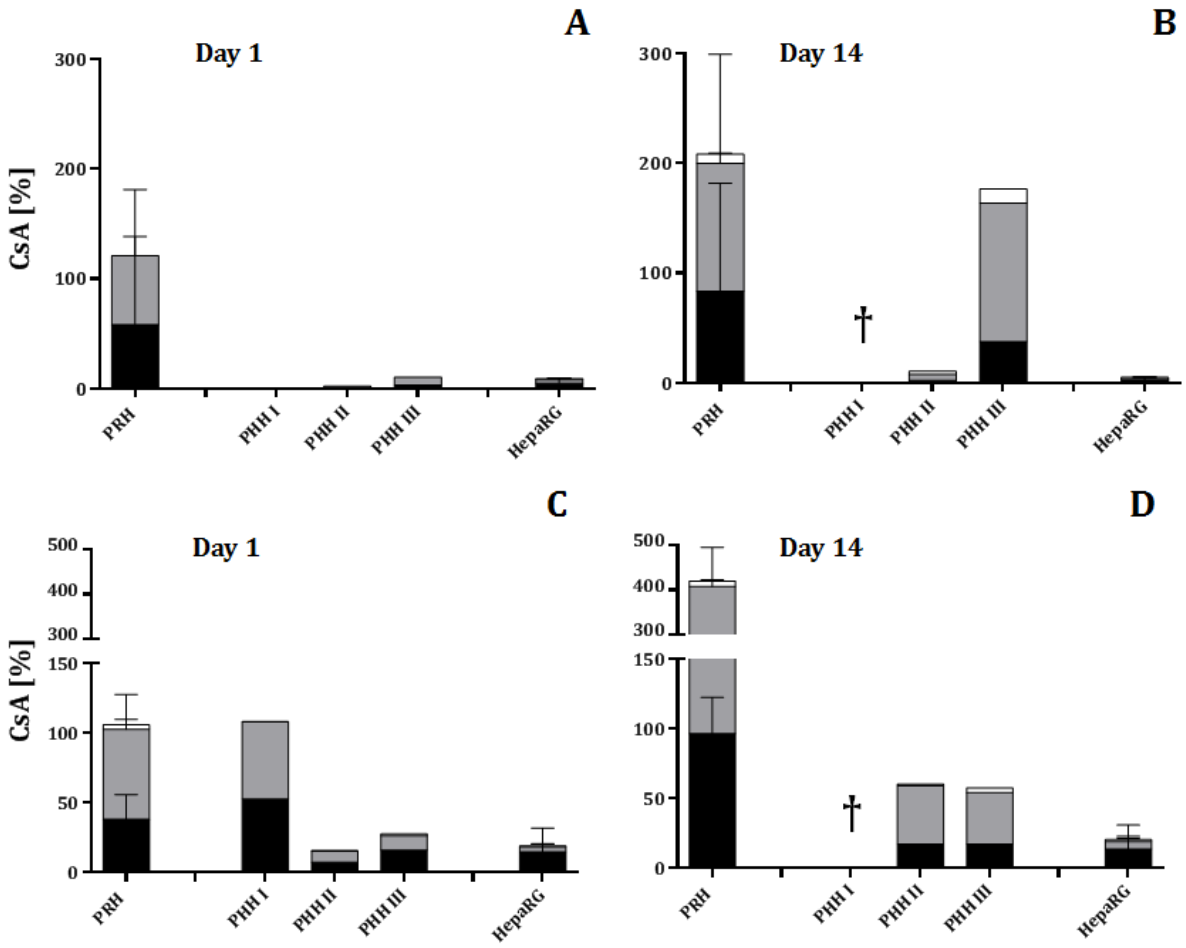

Figure 6. *Cyclosporine A mass balances in three hepatic in vitro models. Measured CsA concentrations in medium (■), cells (▭) and plastic adsorption samples (▭) were normalized to CsA concentrations determined in vehicle as described in 2.6.1. Mass balances were calculated after 1 day (A,C) and 14 days (B,D) of treatment with the respective low (A,B) and high (C,D) CsA concentration. Mean (± SD) of three biological replicates is given for PRH and HepaRG cells. For PHH each replicate is presented separately, while for PHH I mass balances could not be generated after 14 days due to contamination (†).*

Determined CsA amounts in plastic adsorption samples were under the LOQ after exposure to 0.25 µM CsA on day 0, but increased after repeated exposure. Due to strong fluctuations between replicates (0-13 % of the administered CsA amount), the increase was not statistically significant. By contrast, exposure to 2.5 µM CsA revealed quantifiable CsA amounts (1 to 8%) on day 0, increasing statistically significant to 12 ± 3% after 14 days (1 day vs. 14 days: p value = 0.04; unpaired, two-tailed Student's *t*-test). These results indicate that CsA adsorption to the plastic of culture dishes should not be neglected.

In order to investigate the potential of CsA trapping to collagen and therefore to estimate the bias of CsA accumulation in cells, blank studies were performed. Repeated CsA treatment for up to 14 days showed for collagen coated wells no significant CsA trapping to the collagen layers for both 0.25 µM (Figure 7 A) and 2.5 µM CsA (Figure 7 B). On the contrary, at the last sampling time-point CsA showed a high CsA loss for collagen coated wells (38 ± 18% of the administered CsA amount) after incubation with 0.25 µM, which cannot be attributed to biotransformation due to the absence of cells.

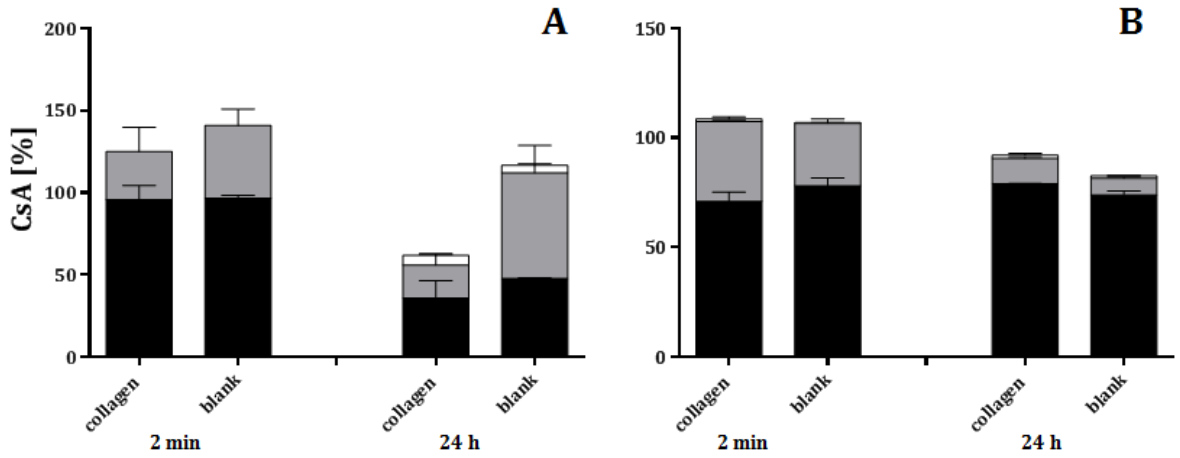

Figure 7. *Cyclosporine A mass balance in PRH blank experiments. Measured CsA concentrations in medium (■), cells (▭) and plastic adsorption samples (▭) were normalized to CsA concentrations determined in vehicle as described in 2.6.1. Culture plates with ("collagen") and without ("blank") sandwich layers were incubated with 0.25 µM (A) and 2.5 µM CsA (B) for up to 14 days. CsA containing medium was refreshed every 24 h and samples were generated after 2 min and 24 h on day 13. Mean (± SD) is given for two technical replicates.*

3.1.2. Primary human hepatocytes (PHH)

For PHH I, approximately 39% (day 0) and 123% (day 13) of the nominal CsA concentration was recovered in low concentration vehicles (0.7 µM). Similar deviations were determined in vehicles for the high (7µM) concentrations (day 0: 62% and day 13: 117%). CsA concentrations in medium decreased slowly under the LOQ within 24 h after treatment with 0.7 µM CsA on day 0 (Figure 8 A). Simultaneously, intracellular CsA levels increased reaching a peak concentration (0.83 nmol/well) after 3 h, followed by a compound decrease within the following 21 h (<LOQ). Similar observations were made for treatment with 7 µM CsA on day 0 (Figure 8 C), with the exception of an increased intracellular CsA level (4.79 nmol/well) after 24 h and CsA concentrations in medium decreasing to a lesser extent (2.3 µM). Repeated exposure did not influence the CsA kinetic profile in medium for both treatment concentrations within 3 h on the last

sampling day (Figure 8 C and D). Nevertheless, the intracellular CsA levels were elevated on day 13 and were found to be in a range from 0.65 to 0.83 nmol/well for 0.7 µM CsA treatment and from 3.14 to 4.70 nmol/well for 7 µM CsA (Figure 8 B and D). While CsA concentrations decreased in medium (0.17 µM) from low concentration samples within 3 h on day 13 (Figure 8 B), stable CsA concentrations (2.0 µM) were reached in high concentration samples within 1 h (Figure 8 D).

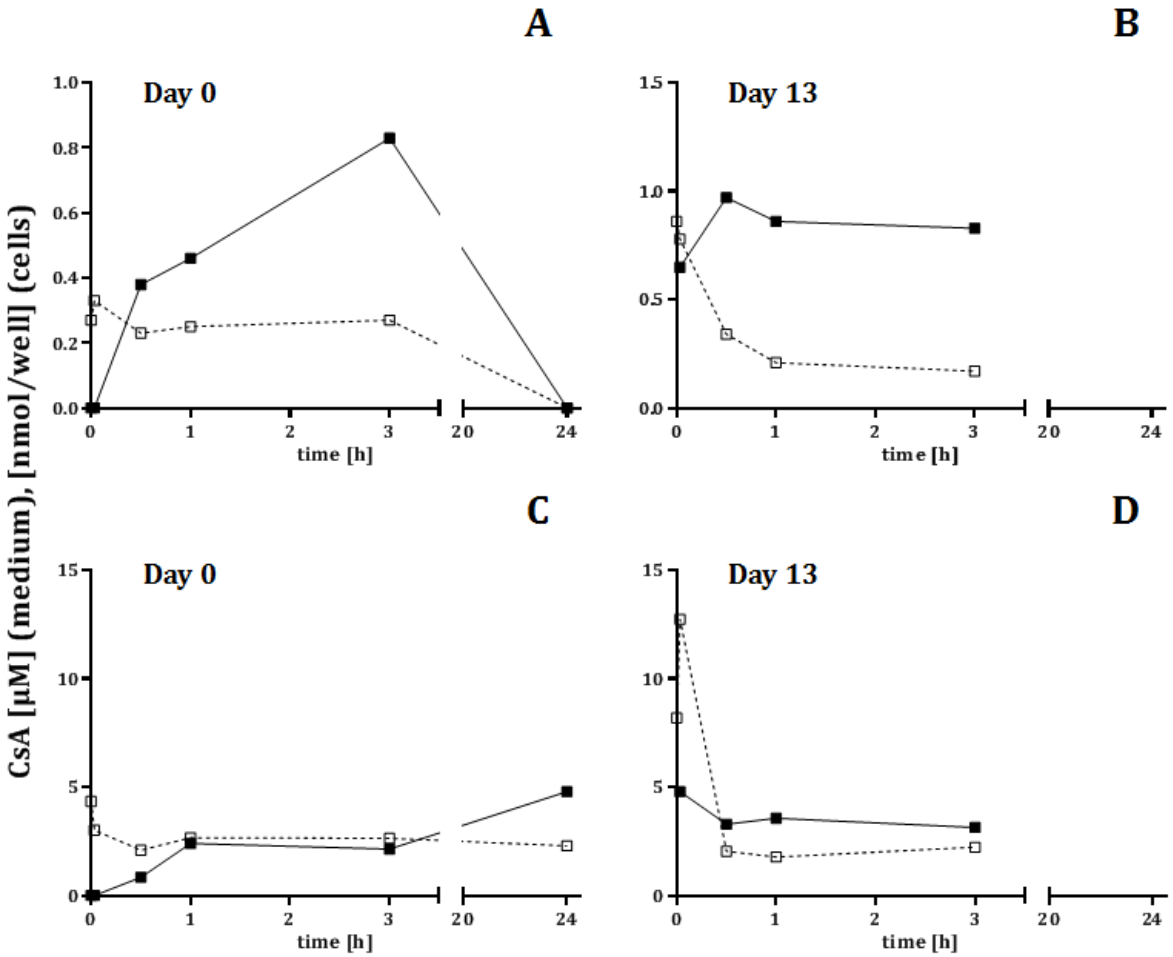

Figure 8. *Extra- and intracellular cyclosporine A concentration-time curves in primary human hepatocytes. PHH I were obtained from a human donor as described in 2.2.2. CsA concentrations were measured by LC-MS/MS (2.4.1 and 2.5.1) in vehicle (time-point 0 min □), medium (□) and cells (■) of PHH I after treatment with 0.7 µM (A,B) and 7 µM CsA (C,D). Samples were generated after 2 min, 30 min, 1 h, 3 h and 24 h on day 0 (A,C) and after 2 min, 30 min, 1 h and 3 h on day 13 (B,D). As data for PHH were not pooled each replicate is illustrated separately, hence, a single data point is plotted for each sampling time-point.*

For both concentration levels, no statement can be made regarding potential CsA bioaccumulation, as no samples were generated due to contamination after 14 days (Figure 6 B and D). Although it seems that CsA bioaccumulation occurs, this might be a

result of treatment with a higher CsA concentration on day 13 than on day 0. The total CsA recovery was 88.4% for the low concentration and 112.0% for the high concentration after 30 min on day 13, indicating that no bioaccumulation occurred.

The amount adsorbed to plastic was <LOQ after treatment with 0.7µM CsA and 0.6 ± 0.3% after exposure to 7 µM CsA on the first day and increased after repeated low and high concentration treatment to 4.7 ± 1.1% and 3.2 ± 1.4%, respectively, which was statistically significant for exposure to 7 µM CsA (for 7 µM day 1 vs. day 14: p value = 0.01; unpaired, two-tailed Student's *t*-test).

For PHH II, similar aberrations from the nominal CsA concentrations were determined in vehicles with 37.6% and 69.9% of the nominal low (0.7 µM) concentration on day 0 and day 13, respectively, and 55.3% and 68.0% of the nominal high (7 µM) CsA concentration. The CsA concentrations measured in medium decreased to <LOQ and 0.29 µM within 24 h after low and high concentration treatment, respectively, following a 1st order kinetics on day 0 (Figure 9 A and C). A similar CsA decrease was observed within 24 h on day 13 (low concentration: 0.01 µM; high concentration: 0.82 µM) (Figure 9 B and D). In cells treated with 0.7 µM the CsA amount increased to a peak concentration (0.37 nmol/well) within 1 h on day 0 and within 3 h on day 13 (Figure 9 A and B). Furthermore, intracellular CsA levels decreased following a 1st order kinetics to 0.01 nmol/well on day 0 and 0.05 nmol/well on day 13. For cells treated with 7 µM CsA the intracellular peak level (2.56 nmol/well) was reached within 3 h on day 0 and decreased to 0.60 nmol/well within the following 21 h (Figure 9 C). Similar observations were made for high concentration treated cells on day 13 (Figure 9 D), albeit intracellular CsA levels were statistically significant higher after repeated exposure (p value = 0.005; unpaired, two-tailed Student's *t*-test). Despite the high intracellular CsA concentrations, the obtained mass balances indicate no remarkable CsA bioaccumulation with the total CsA recovery being 10.6% and 60.3% of the administered low and high CsA amount, respectively, after 14 days (Figure 6 B and D).

Regarding the CsA amount adsorbed to plastic, the obtained results confirmed observations made previously on PHH I. No CsA amount could be quantified in low concentration samples (<LOQ) and 0.4 ± 0.2% of the administered CsA amount was recovered in high concentration samples on day 0. Both increased within 14 days of treatment to 3.4 ± 1.4% of the low and statistically significant to 1.9 ± 0.5% of the high

CsA concentration (for 7 µM day 1 vs. day 14: p value = 0.001; unpaired, two-tailed Student's *t*-test).

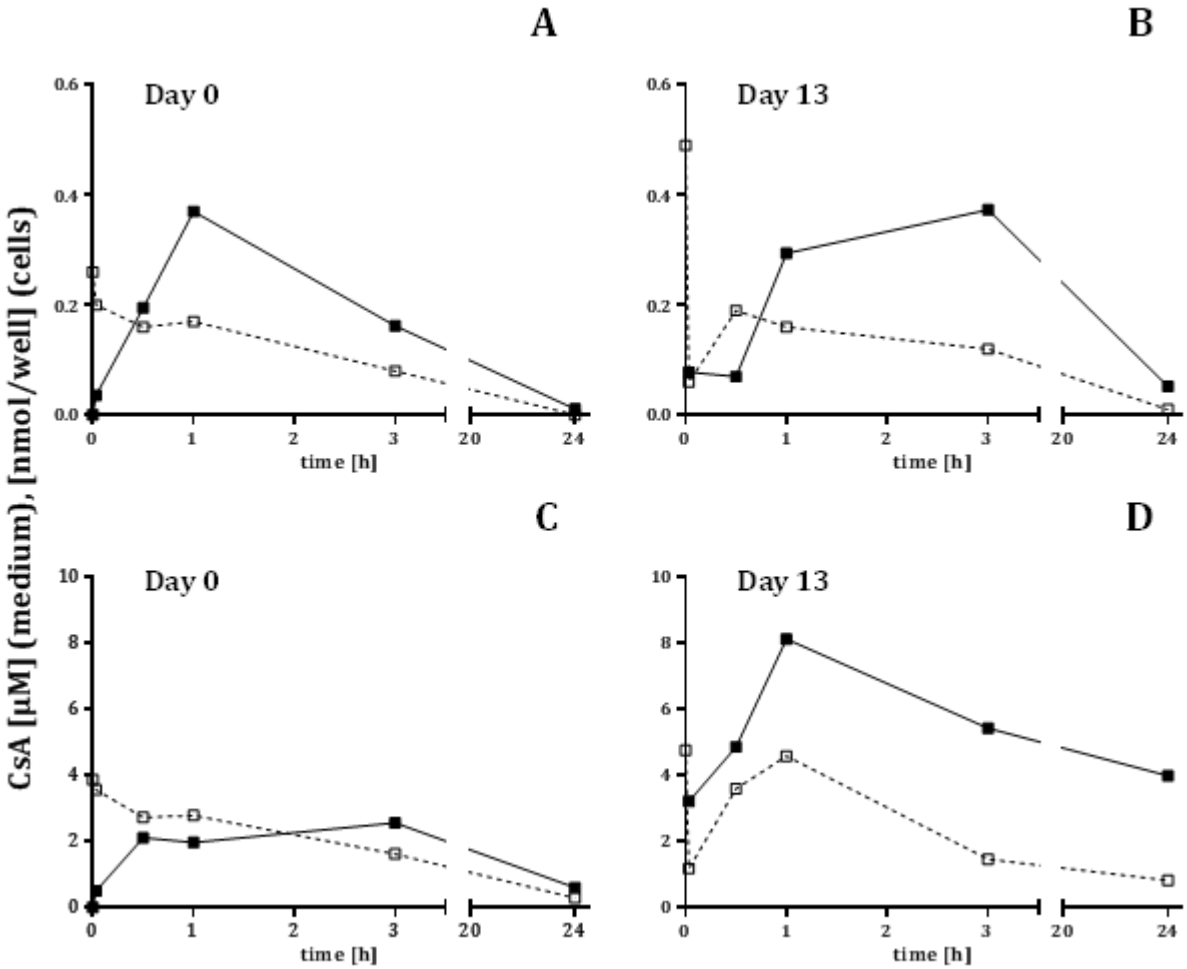

Figure 9. *Extra- and intracellular cyclosporine A concentration-time curves in primary human hepatocytes. PHH II were obtained from a human donor as described in 2.2.2. CsA concentrations were measured by LC-MS/MS (2.4.1 and 2.5.1) in vehicle (time-point 0 min □), medium (□) and cells (■) of PHH II after treatment with 0.7 µM (A,B) and 7 µM CsA (C,D). Samples were generated after 2 min, 30 min, 1 h, 3 h and 24 h on day 0 (A,C) and day 13 (B,D). As data for PHH were not pooled each replicate is illustrated separately, hence, a single data point is plotted for each sampling time-point.*

CsA concentrations in vehicle were lower than the nominal concentrations for PHH III. For 0.7 µM CsA, the recovery in vehicles was 66.6% on day 0 and 59.6% on day 13. For 7 µM CsA, the determined amounts were 85.2% and 56.3% on day 0 and day 13, respectively.

Determination of CsA concentrations in medium revealed a time-dependent decrease to 0.02 µM and 0.95 µM after low and high concentration treatment, respectively, within 24 h on day 0 (Figure 10 A and C) and to 0.16 µM (low concentration) and 0.68 µM (high

concentration) on day 13 (Figure 10 B and D). Intracellular peak levels were reached within 1 h after low concentration treatment (0.54 nmol/well) and decreased to 0.06 nmol/well after 24 h (Figure 10 A). Similar results were obtained after high concentration treatment with the peak level (3.66 nmol/well) being reached after 3 h and a decrease to 1.22 nmol/well after 24 h (Figure 10 C). By contrast, measured CsA concentrations on day 13 fluctuated strongly for both treatment levels (Figure 10 B and D). Samples of the first two sampling time-points (2 and 30 min) from treatment with 0.7 µM CsA and the second sampling time-point (30 min) from treatment with 7 µM CsA were missing due to contamination.

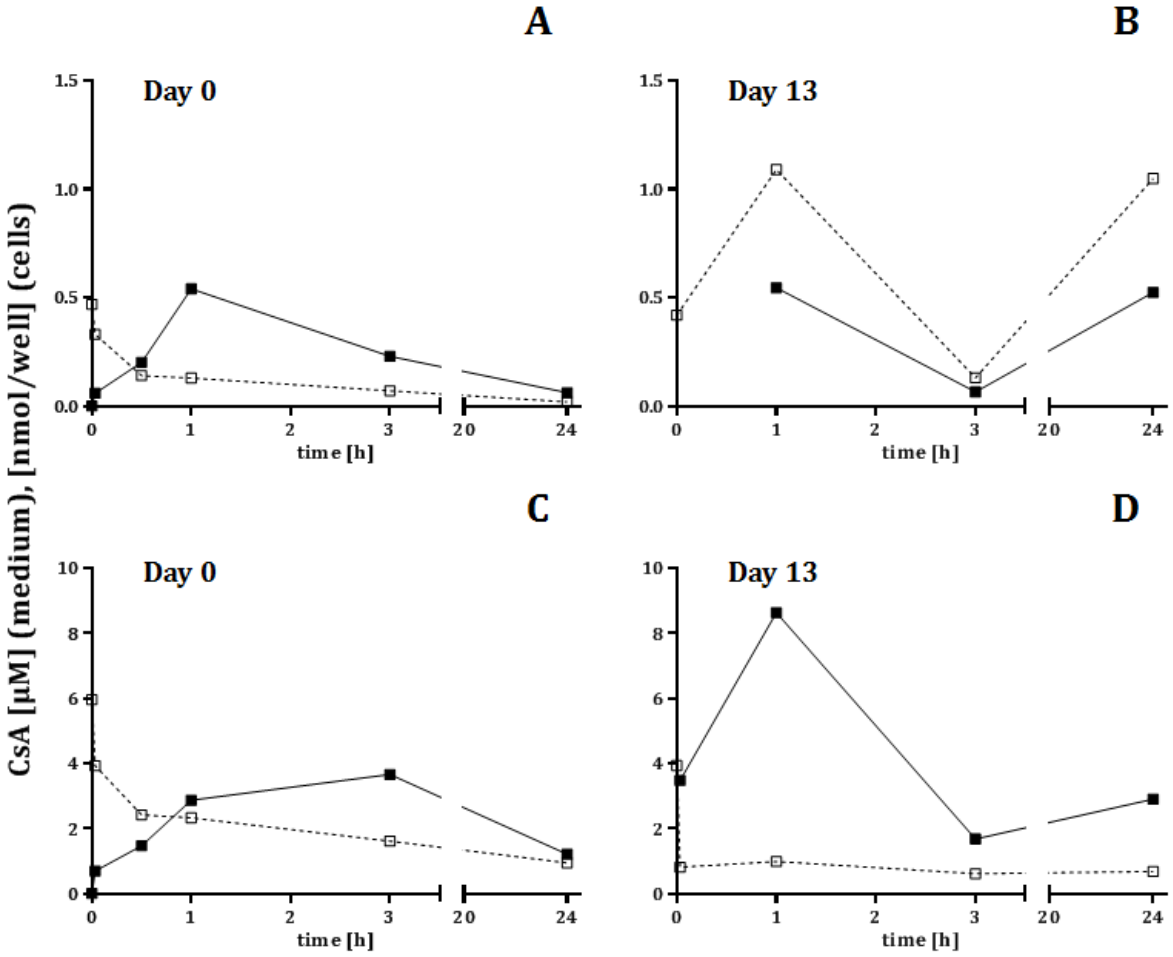

Figure 10. *Extra- and intracellular cyclosporine A concentration-time curves in primary human hepatocytes. PHH III were obtained from a human donor as described in 2.2.2. CsA concentrations were measured by LC-MS/MS (2.4.1 and 2.5.1) in vehicle (time-point 0 min □), medium (□) and cells (■) of PHH III after treatment with 0.7 µM (A,B) and 7 µM CsA (C,D). Samples were generated for 0.7 and 7 µM CsA after 2 min, 30 min, 1 h, 3 h and 24 h on day 0 (A,C), for 0.7 µM CsA after 1 h, 3 h and 24 h on day 13 (B) and for 7 µM after 2 min, 1 h, 3 h and 24 h on day 13 (D). As data for PHH were not pooled each replicate is illustrated separately, hence, a single data point is plotted for each sampling time-point.*

Although the mass balance indicates a bioaccumulation after low concentration treatment with a total CsA recovery of 176.4% of the administered CsA amount after 14 days (Figure 6 B), this observation could not be confirmed by high concentration treated cells (57.7%) (Figure 6 D).

Analyses of plastic adsorption samples showed CsA amounts under the LOQ after low concentration treatment on day 0. Repeated treatment led to increased CsA amounts, albeit strong variations were determined ranging from 1.8% to 12.8% of the administered CsA amount. High concentration samples contained 1.1 ± 0.6% CsA on day 0 and increased to 2.2 ± 1.2% after 14 days, which was not statistically significant (day 1 vs. day 14: p value = 0.103; unpaired, two-tailed Student's *t*-test).

PRH and PHH sandwich layers consisted of collagen and Geltrex™, respectively. As both sandwich layers are containing different ingredients that might affect CsA trapping, a separate blank study was conducted for PHH layers. The CsA amount was not determined in vehicle. Hence, measured concentrations were referred to the nominal CsA treatment concentration (7 µM), in order to calculate CsA mass balances. Obtained results indicate statistical significant CsA trapping to the Geltrex™ layers after repeated exposure for 14 days (Figure 11). Thus, potential CsA bioaccumulation in PHH might be biased by CsA trapping to the Geltrex™ layers.

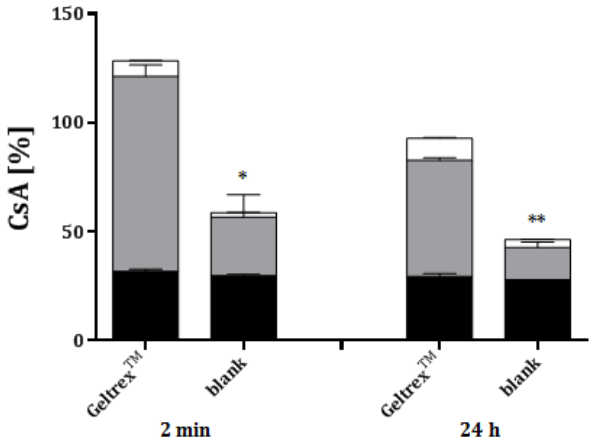

Figure 11. *Cyclosporine A mass balance in PHH blank experiments. Measured CsA concentrations in medium (■), cells (▭) and plastic adsorption samples (▭) were normalized to the nominal CsA concentration as described in 2.6.1. Culture plates with ("Geltrex™") and without ("blank") sandwich layers were incubated with 7 µM CsA (B) for up to 14 days. CsA containing medium was refreshed every 24 h and samples were generated on day 13 after 2 min and 24 h. Mean (± SD) is given for two technical replicates. Statistical significance was tested by two-tailed, unpaired Student's t-test. Asterisk (*) indicates p-values < 0.05 and (**) p<0.01.*

3.1.3. HepaRG cells

CsA concentrations in vehicles were measured in two of three replicates and high variations were determined between replicates. For 0.5 µM CsA treatment, the quantified CsA amount was 88.9 ± 1% and 100.4 ± 0.3% of the nominal CsA concentration in vehicles of the first replicate on day 0 and 13, respectively, while in samples of the second replicate the recovered CsA amount was 31.8 ± 3% and 37.9 ± 2.1% of the nominal concentration on day 0 and day 13, respectively. Similar results were obtained for high concentration vehicles (5 µM) with determined CsA recoveries of 103.8 ± 1.4% (day 0) and 100.0 ± 1.7% (day 13) for the first replicate and 56.0 ± 5.6% (day 0) and 67.0 ± 3.0% (day 13) for the second replicate.

CsA concentrations in medium decreased to 0.02 ± 0.01 µM within 24 h on day 0 after low concentration treatment. Simultaneously, the intracellular CsA peak concentration (0.19 ± 0.01 nmol/well) was reached within 2 h and decreased (0.02 ± 0.01nmol/well) within the next 22 h following 1st order kinetics (Figure 12 A). Repeated exposure did not significantly influence the CsA kinetic profile in low concentration samples. A time-dependent CsA decrease to 0.01 ± 0.01 µM was observed in medium within 24 h and concurrent intracellular CsA increase within 1 h (0.20 ± 0.05 nmol/well), which decreased (0.01 ± 0.01 nmol/well) until the end of the treatment day (Figure 12 B). Treatment with 5 µM CsA revealed a concentration decrease to 0.59 ± 0.7 µM in medium within 24 h on day 0 (Figure 12 C). Intracellular CsA peak concentrations (0.68 ± 0.19 nmol/well) were reached within 2 h on day 0 and declined to 0.27 ± 0.19 nmol/well after 24 h (Figure 12 C). Similar kinetic profiles in medium and cells were observed after 13 days of high concentration treatment with the exception of constantly two-fold higher intracellular CsA levels (Figure 12 D). The calculated CsA mass balances indicate no CsA bioaccumulation with the total recovery being 9.1 ± 6.4% (day 1) and 5.2 ± 3.7% (day 14) after treatment with 0.5 µM CsA (Figure 6 A and B) as well as 19.3 ± 21.2% (day 1) and 20.6 ± 21.6% (day 14) after treatment with 5 µM CsA (Figure 6 C and D).

The percentage of the administered CsA amount adsorbed to plastic devices was 5.3 ± 2.4% (low concentration treatment) and 2.1 ± 1.4% (high concentration treatment) after 1 h on day 0, but decreased to approximately 1% after 24 h for both 0.5 µM and 5 µM CsA treatment. Identical observations were made after repeated

exposure, namely 5.1 ± 0.9% (low concentration) and 4.1 ± 3.9% (high concentration) recovered after 1 h, followed by a decrease to approximately 1% after 24 h.

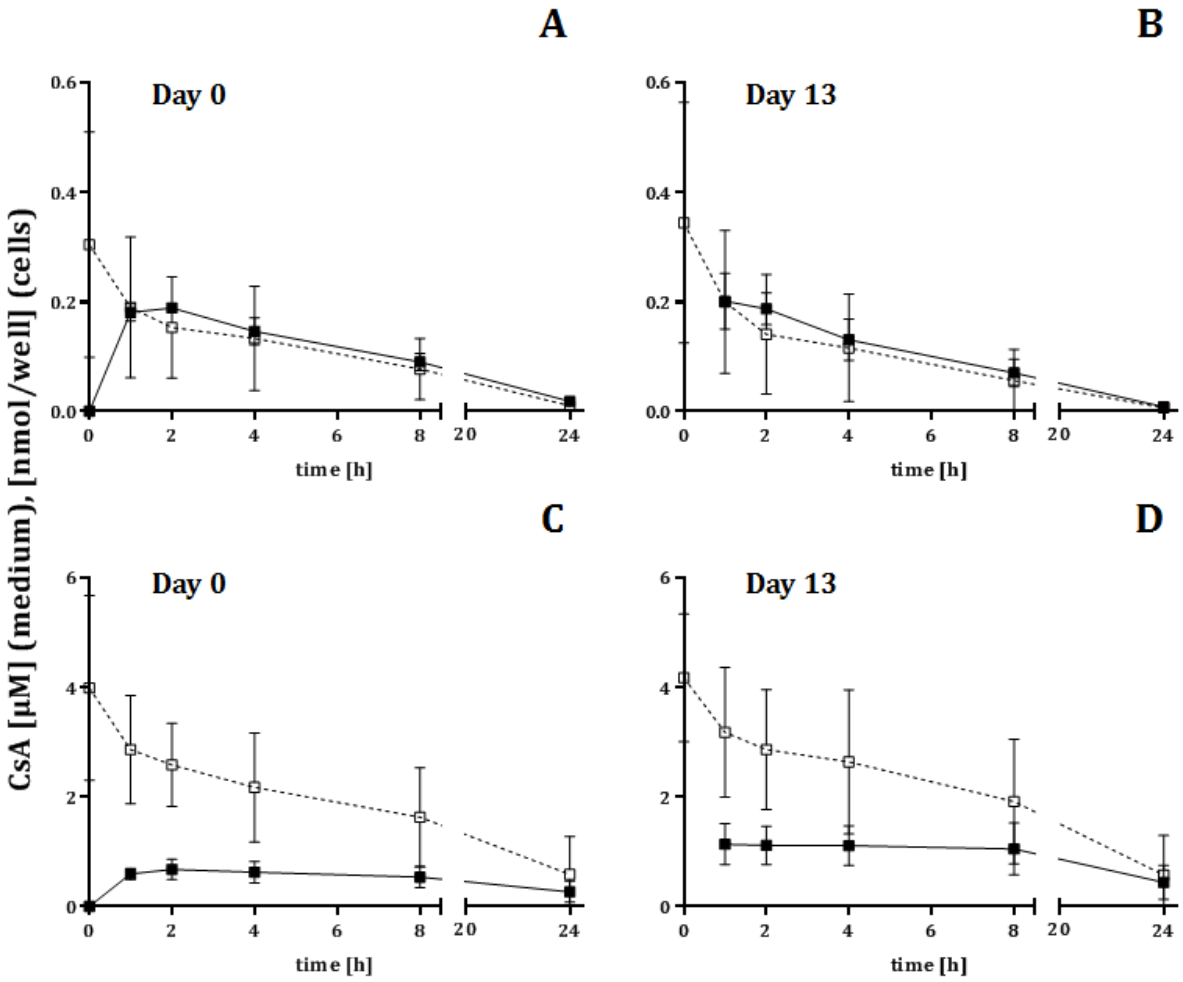

Figure 12. *Extra- and intracellular cyclosporine A concentration-time curves in HepaRG cells. HepaRG cells were cultured as described in the method section (2.2.3). CsA concentrations were measured by LC-MS/MS (2.4.1 and 2.5.1) in vehicle (time point 0 min □), medium (□) and HepaRG cells (■) after treatment with 0.5 µM (A,B) and 5 µM CsA (C,D). Samples were generated after 1 h, 2 h, 4 h, 8 h and 24 h on day 0 (A,C) and day 13 (B,D). Mean (± SD) of three biological replicates is shown. For vehicles mean (± SD) of two biological replicates is illustrated.*

3.1.4. Cyclosporine A clearance *in vitro*

Determined CsA concentrations in cells were used for estimation of *in vitro* clearances, which were scaled to *in vivo*. Scaled $Cl_{in\ vitro}$ are summarized in Table 11. PRH showed 150- to 190-fold lower clearances in comparison to PHH and HepaRG cells. Treatment with the low CsA concentration had an impact on PRH clearances after repeated exposure, which were significantly lower after 14 day repeated exposure to both the low (p value = 0.049; unpaired, two-tailed Student's *t*-test) and high CsA concentration (p value = 0.004; unpaired, two-tailed Student's *t*-test). For PHH, scaled clearances were

approximately 0.8-fold lower compared to HepaRG. Further, clearance for PHH I was lower than for PHH II and PHH III, confirming the determined low CYP3A4/5 activity in this donor. Clearances were not calculated for the last treatment day for PHH I due to missing samples for the last sampling time-point. Clearances for PHH II and III were constant and neither CsA concentration nor duration of treatment had an impact on obtained clearances. For PHH III, the obtained clearance was approximately as high as for PHH II, which is inconsistent with the ascertained CYP3A4/5 activities. HepaRG cells revealed high and constant clearances for both CsA treatment levels, which were not influenced by repeated exposure. Comparison of the scaled clearances with the *in vivo* situation indicates an allover 10-fold overestimation of rat clearances by PRH, while PHH are in good accordance with *in vivo* clearances and HepaRG about 2-fold overestimated.

Table 11. *Scaled clearances to in vivo [L/h] obtained after respective low and high CsA treatment of PRH, PHH and HepaRG cells for 1 and 14 days.*

CsA level	Treatment duration [d]	PRH	PHH			HepaRG
			PHH I	PHH II	PHH III	
Low	1	0.61 ± 0.07	55.5	77.8	78.8	89.1± 0.5
	14	0.43 ± 0.09	-	76.6	80.5	89.4 ± 0.3
High	1	0.63 ± 0.09	69.6	77.2	77.5	89.6 ± 0.1
	14	0.24 ± 0.07	-	66.1	72.6	89.3 ± 0.4
Ratio in vitro/ in vivo		9.9 ± 3.7 [a]	1.7 ± 0.2 [b]; 4.0 ± 0.4 [c]			2.1 ± 0.0 [b]; 4.9 ±0.0 [c]

[a] *Rat clearance (164.5 ± 5 mL/min/kg) was obtained from Bernareggi and Rowland (1991) and Kawai et al. (1998). A standard body weight of 250 g for rat was used to scale clearance to whole body.*

[b] *Human clearances (0.60 ± 0.15 L/h/kg) were determined by Gupta et al. (1987). CsA was administered to renal transplant patients as constant CsA infusion until steady state. The standard body weight for man was set to 70 kg.*

[c] *Human clearances (0.26 ± 0.05 L/h/kg) were determined after i.v. CsA administration to healthy volunteers (Ducharme et al., 1995; Min et al., 2000). The standard body weight for man was set to 70 kg.*

3.2. Cyclosporine A in brain cell cultures

Two different brain cell culture models were utilized for the investigation of CsA kinetics. Hence, cells were exposed to two different CsA concentrations that were determined by measurement of cytotoxicity after repeated CsA treatment for 14 days. High concentrations are equivalent to TC_{10} and low concentrations were either $1/20^{th}$ (2D model) or $1/5^{th}$ (3D model) of TC_{10}. Cells of the 2D and 3D model were treated every second day for up to 14 and 13 days, respectively. Samples were generated on day 0 and day 12 (3D model) or day 13 (2D model) at five different time-points. The determined CsA concentrations in vehicle, media and cells were used to assess the kinetic profile of CsA and to obtain indications regarding CsA biotransformation and bioaccumulation in the studied *in vitro* models.

3.2.1. Primary neuronal mouse cells (2D model)

Vehicles of the low (0.1 µM) and high (2 µM) CsA concentration were analyzed regarding the administered CsA amount on day 0. The recovered CsA content was 18.1 ± 3.2% of the nominal low concentration and 46.2 ± 7.8% of the nominal high concentration.

Although the applied CsA concentration was 0.02 ± 0.00 µM in low concentration vehicles, the determined CsA concentration in medium was 0.03 ± 0.01 µM after 30 min on day 0 (Figure 13 A) and remained stable for 14 days (Figure 13 B). Intracellular CsA steady state levels (0.02 ± 0.01 nmol/well) were reached within 30 min on day 0 and stayed unchanged until the end of the experiment period (Figure 13 A and B). High concentration treatment did not influence the CsA kinetic profile with fast achieved steady state concentrations (medium: 0.64 ± 0.13 µM, cells: 0.12 ± 0.02 nmol/well) on day 0 (Figure 13 C), which stayed constant for 14 days (Figure 13 D).

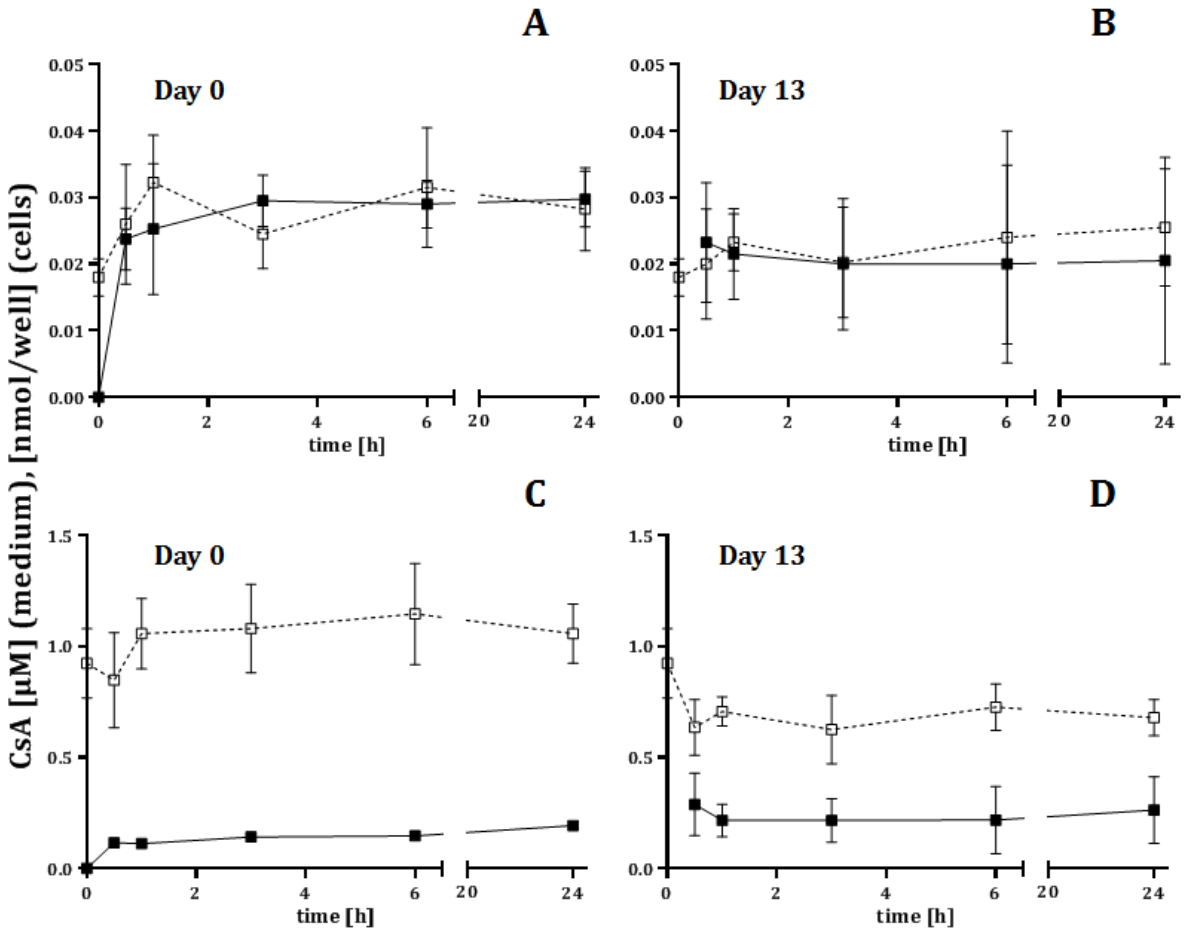

Figure 13. *Extra- and intracellular cyclosporine A concentration-time curves in primary neuronal mouse cells. Cells of the 2D model derived from embryonic frontal cortex tissue from NMRI mice as described in the method section (2.2.4). CsA concentrations were measured by LC-MS/MS (2.4.1 and 2.5.1) in vehicle (time point 0 min □), medium (□) and cells (■) of the 2Dmodel after treatment with 0.1 µM (A,B) and 2 µM CsA (C,D). Samples were generated after 30 min, 1 h, 3 h, 6 h and 24 h on day 0 (A,C) and day 13 (B,D). Mean (± SD) of four biological replicates is shown.*

Due to discrepancies between measured CsA concentrations in low concentration vehicles and related medium and cell lysate samples, the generated mass balance exceeded 100% (232.9 ± 23.7% of the administered CsA amount) after 24 h, but did not change after repeated exposure (Figure 14 A). For high concentration samples the total CsA recovery was 129.7 ± 14.3% after 24 h (Figure 14 B). After 14 days the mass balance was 90.5 ± 14.7%. Hence, the total CsA recovery was significantly lower after repeated treatment (p value = 0.008; unpaired, two-tailed Student's *t*-test), which seems not to be of biological relevance.

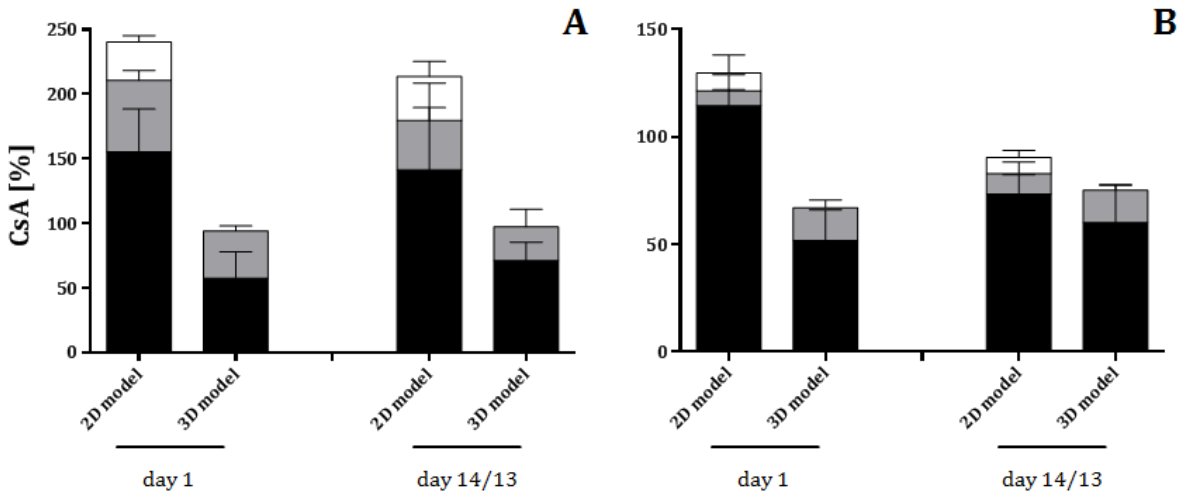

Figure 14. *Cyclosporine A mass balances in two in vitro brain cell culture models. Measured CsA concentrations in medium (■), cells (▭) and plastic adsorption samples (▭) were normalized to concentrations determined in vehicle as described in 2.6.1. Mass balances were calculated after treatment with the respective low (A) and high (B) CsA concentration for 1 day and 13 or 14 days for the 3D or 2D model, respectively. Mean (± SD) of three and four biological replicates is given for the 3D and 2D model, respectively. For the 3D model no plastic adsorption samples were generated due to culturing in glass flasks.*

The CsA content in plastic adsorption samples of the 2D model was under the LOQ for 0.1 µM CsA treatment on day 0, but increased to 0.02 ± 0.00 µM (29.9 ± 5.1% of the administered CsA amount) after 24 h and did not change within the following 13 days (34.1 ± 11.7% of the administered CsA amount). By contrast, in high concentration samples plastic adsorption was already completed after 30 min on day 0 with stable CsA concentrations of 0.14 ± 0.03 µM (1 day: 7.4 ± 1.8% of the administered CsA amount, 13 days: 7.6 ±3.2%).

3.2.2. Primary aggregating rat brain cells (3D model)

Minor differences were detected between the applied CsA contents and the nominal concentrations. For low concentration (0.2 µM) treatment 79.8 ± 22.1% (day 0) and 102.3 ± 21.3% (day 12) was recovered in vehicles. 113.2 ± 28.4% and 122.7 ± 17.4% of the nominal high concentration (1 µM) was detected in vehicles on day 0 and day 12, respectively.

The CsA content decreased to 0.10 ± 0.02 µM in medium of cells treated with 0.2 µM CsA within 30 min on day 0. No remarkable changes were observed within 24 h or 13 days with the CsA concentration being on average 0.09 ± 0.01 µM (day 0) and 0.15 ± 0.03 µM (day 12) (Figure 15 A and B). Stable CsA concentrations (0.42 ± 0.08 nmol/flask) in cells

were achieved within 30 min on day 0 and no statistical significant change was observed within 24 h and 13 days (30 min. vs. 24 h p value = 0.08; day 1 vs. day 13 p value = 0.80 unpaired, two-tailed Student's *t*-test).

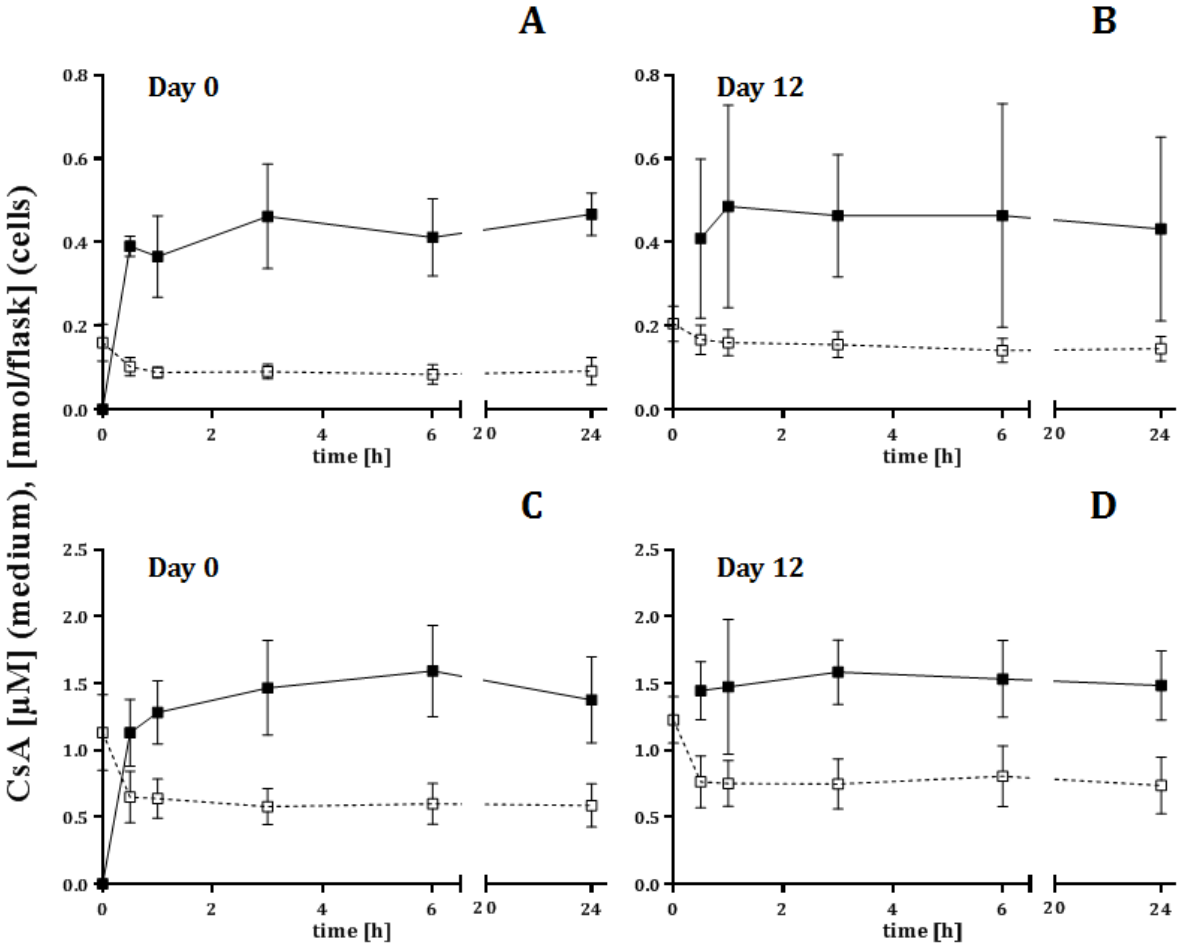

Figure 15. *Extra- and intracellular cyclosporine A concentration-time curves in primary aggregating rat brain cells. Cells of the 3D model derived from 16-days old Sprague-Dawley rat embryos as described in the method section (2.2.5). CsA concentrations were measured by LC-MS/MS (2.4.1 and 2.5.1) in vehicle (time point 0 min □), medium (□) and cells (■) of the 3Dmodel after treatment with 0.2 µM (A,B) and 1 µM CsA (C,D). Samples were generated after 30 min, 1 h, 3 h, 6 h and 24 h on day 0 (A,C) and day 12 (B,D). Mean (± SD) of three biological replicates is shown.*

Same observations were made for high concentration treatment with constant CsA concentrations after 30 min in medium (0.76 ± 0.19 µM) and cells (1.13 ± 0.25 nmol/flask) on day 0 (Figure 15 C). No further alterations were detected within 13 days (Figure 15 D). Obtained mass balances indicate neither biotransformation nor bioaccumulation in the 3D model (Figure 14). For exposure to 0.2 µM the total CsA recovery was 94.0 ± 23.6% and 97.2 ±24.0 after 24 h and 13 days, respectively (Figure 14 A). Although the recovered CsA amount was 67.0 ± 17.3 (day 1)

and 75.2 ± 20.0% (day 13) of the applied high CsA concentration and resulted in a CsA loss (Figure 14 B), this seems not to be related to a possible biotransformation. Calculated mass balances were 69.4 ± 20.8% and 77.0 ± 17.7% already after 30 min on day 0 and 12, respectively. Hence, biotransformation occurring only within 30 min seems very unlikely.

3.3. Transporter experiments

Transporter experiments were performed in order to investigate the potential of CsA to cross a membrane by passive diffusion. Therefore, CsA was administered at a low and high concentration to Caco-2 cells cultured on filter inserts from either AB or BA direction. Additionally, a parallel artificial membrane and blank filter inserts were incubated with CsA. Lucifer yellow was used as permeability marker.

The lucifer yellow amount recovered in acceptor wells was 0.35 ± 0.39% for untreated Caco-2 cells. Lucifer yellow recoveries were 0.12 ± 0.18% (1 µM CsA) and 0.02 ± 0.16% (10 µM CsA) for CsA treated cells in AB direction and 0.49 ± 0.26% (1 µM CsA) as well as 0.32 ± 0.12% (10 µM CsA) for treated cells in BA direction. These results indicate that exposure to CsA for 3 h had no influence on the integrity of Caco-2 cell monolayer. Lucifer yellow permeability was determined for a parallel artificial membrane and blank filter inserts. 2.41 ± 1.14% and 7.27 ± 3.5% of the initial lucifer yellow amount was able to diffuse through the membrane and filter inserts, respectively. Hence, limited lucifer yellow permeability through Caco-2 monolayer was not biased by filter inserts.

For transport experiments performed on Caco-2 cells, the majority of the applied CsA amount was recovered in the donor well accounting for 33.6 ± 3.4% (AB) and 48.3 ± 5.3% (BA) after low concentration treatment (Figure 16 A) as well as 15.5 ± 1.3% (AB) and 46.9 ± 10.7% (BA) after high concentration treatment (Figure 16 B). The total CsA recovery was significantly lower for cells treated from the apical chamber (AB direction) for both exposure levels (for 1 µM p value = 0.026; for 10 µM p value = 0.024; unpaired, two-tailed Student's *t*-test). PAMPA experiments revealed low CsA recoveries in the acceptor wells (2.6 ± 0.3% for 1 µM CsA and 2.7 ± 0.5% for 10 µM CsA), 13.4 ± 9.9% (1 µM CsA) and 23.6 ±6.3% (10 µM CsA) left in the donor well and majority retrieved trapped to the membrane and plastic (65.2 ± 6.6% for 1 µM CsA and 72.7 ± 1.4% for 10 µM CsA) (Figure 16 A and B). An almost complete CsA adsorption to plastic occurred after incubation of empty filter inserts with 1 µM CsA for 3 h, while CsA

values were determined to be under the LOQ in both donor and acceptor wells (Figure 16 A). Similar observations were made after 10 µM CsA incubation, but quantifiable CsA amounts were measured in the donor (1.4 ± 0.6%) and acceptor wells (8.8 ± 3.2%) (Figure 16 B).

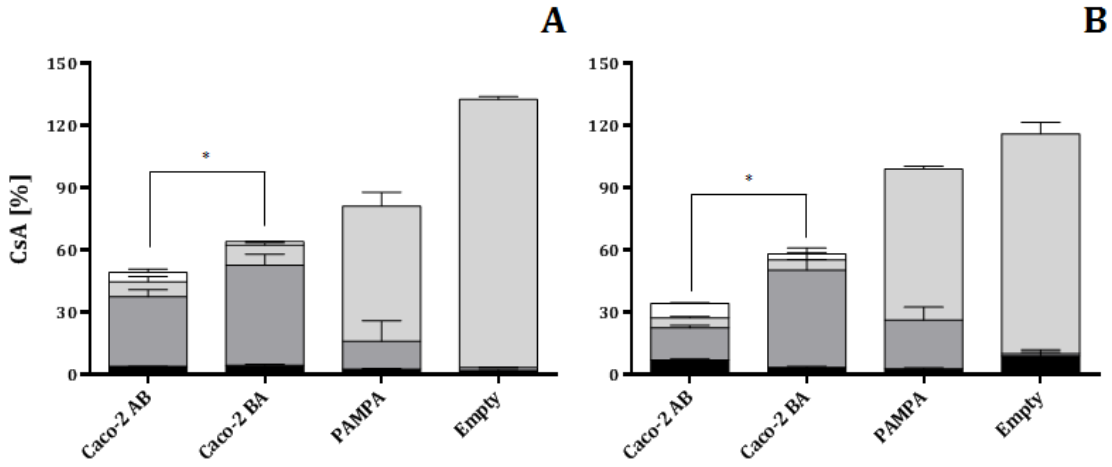

Figure 16. *Cyclosporine A mass balances in Caco-2 cells, a parallel artificial membrane and wells containing blank filter inserts. Caco-2 cells were cultured on filter inserts as described in the method section (2.2.7). Cells were treated either from the apical (AB) or from the basolateral (BA) compartment, while PAMPA and blank experiments were incubated with CsA containing medium from the apical side only. The compartment containing CsA was denoted as "donor" and the compartment without CsA as "acceptor". Measured CsA concentrations in acceptor (■) and donor (▭) medium, plastic adsorption samples (▭) and cells (▭) were related to the CsA concentrations determined in vehicle as described in 2.6.1. Mass balances were calculated after treatment with the 1 µM (A) and 10 µM (B) CsA for 3 h. Mean (± SD) of three replicates is given. Statistical significance was tested by two-tailed, unpaired Student's t-test. Asterisk (*) indicates p-values < 0.05.*

Calculated P_{app} values are illustrated in Figure 17 and were high for Caco-2 cells treated in BA direction for both CsA concentrations. Although Caco-2 cells treated in AB direction, PAMPA and blank experiments revealed low CsA permeability, statistically significant higher P_{app} values were obtained for Caco-2 cells (AB) in comparison to PAMPA (p value = 0.035 for 1 µM CsA and p value = 0.001 for 10 µM CsA; unpaired, two-tailed Student's *t*-test) and blank filter inserts (p value = 0.0001 for 1 µM CsA and p value = 0.014 for 10 µM CsA; unpaired, two-tailed Student's *t*-test). Efflux ratios, i.e. ratio $P_{app}(BA)/P_{app}(AB)$, were high for both 1 µM CsA (31.0 ± 4.3) and 10 µM CsA (14.1 ± 1.9) treatment, but were significantly lower for exposure to 10 µM (p value = 0.003; unpaired, two-tailed Student's *t*-test), indicating active efflux transport, which seems to be inhibited at higher concentration.

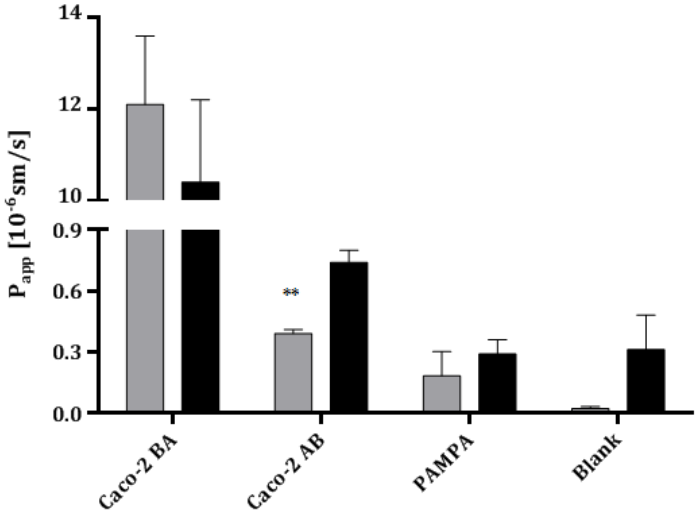

Figure 17. *Calculated apparent permeability coefficients of CsA on Caco-2 cells, a parallel artificial membrane and wells containing blank filter inserts. P_{app} values were obtained after treatment with 1 µM (▭) and 10 µM (■) CsA as described in 2.3.2. Caco-2 cells were treated either from the apical (AB) or from the basolateral (BA) compartment, while PAMPA and blank experiments were incubated with CsA containing medium from the apical side only. Mean (± SD) of three replicates is given.*

3.4. Adefovir dipivoxil in the kidney model

3.4.1. Kinetics – "lab 6"

Cells from the human kidney cell line RPTEC/TERT1 were exposed to 2.5 µM and 8 µM ADVd for up to 14 days. ADVd content was under the limit of quantification in all vehicles, while the recovered amount of its major metabolite ADV was 64.3 ± 1.3% of the nominal 2.5 µM ADVd concentration and 83.4 ± 2.0% of the nominal 8 µM ADVd concentration.

Figure 18 represents a chromatogram of the 2.5 µM ADVd vehicle solution. Although only the parent drug was added to the medium, almost no ADVd was detected. Instead, a clear signal for ADV was recorded in the same sample. Therefore, only the major metabolite ADV was quantified by LC-MS/MS after quantitative hydrolysis of ADVd to ADV.

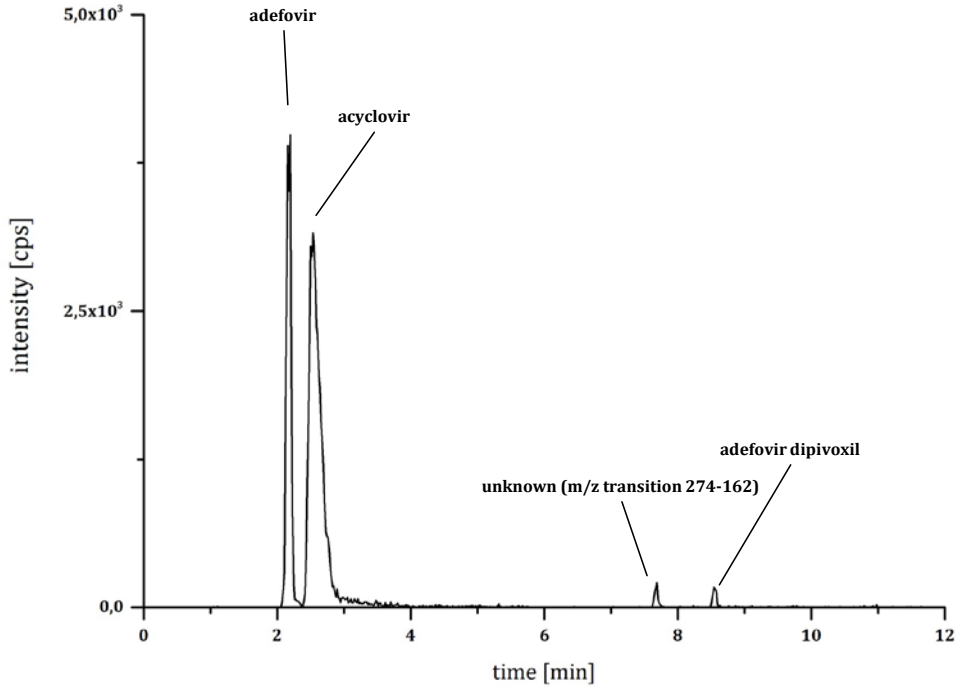

Figure 18. *LC-MS/MS chromatogram of adefovir dipivoxil (m/z transition 502→256), adefovir (m/z transition 274→162) and acyclovir (m/z transition 226→152) in the 2.5 µM vehicle solution from "lab 6" recorded as described in 2.5.2.*

After quantitative hydrolysis, the recovered ADV amount in vehicles was 85.0 ± 5.9% on day 0 and 98.2 ± 4.8% on day 13 of the nominal low concentration (2.5 µM). For high concentration (8 µM) vehicles, the content was 94.1 ± 6.7% on day 0 and 108 ± 8.4% on day 13.

ADV determination revealed stable concentrations in medium after treatment with 2.5 µM on day 0 (apical: 2.3 ± 0.1 µM, basolateral: 2.3 ± 0.2 µM) and day 13 (apical: 2.5 ± 0.1 µM, basolateral: 2.5 ± 0.1 µM). Further, no ADV was detected in cells at any sampling time-point (Figure 19 A and B). Similar observations were made for treatment with 8 µM ADVd: stable ADV concentrations in medium on day 0 (apical: 7.6 ± 0.5 µM, basolateral: 7.5 ± 0.7 µM) as well as on day 13 (apical: 8.6 ± 0.9 µM, basolateral: 7.8 ± 0.6 µM) and no intracellular ADV recovery (Figure 19 C and D).

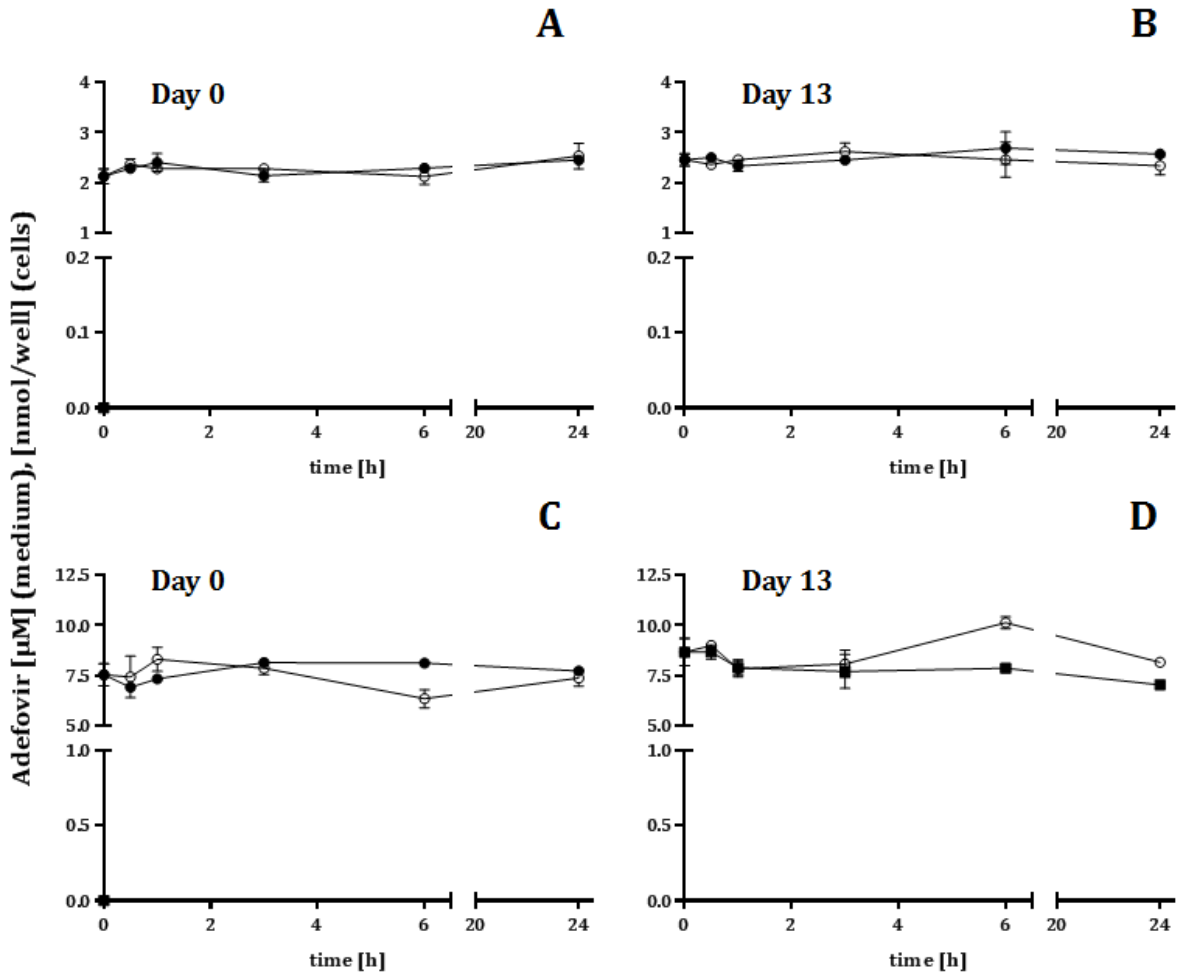

Figure 19. *Extra- and intracellular adefovir concentration-time curves in RPTECT/TERT1 cells. Cells were cultured as described in the method section (2.2.6). Adefovir concentrations were measured by LC-MS/MS (2.4.3 and 2.5.3) in vehicle (time point 0 min), medium (● apical, ○ basolateral) and RPTEC/TERT1 cells (■) after treatment with 2.5 µM (A,B) and 8 µM adefovir dipivoxil (C,D). Samples were generated after 30 min, 1 h, 3 h, 6 h and 24 h on day 0 (A,C) and day 13 (B,D). Mean (± SD) of two technical replicates for one biological replicate is shown.*

Calculated mass balances indicate neither significant ADV bioaccumulation nor biotransformation with the total ADV recovery being 117.8 ± 2.7% after 24 h and 98.4 ±5.2% after 14 days of treatment with 2.5 µM ADVd (Figure 20 A). Recovered ADV

amount after exposure to 8 µM ADVd was 99.2 ± 4.5% after 24 h and 85.6 ± 1.2% after 14 days. No ADV was detected in cells and plastic.

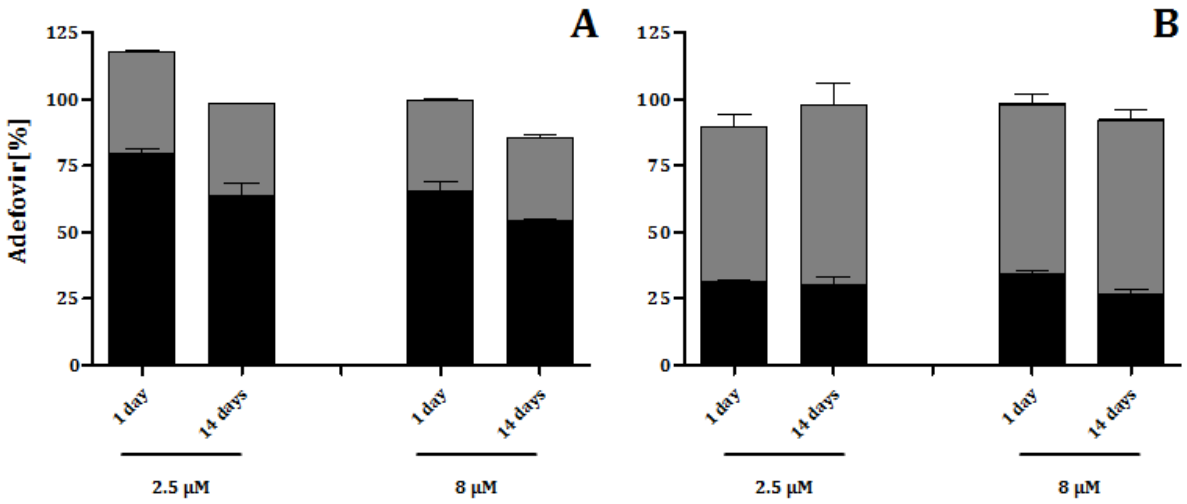

Figure 20. *Adefovir mass balances in RPTEC/TERT1 cells. Measured adefovir concentrations in basolateral medium (■), apical medium (■) and cells (□) were normalized to concentrations determined in vehicle as described in 2.5.3. Mass balances were calculated after treatment with 2.5 µM and 8 µM adefovir dipivoxil for 1 and 14 days. Experiments were performed in "lab 6" (A) and "lab 7" (B). Mean (± SD) is given for two technical replicates ("lab 6") and two biological replicates ("lab 7").*

3.4.2. Kinetics – "lab 7"

The 2.5 µM ADVd vehicle was analyzed regarding both ADVd and ADV content. The recovered ADVd amount was 1.1 ± 0.1% of the nominal concentration, while no signal was recorded for ADV. Instead, a signal was detected after 7.7 min at the specific transitions for ADV (274→162 and 274→136) (Figure 21). ADVd was hydrolyzed quantitatively to ADV in all medium samples and samples were reanalyzed regarding the ADV content.

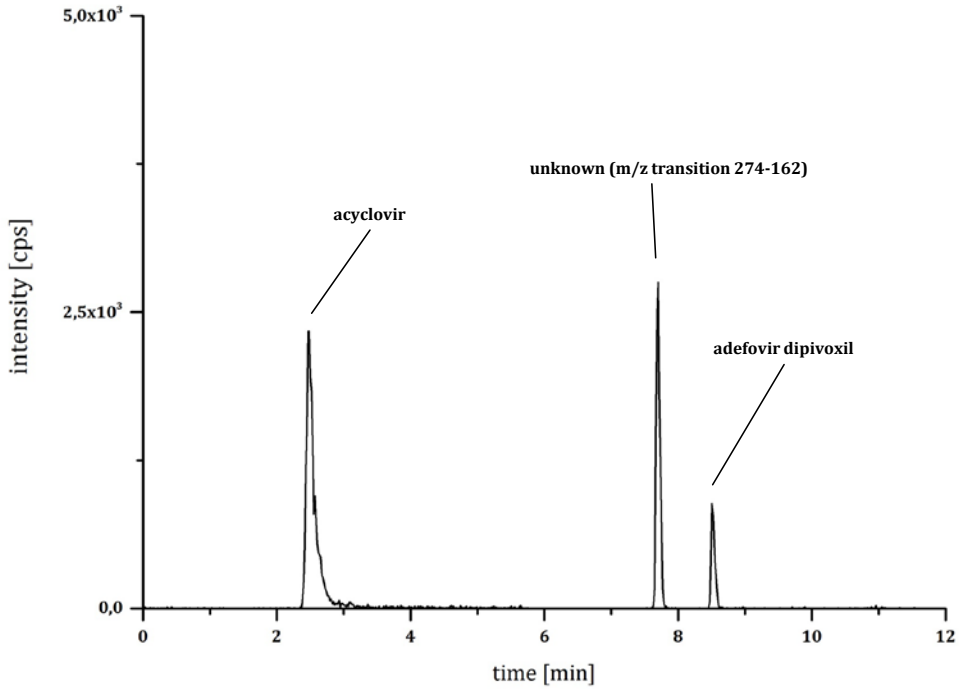

Figure 21. *LC-MS/MS chromatogram of adefovir dipivoxil (m/z transition 502→256), adefovir (m/z transition 274→162) and acyclovir (m/z transition 226→152) in the 2.5 µM vehicle solution from "lab 7" recorded as described in 2.5.2.*

Vehicles were available for the first treatment day. ADV concentrations were assessed in vehicles with a recovery of 93.0 ± 5.4% of the nominal low ADVd content and 94.6 ± 9.7% of the nominal high concentration.

For exposure to 2.5 µM ADVd, ADV quantification in medium showed in the basolateral samples stable ADV concentrations for all time points on day 0 (2.1 ± 0.1 µM) and day 13 (2.3 ± 0.2 µM), while the ADV content in the apical samples decreased within 1 h to 1.7 ± 0.1 µM on day 0 and 1.8 ± 0.1 µM on day 13 (Figure 22 A and B). Further in the apical compartment, ADV increased within the following 23 h to 2.1 ± 0.1 µM on day 0 and 2.2 ± 0.1 µM on day 13 (Figure 22 A and B). A similar observation was made after exposure to 8 µM ADVd (Figure 22 C and D). The determined ADV concentrations in cells

showed for all treatment days and both treatment concentrations the same outcome. ADV peak levels were reached after 1 h (0.16 ± 0.03 nmol/well for 2.5 µM treatment and 1.2 ± 0.4 nmol/well for 8 µM treatment) on day 0 and (0.18 ± 0.02 nmol/well for 2.5 µM treatment and 0.86 ± 0.07 nmol/well for 8 µM treatment) day 13, followed by a decrease to concentrations <LOQ following a 1st order kinetics within the next 23 h, although the drug was still available in medium (Figure 22).

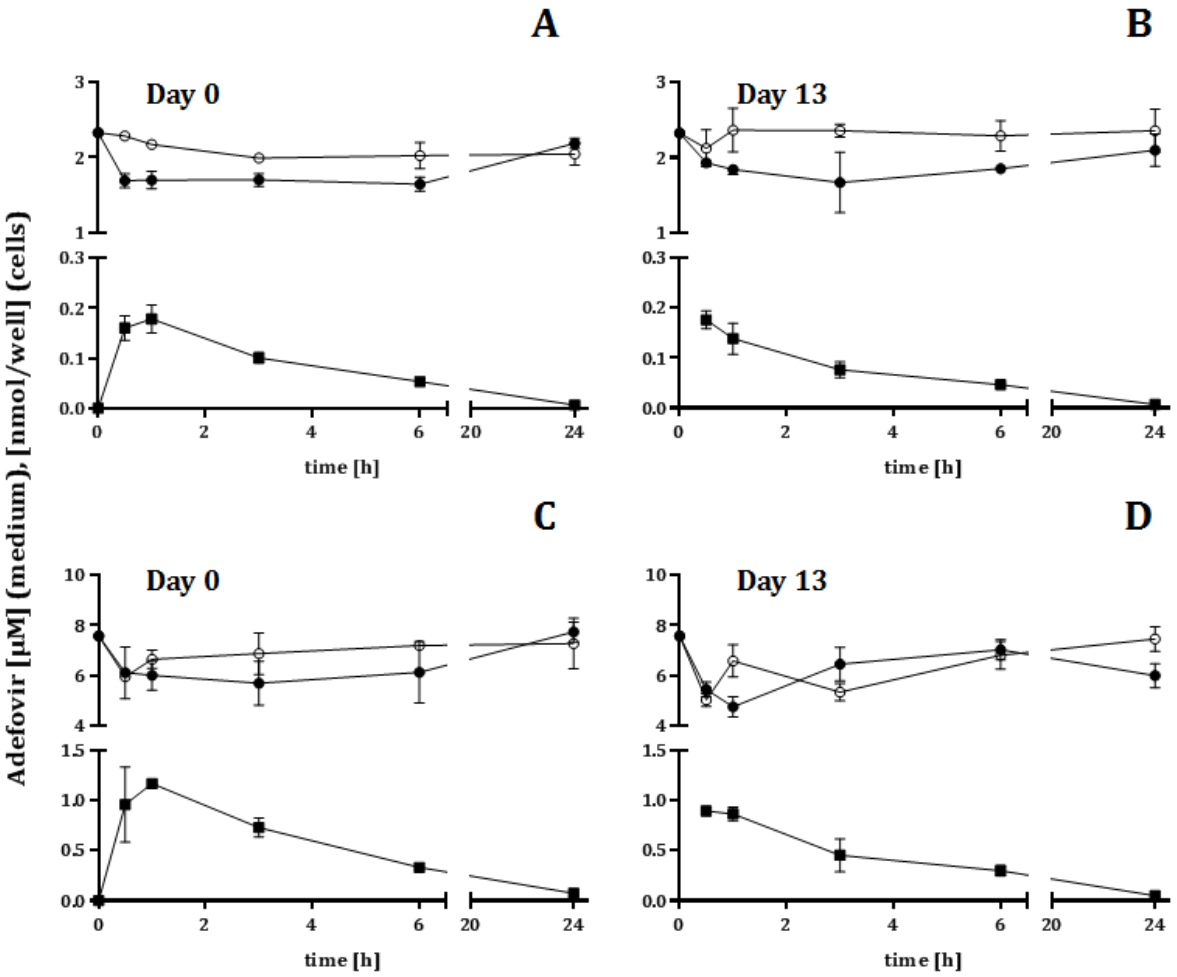

Figure 22. *Extra- and intracellular adefovir concentration-time curves in RPTECT/TERT1 cells. Cells were cultured as described in the method section (2.2.6). Adefovir concentrations were measured by LC-MS/MS (2.4.3 and 2.5.3) in vehicle (time point 0 min), medium (●apical, ○ basolateral) and RPTEC/TERT1 cells (■) after treatment with 2.5 µM (A,B) and 8 µM adefovir dipivoxil (C,D). Samples were generated after 30 min, 1 h, 3 h, 6 h and 24 h on day 0 (A,C) and day 13 (B,D). Mean (± SD) of two biological replicates is shown.*

Similar to "lab 6" no significant changes were detected in the total ADV recovery, which can be ascribed to lack of biotransformation and –accumulation (Figure 20 B). For 2.5 µM treatment the total mass balance was 90.0 ± 5.2% and 97.7 ± 8.2% after 24 h and 14 days, respectively, with no ADV being detected in cells. For high concentration

treatment, ADV recovery was 102.3 ± 4.7% after 24 h and 92.2 ± 5.8% after 14 days with intracellular ADV contents <1%. ADV was not recovered in plastic adsorption samples.

3.4.3. Differences between treatment solutions and stability test

The three biological replicates of RPTEC/TERT1 cells treated with ADVd for up to 14 days were performed in two different laboratories ("lab 6" and "lab 7") and drug quantification by LC-MS/MS was run in-house ("Wuerzburg"). In order to explain the observed aberrations in the kinetic profiles in RPTEC/TERT1 cells after exposure to ADVd, vehicle solutions were compared across the three different laboratories. Figure 23 shows the spectra of the 2.5 µM ADVd vehicle prepared in the three different laboratories. A signal for ADVd (RT 8.5 min) was recorded in "Wuerzburg" samples, while no ADVd, but ADV (RT 2.2 min) was detected in "lab 6" samples and no ADV, minor ADVd and an unidentified peak (RT 7.7 min), accounting for the major fraction, was observed in samples received from "lab 7".

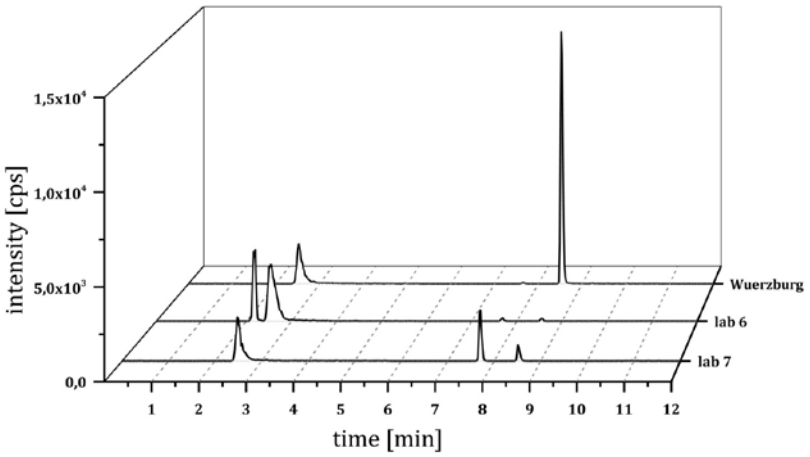

Figure 23. *Spectra of 2.5 µM adefovir dipivoxil in vehicle solutions from "lab 6", "lab 7" and in-house preparation recorded by LC-MS/MS as described in 2.5.2.*

Within the repeated analyses of calibration curves containing defined ADVd and ADV concentrations during three days, it turned out that ADVd concentrations slightly decreased. As measurements were performed at room temperature the question arose, whether ADVd is stable under cell culture conditions for 24 h. Therefore, the parent drug ADVd was diluted in RPTEC/TERT1 culture medium and incubated at 37°C for 24 h. Aliquots were taken after 30 min, 1 h, 3 h and 24 h. ADVd determination in medium revealed a time-dependent concentration decrease for the parent compound (Figure 24 A), where approximately 14.2 ± 2.0% of the nominal 2.5 µM ADVd and 9.3 ± 0.7% of the nominal 8 µM ADVd were recovered after 3 h. The ADVd content was

under the limit of quantification for all samples after 24 h. No ADV was detected within 30 min for both concentrations, but approximately 2.2 ± 0.0% and 2.5 ± 0.2% ADV were recovered for the nominal 2.5 µM and 8 µM ADVd concentration, respectively, after 24 h. These results indicate a time-dependent degradation of ADVd partly to ADV and at least one intermediate under culture condition.

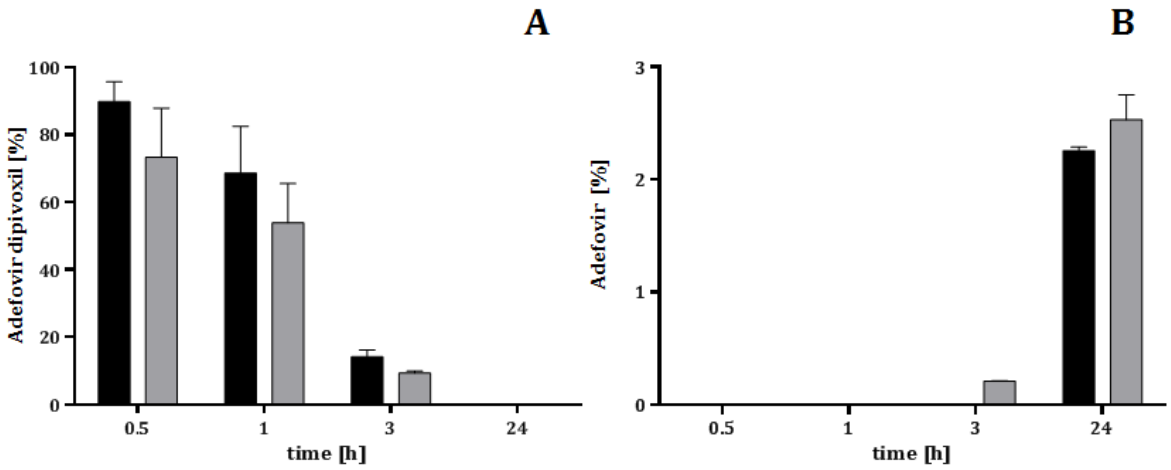

Figure 24. *Adefovir dipivoxil and adefovir recovery in vehicles incubated at 37°C. Adefovir dipivoxil was diluted in serum-free RPTEC/TERT1 cell culture medium yielding final concentrations of 2.5 µM (■) and 8 µM (▭). Solutions were incubated without cells at 37°C for up to 24 h (2.3.3). Samples were taken after 30 min, 1 h, 3 h and 24 h and analyzed regarding the adefovir dipivoxil (A) and adefovir (B) content as described in the methods (2.4.2 and 2.5.2). Determined concentrations were normalized to the nominal concentrations. Mean (± SD) is given for two technical replicates.*

3.5. Cisplatinum in the kidney model

RPTECT/TERT1 cells were treated with a low and a high concentration of the anti-cancer drug cisplatinum. Generated samples were analyzed by ICP-MS, which leads to partial element breakdown of organic structures and inorganic compounds are detected afterwards. Hence, prior to analysis samples were decomposed by aqua regia and additional microwave heating (cell lysate samples), in order to quantitatively release platinum from binding to organic structures.

Vehicles were available for one biological replicate. The platinum amount in vehicles was determined to be 97.4% on day 0 and 94% on day 13 for the low (0.5 µM) cisplatinum concentration. For the high (2 µM) concentration vehicles, the detected platinum percentages were 100.0% and 94.9% on day 0 and day 13, respectively.

For 0.5 µM cisplatinum exposure, platinum concentrations in apical medium seem to increase within 24 h on day 0 (0.58 ± 0.10 µM) and day 13 (0.55 ± 0.04 µM), while concentrations in the basolateral medium decreased (day 0: 0.45 ± 0.05 µM, day 13: 0.46 ± 0.00 µM). Same results were obtained for treatment with 2 µM cisplatinum for 24 h on day 0, with increasing platinum concentration in the apical compartment (2.36 ± 0.19 µM) and decreasing amounts (1.68 ± 0.12 µM) in the basolateral compartment. However, stable platinum concentrations were achieved in apical medium samples (2.14 ± 0.12 µM) after 14 days, while platinum concentrations decreased at the basolateral side (1.89 ± 0.10 µM). Intracellular platinum concentrations were <LOQ for both treatment levels on day 0 (Figure 25 A and C), but increased to 0.02 ± 0.00 nmol/well within 24 h for cells treated with 2 µM cisplatinum (Figure 25 C). Repeated exposure revealed increased, but stable intracellular platinum levels for cells exposed to 0.5 µM (0.03 ± 0.01 nmol/well, Figure 25 B) and 2 µM cisplatinum (0.09 ± 0.03 nmol/well, Figure 25 D).

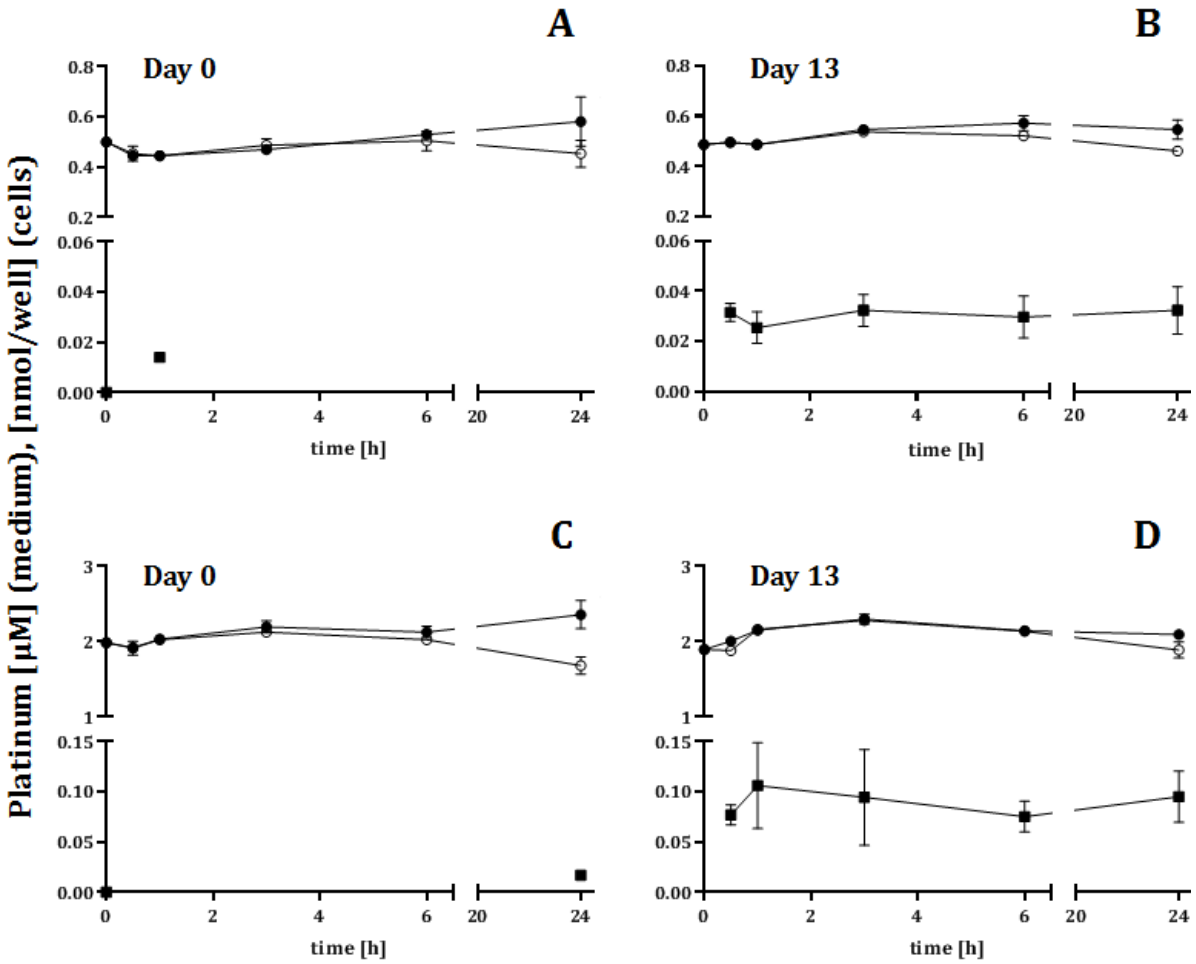

Figure 25. *Extra- and intracellular platinum concentration-time curves in RPTECT/TERT1 cells. Cells were cultured as described in the method section (2.2.6). Platinum concentrations were determined by ICP-MS in vehicle (time point 0 min), medium (● apical, ○ basolateral) and RPTEC/TERT1 cells (■) after treatment with 0.5 µM (A,B) and 2 µM cisplatinum (C,D). Samples were generated after 30 min, 1 h, 3 h, 6 h and 24 h on day 0 (A,C) and day 13 (B,D). Mean (± SD) of three biological replicates is shown. One replicate is given for vehicles.*

In order to investigate the platinum increase and decrease in the apical and basolateral compartments, respectively, medium samples from day 3, 5, 7 and 10 were analyzed additionally. Figure 26 illustrates the significantly higher and lower platinum concentrations at the apical and basolateral side, respectively, for both treatment levels. No statistical significant difference was gained after 24 h and 10 days for 0.5 µM cisplatinum and after 3 and 7 days for 2 µM cisplatinum administration.

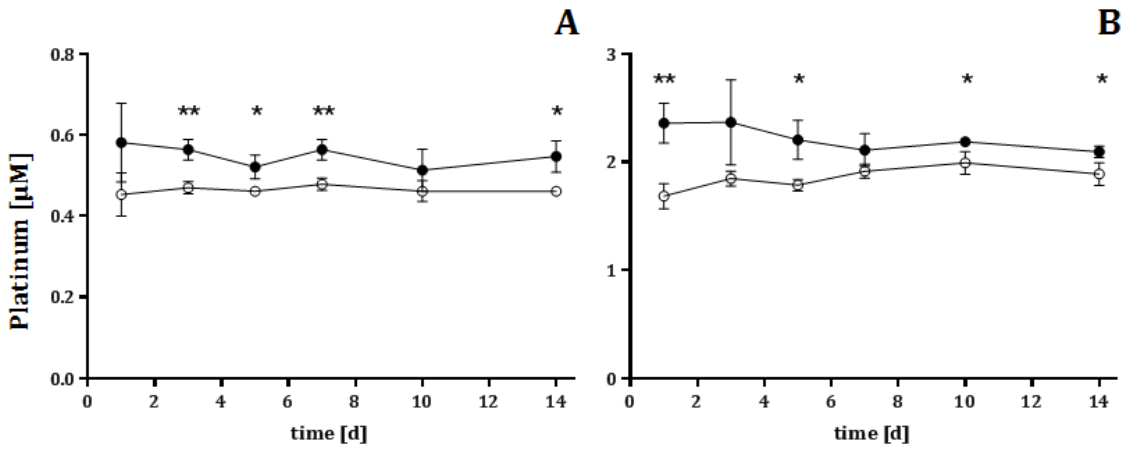

Figure 26. *Extracellular platinum concentration-time curves in RPTECT/TERT1 cells. Platinum concentrations were measured by ICP-MS in medium (● apical, ○ basolateral) after treatment with 0.5 µM (A) and 2 µM cisplatinum (B) for 24 h on day 0, 2, 4, 6, 9 and 13. Mean (± SD) of three biological replicates is shown. Statistical significance was tested by two-tailed, unpaired Student's t-test. Asterisk (*) indicates p-values < 0.05 and (**) p<0.01.*

Although intracellular platinum concentrations were higher after multiple exposures, generated mass balances indicate no bioaccumulation after 0.5 and 2 µM cisplatinum treatment for 14 days (Figure 27). The intracellular platinum content accounts for 2.1 ± 0.5% and 1.6 ± 0.5% of the administered low and high concentrations, respectively, after 14 days. No statement can be made regarding cisplatinum biotransformation, because the whole platinum amount was analyzed. No platinum was detected in plastic adsorption samples.

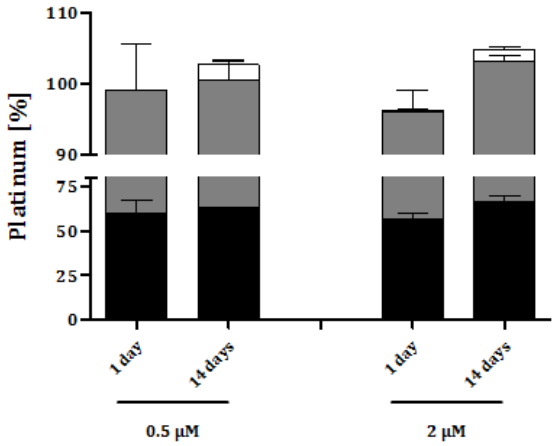

Figure 27. *Platinum mass balances in RPTEC/TERT1 cells. Measured platinum concentrations in medium (■ basolateral and ▭ apical) and cells (▭) were related to concentrations determined in vehicle. Mass balances were calculated after treatment with 0.5 µM and 2 µM cisplatinum for 1 and 14 days. Mean (± SD) is given for three biological replicates.*

4. Discussion

4.1. Cyclosporine A kinetics

4.1.1. Hepatic *in vitro* models

Nephro-, hepato- and neurotoxicity are known to be induced by the cyclic peptide CsA (Klintmalm *et al.*, 1981; Atkinson *et al.*, 1983; Bennett and Pulliam, 1983; Palestine *et al.*, 1984; Klintmalm *et al.*, 1985; Gijtenbeek *et al.*, 1999). Nephrotoxicity in humans and hepatotoxicity in rats are related to CsA bioaccumulation, while hepatotoxicity in humans occurred, despite lack of bioaccumulation (Cunningham *et al.*, 1985; Lu *et al.*, 2004). The mechanism of hepatotoxicity involves inhibition of transporters and enzymes leading to cholestasis and pericholangitis (Moran *et al.*, 1998; Oto *et al.*, 2010; Sharanek *et al.*, 2014).

Three different hepatic cell culture models were chosen for the investigation of CsA kinetics after repeated daily exposure at two different CsA concentrations. CsA treatment levels were selected by TC_{10} determination after 14 days, specifically determined for each *in vitro* system. The low, non-toxic CsA concentration was 10% of the respective high concentration. PRH, PHH and HepaRG cells were exposed repeatedly to CsA for up to 14 days. CsA amounts were determined in medium, cells and adsorbed to plastic at five different sampling time-points on the first and last exposure day. The resulting CsA kinetic profiles were different in the three *in vitro* approaches.

Limited CsA uptake in PRH treated with 0.25 µM might be attributed to efficient active efflux by Pgp, which results in absence of bioaccumulation after 14 days (Fricker and Fahr, 1997). By contrast, high concentration (2.5 µM) treatment led to significant CsA accumulation. Although, this effect can be biased by CsA trapping to sandwich layers consisting of collagen, generated blank studies revealed only minor and inconsistent CsA binding to collagen. Hence, the assessed accumulation is presumably occurring inside the cells. CsA kinetics in PHH showed efficient CsA uptake and biotransformation. For PHH I, the demonstrated low CYP3A4/5 activity was in accordance with the CsA kinetic profile illustrating low extent of CsA biotransformation. Equally, PHH II expressing high enzyme activity also exhibited efficient CsA biotransformation. Although CYP3A4/5 activity in PHH III was categorized as low, it was higher than in PHH I. In fact, CsA biotransformation was approximately in the same magnitude as for PHH II. Both, CsA

and midazolam, the test substrate to evaluate CYP3A4/5 activity, are known substrates for CYP3A4/5 (Combalbert *et al.*, 1989; Christians and Sewing, 1993; Fahr, 1993; Hamaoka *et al.*, 2001; Kelly and Kahan, 2002). However, contrary data are available regarding midazolam biotransformation with midazolam being mainly metabolized by CYP3A4/5, but also being a substrate for CYP2D6 (10% contribution) and CYP2C19 (2% contribution) (Ekins *et al.*, 1998; Turpeinen *et al.*, 2005). In this study, the contribution of CYP2D6 on midazolam biotransformation seems to be of less relevance as both PHH II and PHH III showed high CYP2D6 activity. CYP2C19 activity could not be assessed by the applied mixture for enzyme activity assessment. Hence, the determined CYP3A4/5 activity in PHH II might be overestimated due to high CYP2C19 activity and could be in the same range as for PHH III, but for both still being higher than for PHH I. However, CsA levels were enriched in cells of all donors after repeated exposure to 7 µM. This can be a result of three different effects caused by CsA. First, blank studies demonstrated significant CsA binding to the sandwich layers (Geltrex™). Second, besides CsA being a substrate for CYP3A4/5, it also inhibits CYP3A4/5 (Amundsen *et al.*, 2012). Finally, primary cell cultures lose time-dependently enzyme activity during culture (LeCluyse *et al.*, 2012; Soldatow *et al.*, 2013). Indeed, when CYP3A4/5 activity in PHH I-III was determined after 14 days with and without CsA treatment, a time-dependent decrease without CsA was observed, which was more emphasized by CsA exposure. Therefore, the observed enrichment, which did not lead to significant CsA bioaccumulation, might be an effect of both Geltrex™ trapping and enzyme inhibition. Efficient CsA uptake and biotransformation was detected in HepaRG cells for both treatment levels over 14 days. Although CYP3A4/5 activity is increasing with time at confluence, CsA biotransformation was constant (Josse *et al.*, 2008). It might be possible that increasing enzyme activity was abolished by CsA-induced CYP3A4/5 inhibition.

Determination of the actual applied CsA concentration in vehicles was beneficial. Although, PHH were supposed to be treated with 0.7 and 7 µM CsA, the actual concentration was significantly lower. This difference from the nominal concentration would be accounted to biotransformation and would result in a significant overestimation of clearances. Further, high standard deviations were observed for PRH and HepaRG cells, which should not be attributed to biological inter-assay variability of the systems, but rather to different applied CsA concentrations between replicates as a consequence of pipetting errors or storage of stock solution in plastic devices.

Scaled $Cl_{in\ vitro}$ could be directly compared to clearances obtained *in vivo* after intravenous administration. As CsA is eliminated predominantly by the liver, systemic clearance can be assumed to equal hepatic clearance (Ducharme *et al.*, 1995). Calculated clearances confirmed that PRH possess the lowest biotransformation capacity in comparison to PHH and HepaRG cells. This is supported by *in vivo* studies identifying the rat as a poor model for biotransformation via CYP3A4/5 (Zuber *et al.*, 2002). The rat orthologous CYP3A1 does not metabolize many typical substrates of human CYP3A (Zuber *et al.*, 2002). However, PRH clearances are 10–fold overestimated in comparison to *in vivo*. A reason for this outcome might be explained by inadequate assumptions made for scaling, particularly the fraction unbound in blood, where parameters were estimated for humans and assumed to be identical for rats (Jamei *et al.*, 2014). Further, the nonspecific binding of CsA in hepatocytes was assumed for both systems to be 1, which might be different for PRH. In fact, nonspecific binding to hepatocytes has a significant impact on the estimation of intrinsic clearances of drugs and prediction of nonspecific binding is hampered by inaccurate determination of partition (logP) and distribution coefficients (logD) in the lipophilicity area > 3 (CsA logP = 2.92) (Lewis, 2000; Kilford *et al.*, 2008). For PHH, scaled clearances were approximately 2-fold overestimated, albeit one would expect major inter-donor variability and an underestimation due to different, but low, CYP3A4/5 activities between donors. Obtained clearances for HepaRG cells were approximately 2-fold overestimated. For clearance calculations the seeded cell number was used for HepaRG cells (0.25×10^6 cells per well). In fact, the cell number increases until the start of experiment and cells differentiate to hepatocytes and not-metabolizing biliary cells. However, recalculations integrating higher cell numbers (up to 2.0×10^6 cells per well) had no large influence on this outcome. Another possibility might be the constantly higher CYP3A4/5 activity in HepaRG cells. It should be assessed, if the 2-fold overestimation by PHH and HepaRG cells in this experimental design is in accordance with other compounds underlying only CYP3A4/5 biotransformation. In that case, the factor 0.5 could be included as scaling factor in estimations by similar experiments performed on PHH and HepaRG cells. It has to be considered that a very simplified method for calculation of *in vitro* clearances was used. Hence, calculated clearances should be verified by physiologically-based pharmacokinetic modeling, where more complex biological processes are included, e.g. transporter and enzyme activities.

Most studies for evaluation of clearances *in vitro* are conducted in cell suspensions and, similar to this study, the depletion of parent compounds is determined in advance of metabolite formation (Lu *et al.*, 2006; Zanelli *et al.*, 2012). Although the applied compound concentration is considered, plastic binding is completely ignored. In the case of CsA, the assessed data clearly indicate a significant contribution of adsorption to plastic devices, resulting in a nominal decrease of CsA concentrations not due to biological processes, which should be included for correct data interpretation. Here, *in vitro* clearances were obtained only from intracellular CsA kinetics. For extrapolation to the *in vivo* situation, e.g. concentration-time profiles in blood or tissue concentrations, determined concentrations in all compartments (vehicle, medium, cells and plastic) need to be taken into account by physiologically-based pharmacokinetic modeling.

Concentration-range experiments revealed that PRH were more susceptible than human derived hepatocytes. This outcome together with low observed capacity for biotransformation in PRH, would lead to the conclusion that CsA biotransformation results in detoxification. In fact, CsA biotransformation products were shown to be significantly less active than CsA (Beauchesne *et al.*, 2007). Finally, CsA trough levels determined after 14 day exposure were approximately 0.05 µM and 1.5 for PHH after low and high concentration treatment, respectively, as well as 0.01 µM and 0.5 µM for HepaRG cells. Hence, CsA treatment leading to constant blood concentration in a range from 0.01 to 0.05 µM, should not lead to hepatotoxicity in patients. It has to be considered that measured CsA trough concentrations in PHH and HepaRG cells were evaluated in serum-free and medium containing only 2% FCS, respectively. Taking into account CsA binding in whole blood, where 33% of CsA is recovered in plasma and out of this 2% is unbound to plasma proteins, results in putative non-toxic CsA concentration in a range from 1.5 to 7.5 µM. The therapeutic window of CsA trough levels ranges from 0.08 µM to 0.166 µM in whole blood and exceeding CsA concentrations lead to adverse effects (Beauchesne *et al.*, 2007; Aktories *et al.*, 2013). Hence, the estimated "non-toxic" range would result in lethal concentrations for human, but might be diminished by the implementation of safety factors. This must be validated by additional experiments.

4.1.2. Brain cell culture models

CsA-induced neurotoxicity is not necessarily related to elevated blood levels, as neurotoxicity was also observed in patients with CsA blood levels within the therapeutic range (Serkova *et al.*, 2004). Various symptoms have been reported in patients receiving

CsA, while the common feature is that termination of CsA treatment leads to convalescence (Gijtenbeek *et al.*, 1999). There is lack of data describing both neurotoxicity and CsA kinetics in brain tissue. Hence, CsA kinetics was studied in rodent brain culture models at a high (TC_{10}) and low (non-toxic) CsA concentration after single and repeated exposure every second day.

For both the 2D and the 3D model, CsA steady state levels were achieved within 30 min on the first treatment day. Neither concentration- nor time-dependent changes of the kinetic profiles were observed for both *in vitro* models resulting in missing bioaccumulation and biotransformation. This indicates a chemical equilibrium of CsA distribution between the aqueous (medium) and organic (cell membrane, myelin, plastic) phase, which is in correlation with previous observations (Cefalu and Pardridge, 1985). Simultaneously, CsA-induced cyclophilin B secretion, an indicator for intracellular CsA uptake, was determined for the 3D model after low and high concentration treatment (evaluated by project participant) (Wilmes *et al.*, 2013; Bellwon *et al.*, 2015 DOI: 10.1016/j.tiv.2015.01.003). On the contrary, rapidly achieved CsA equilibrium and missing biological activity (biotransformation, accumulation) detected for both brain cell cultures suggest major CsA content outside the cells attached to the membrane. In comparison to the hepatic models, particularly to PRH, similar results were obtained with fast achieved apparent CsA steady state levels, but repeated high concentration treatment led to CsA bioaccumulation in PRH. The hypothesis arose that the major uptake route of CsA is not via passive diffusion, but mediated by active transporters present in the hepatic models and missing in the brain cell cultures.

The relevance of the obtained results for the *in vivo* scenario regarding CsA-induced neurotoxicity, remains a major question. In order to relate the generated *in vitro* data to *in vivo* brain tissue, it is essential to know the potential of CsA crossing the blood-brain barrier. *In vivo* data describe low CsA levels in human, rat and mouse brain tissue (Atkinson *et al.*, 1982; Niederberger *et al.*, 1983; Boland *et al.*, 1984; Wagner *et al.*, 1987; Lensmeyer *et al.*, 1991). Simultaneously, studies on a blood-brain barrier model were performed within “Predict-IV” and revealed very low permeability for CsA across the blood-brain barrier as well as no damage of the blood-brain barrier integrity by repeated CsA treatment for 14 days, which is in agreement with previous reports (Pardridge *et al.*, 1990; Lohmann *et al.*, 2002). In addition, the free available CsA amount in brain tissue was modeled for therapeutic plasma levels to be in a range from 3 to

10 nM, indicating that cytotoxic CsA concentrations are not reached in brain tissue (Schultz *et al.*, 2015, submitted). However, CsA-induced neurotoxicity is occurring and it might be possible, that it is not an effect of CsA directly in the CNS. CsA is a potent inhibitor of enzymes and transporters, including Pgp, bile salt export pump (BSEP) and multidrug resistance associated protein 3 (MRP3) (Saeki *et al.*, 1993; Tsuji *et al.*, 1993; Giacomini *et al.*, 2010). The saturation of blood-brain barrier efflux transporters by CsA might be relevant regarding elevated brain tissue levels of other substances than CsA itself as observed for colchicine, ivermectin, paclitaxel and verapamil (Hendrikse *et al.*, 1998; Marques-Santos *et al.*, 1999; Kemper *et al.*, 2003; Hsiao *et al.*, 2006; Wason *et al.*, 2012; Fabulas-da Costa *et al.*, 2013). Therefore CsA might facilitate neurotoxicity induced by exogenous and endogenous substances due to CsA-induced impairment of the blood-brain barrier homeostasis by inhibition of transport systems.

4.1.3. Transporter experiments

Although it is widely assumed that CsA is crossing the membrane by simple passive diffusion, contrary observations were reported (Ziegler *et al.*, 1988; Sanghvi *et al.*, 1989; Takayama *et al.*, 1991; Augustijns *et al.*, 1993; Fricker *et al.*, 1996). The molecular mass, chemical structure and properties indicate limited ability of CsA crossing the membrane by diffusion (Lipinski *et al.*, 1997; Ghose *et al.*, 1999). Comparison of obtained CsA kinetic profiles on the hepatic models and brain cell cultures indicates that in brain culture models biological processes play a minor role. It seems that CsA is mostly trapped to the cell membrane, which implicates that CsA major uptake route is active or carrier-mediated. Aim of the study was not to discover a potential transport system for CsA, but to prove whether CsA diffusion across membranes is a feasible uptake route. This aspect can be kept by PAMPA, which accounts only for passive diffusion (Kansy *et al.*, 1998). However, a combination of PAMPA and Caco-2 cells, possessing functional transport systems, is advised as comparison of gained data on both systems provide higher confidence of predicted permeability (Kerns *et al.*, 2004).

PAMPA and blank experiments showed, that the majority of CsA was trapped in lipophilic compartments, i.e. artificial membrane, plastic of well walls and filter inserts. Calculated P_{app} values obtained by PAMPA and blank studies indicate low permeability when comparing with data of high, e.g. verapamil (8.16×10^{-6} cm/s), and low permeability standards, e.g. theophylline (0.12×10^{-6} cm/s), ergonivine ($0.00\text{-}0.04 \times 10^{-6}$ cm/s) (Liu *et al.*, 2003; Kerns *et al.*, 2004). This outcome might be

questioned as poor predictability of diffusion for substances with low aqueous solubility has been reported and should be avoided by use of solubilizer (Liu *et al.*, 2003). However, this aspect is only correct for substances that precipitate in the aqueous solvent used, which was not observed for CsA under the chosen conditions. Findings on Caco-2 cells revealed significant CsA uptake and biotransformation, which was more emphasized in AB than BA direction confirming previous reported data (Gan *et al.*, 1996). Reason for this is the interaction of CYP3A4/5 and Pgp efflux pump with the latter being located at the apical membrane in Caco-2 cells (Cordon-Cardo *et al.*, 1990). CsA is taken up by the cells and is metabolized partly by CYP3A4/5 or extruded by Pgp to the apical compartment. Repeated cycles of this scenario lead to the higher biotransformation in AB direction (Watkins, 1997; Benet and Cummins, 2001). CsA P_{app} values for Caco-2 cells were significantly higher than for PAMPA and blank experiments after low and high concentration treatment, indicating that transporters might be involved for both intracellular influx and efflux. Overall highest P_{app} values were obtained for Caco-2 BA experiments, these can be explained by significant CsA extrusion by Pgp into the apical compartment (Cordon-Cardo *et al.*, 1990). Further, calculated efflux ratios (P_{app} BA/P_{app} AB), which decreased with higher CsA concentration, confirm active efflux mediated by Pgp and its inhibition by CsA due to saturation of the transporters capacity (Saeki *et al.*, 1993; Takeguchi *et al.*, 1993). Taken all together, obtained results underline the possibility that CsA is presumably located in the membrane when uptake pathways other than passive diffusion are not present. A possible carrier-mediated CsA uptake mechanism was suggested to occur via the low density lipoprotein receptor (Sanghvi *et al.*, 1989; Chung and Wasan, 2004).

4.2. Adefovir dipivoxil

ADV acts as nucleotide analog for endogenous deoxyadenosine triphosphate after intracellular activation to ADV diphosphate (Qaqish *et al.*, 2003). ADV diphosphate is incorporated specifically into viral DNA during DNA elongation with exhibiting higher affinity to viral polymerase than to human (Danta and Dusheiko, 2004). ADV has poor oral bioavailability (approximately 12%) (Cundy *et al.*, 1995). Hence, the diester prodrug ADVd was developed in order to mask the negative charge of ADV at physiological pH and consequently to improve membrane permeability (Cundy *et al.*, 1995; Bi *et al.*, 2005; Ming and Thakker, 2010). For treatment, 10 mg ADVd is applied once daily and is well tolerated following 48 week of treatment (Kahn *et al.*, 1999).

However, nephrotoxicity was also observed in patients following 10 mg ADVd long-term treatment for up to 30 months (Ha *et al.*, 2009).

ADVd was added daily at a low, non-cytotoxic (2.5 µM) and high, TC_{10} (8 µM) concentration to the human derived cell line RPTEC/TERT1 for up to 14 days. ADVd and ADV were determined in vehicle, medium, cells and plastic at five different time-points on day 0 and day 13. Due to detected degradation of ADVd during LC-MS/MS analyses performed at room temperature (22°C), ADVd stability was examined in RPTEC/TERT1 serum-free culture medium at 37°C for 24 h. Time-dependent ADVd degradation was detected, where ADVd decomposed to at least one unknown intermediate and ADV. In addition to ADV, ADV monopivoxil (Figure 28) formation was observed *in vitro* after ADVd treatment, while both ADVd and ADV monopivoxil are undetectable in blood *in vivo* after oral administration of ADVd (Cundy *et al.*, 1994; Shaw *et al.*, 1997; Sun *et al.*, 2007; Maeng *et al.*, 2012). However, obtained results suggest that the observed degradation of ADVd occurs without enzyme activity and is time- as well as temperature-dependent. The differences between vehicles received from two laboratories can be explained by dissimilar handling during conduct of experiments. While "lab 6" performed several experiments at the same time leading to longer incubation of ADVd vehicle solutions at room temperature (approximately 29°C), "lab 7" conducted only experiments with ADVd. Explanation for the differences in vehicle composition between project participants and in-house vehicles is the preparation of ADVd solutions. Participants ("lab 6" and "lab 7") dissolved ADVd (9.9 mM) in 1 N sodium hydroxid, which may enhance ADVd degradation, while in-house solutions were prepared in water (0.5 mM).

Discrepancies in composition of vehicles had a major impact on the intracellular ADV kinetic profiles. No ADV was recovered in cells treated with vehicle consisting mainly of ADV ("lab 6"), while intracellular uptake and elimination following 1st order kinetics for cells treated with vehicles consisting mostly of ADVd and an unknown intermediate ("lab 7"). However, the intracellular ADV kinetic profiles obtained from experiments conducted at "lab 7" were unexpected, as the administered drug was still present in medium, while intracellular uptake stopped. ADV is taken up by cells via hOAT1/3 transport systems and due to its hydrophilic character passive diffusion through the cell membrane is limited (Uwai *et al.*, 2007; Ming and Thakker, 2010). RPTEC/TERT1 cells seem to not exhibit functional hOAT1/3 transporters and consequently ADV uptake is

not occurring. On the other hand, ADVd and ADV monopivoxil are more lipophilic due to esterification (Figure 28) and both compounds might be able to cross cell membranes by passive diffusion. The observed intracellular uptake in cells from "lab 7" is a result of ADVd and ADV monopivoxil, being mostly present in vehicles, diffusing through the membrane. Due to the time- and temperature-dependent decomposition, ADVd and ADV monopovoxil are degraded to hydrophilic ADV, which leads to the sudden stop of intracellular uptake, although ADV is still present. Intracellular ADV might be phosphorylated or excreted, which is illustrated by the intracellular ADV decrease.

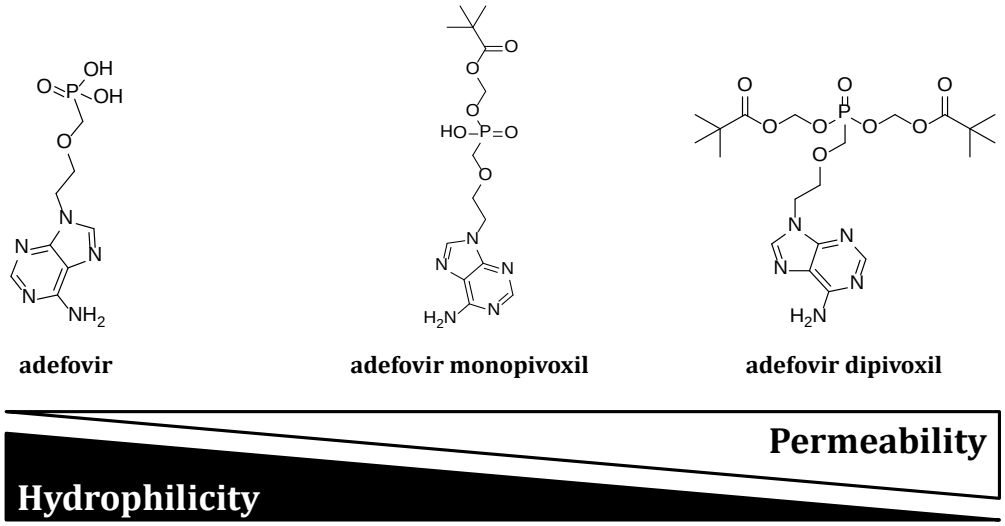

Figure 28. *Chemical structures of adefovir, adefovir monopivoxil and adefovir dipivoxil. Related hydrophilicity is decreasing by esterification. Simultaneously, permeability through membranes is increasing.*

However, not considering the mentioned aspects (ADVd degradation, limited uptake), would lead to the conclusion, that ADVd is poorly taken up by the kidney and 2.5 µM blood concentration will not cause nephrotoxicity. In fact, ADVd is not reaching the molecular target *in vivo*, but ADV. Further, ADV is excreted mainly by the kidneys with 90% of the administered intravenous dose being recovered unchanged in urine (Cundy *et al.*, 1995). Barditch-Crovo *et al.* (1997) determined ADV pharmacokinetics in patients following daily treatment with ADVd at three dose levels (125, 250 and 500 mg) for 14 days. ADV peak concentrations in blood were not significantly elevated after 14 days of treatment (day 1; 125 mg: 0.12 µM, 250 mg; 0.23 µM, 500 mg: 0.42 µM), but even decreased (day 14; 500 mg: 0.32 µM) in the high dose group due to decreased bioavailability. The amount of ADV recovered in urine corresponded to the determined bioavailability (normalized to the administered dose) in patients receiving 125 and

250 mg ADVd. The ADV amount recovered in urine was lower than the adsorbed ADV amount in patients of the high dose group (500 mg) on the first and the last treatment day, suggesting ADV bioaccumulation within the kidneys. By contrast, even 8 µM ADVd exposure to RPTEC/TERT1 cells, seems not to impair biotransformation/elimination.

Again determination of vehicle solutions was a benefit. In this case not the applied concentrations were different, but the composition of the vehicle, which explained the difference in achieved kinetic profiles. Further, a compound's stability is a crucial factor that needs to be determined, prior to conducting *in vitro* studies, otherwise correct data interpretation and *in vitro* to *in vivo* extrapolation is hampered significantly. RPTEC/TERT1 cells possess high differentiation status, lead to reproducible results and are a stable, well-characterized system (Wieser *et al.*, 2008). Although transcriptomics and western blot analyses support the presence of hOAT1/3 transporter systems, their functionality might be doubted with respect to poor ADV uptake into cells. Indeed, poor functionality of hOAT1/3 was proven by independent transporter experiments performed by a project participant.

In comparison to CsA kinetics, low standard deviations obtained for ADVd experiments indicate only minor inter-assay variability. Replicates of the ADVd experiments were performed on the same day reducing aberrations in seeded cell numbers, pipetting errors and influence of storage conditions for stock solutions, when vehicles are prepared.

4.3. Cisplatinum

Cisplatinum is used as antineoplastic agent and has a broad spectrum of activity against malignancies of lung, head, neck, esophagus, bladder, cervix, endometrium and testis (Prestayko *et al.*, 1979; Go and Adjei, 1999; Miller *et al.*, 2010). The drug is administered intravenously either on a single day or during 5 consecutive days and is repeated every three weeks (Ihde *et al.*, 1994). However, major dose-limiting factor is cisplatinum-induced nephrotoxicity (Arany and Safirstein, 2003).

RPTEC/TERT1 cells were exposed daily to 0.5 µM (non-toxic) and 2 µM (TC_{10}) cisplatinum for up to 14 days. Samples were generated at five time-points on the first and last treatment day. Platinum concentrations were quantified in vehicle, medium, cells and plastic by ICP-MS. As total platinum amount was quantified, no statement can be made regarding cisplatinum biotransformation. Analyses of medium samples

revealed significant platinum increase in the apical compartment, while the platinum content decreased simultaneously within 24 h treatment cycles. These findings were made for both treatment levels and are in agreement with the *in vivo* situation. Cisplatinum intracellular uptake is mediated by hOCT2 and CTR1 transporter systems, which are present at the basolateral side (Ciarimboli *et al.*, 2005; Pabla *et al.*, 2009). Extrusion of cisplatinum occurs by active transporter MATE1 at the apical surface (Nakamura *et al.*, 2010). Hence, RPTEC/TERT1 cells possess transporter activities for cisplatinum uptake as well as for extrusion and maintain functional, apical-to-basolateral cell polarization (Wieser *et al.*, 2008). However, no significant platinum bioaccumulation was observed after low and high concentration treatment, although platinum concentrations were slightly enriched after 14 days. Missing bioaccumulation might be explained by the possibility that cisplatinum did not reach the steady state level as modeled by physiologically-based pharmacokinetic modeling (Wilmes *et al.*, 2014). Cisplatinum-induced nephrotoxicity is related to bioaccumulation in the kidney, particularly in the renal cortex, where toxic platinum concentrations range from 2 to 24 nmol/g tissue (Stewart *et al.*, 1985). Most studies analyze total platinum content in blood and tissue, despite that cisplatinum is a highly reactive molecule. In aqueous solutions, the chloride ligands of cisplatinum are replaced reversibly by water resulting in issues regarding the formulation of stable dosage forms of cisplatinum (Long and Repta, 1981). Although, cisplatinum stability is increased by addition of chloride, less is known on its stability in whole blood (Hincal *et al.*, 1978; Long and Repta, 1981). After intravenous administration, 90% of cisplatinum whole blood content is bound to plasma proteins (DeConti *et al.*, 1973). The free available unchanged cisplatinum concentrations seem to correlate with occurring nephrotoxicity in patients recommending that peak concentrations of free cisplatinum should not exceed the range of 5 to 7 nM (Nagai *et al.*, 1996). Comparison with the cisplatinum concentrations applied to RPTEC/TERT1 cells is hampered as total platinum amount was determined and chloride was not added for stabilization. Consequently, formation of cisplatinum complexes with hydroxyl ions cannot be excluded. Himmelstein *et al.* (1981) analyzed total platinum and intact cisplatinum in blood after intravenous cisplatinum administration to human and discovered that approximately 50% of the total platinum amount accounts for cisplatinum at peak levels. Hence, RPTEC/TERT1 cells tolerated about 50-fold higher cisplatinum concentrations not taking into account that *in vivo* applied cisplatinum is distributed across all organs with highest preference

to liver and kidney (Stewart *et al.*, 1982). Although cisplatinum bioaccumulation is also taking place in the liver, cisplatinum-induced hepatotoxicity is infrequently (Stewart *et al.*, 1985). Therefore, beside aquated cisplatinum as potential toxic agent, kidney-specific bioactivation of cisplatinum may lead to formation of nephrotoxins. A potential pathway is proposed by Townsend *et al.* (2003) and is similar to the nephrotoxin formation of halogenated alkenes. This pathway is initiated by glutathione conjugation of cisplatinum, biotransformation in the liver or spontaneously in blood, followed by cleavage of gamma-glutamyl bonds and decomposition to cisplatinum-cysteine conjugates catalyzed by gamma-glutamyl transpeptidase and aminodipeptidase, respectively, at the extracellular, apical surface area of proximal tubule cells (Townsend *et al.*, 2003). Resulting cysteine-conjugates might be taken up inside cells and biotransformation resulting in thiols might appear (Townsend *et al.*, 2003). Therefore, higher tolerated cisplatinum concentrations in RPTEC/TERT1 cells might be related to either slower bioactivation or slower re-uptake of cysteine conjugates. However, future studies using a similar approach can give new insights by considering cisplatinum biotransformation products.

4.4. Conclusion

Repeated daily treatment of stable, well-characterized *in vitro* systems, first introduced by “Predict-IV”, may move the scientific area a step closer to the claimed “3R principles”. Studies were performed successfully under serum-free or nearly serum-free (2% FCS for HepaRG cells) culture conditions. Serum provides a number of factors, e.g. hormonal for stimulation of cell growth, as well as binding and transport proteins, essential for cell culture (Brunner *et al.*, 2010). On the other hand, the use of serum involves variability due to variations between serum batches, may contain adverse factors such as endotoxins and might be a potential source for microbiological contamination (Gstraunthaler, 2003; Brunner *et al.*, 2010). Besides, ethical issues were mentioned regarding harvest, production and process of serum (Gstraunthaler, 2003).

For the first time cell systems have been treated daily for 14 days mimicking the *in vivo* situation without wasting of time and costs. CsA bioaccumulation was clearly evident in PRH, an outcome that is not captured by single administration. In this context, the choice of two treatment levels (toxic and non-toxic) was advantageous, as bioaccumulation was missing after treatment of PRH with the low concentration, while it occurred at the high treatment level. The benefit of long-term exposure to at least two concentration levels

was also confirmed by experiments performed on the brain cell culture models. Kinetic profiles were similar to CsA kinetics in PRH after single administration, but distinguished from PRH after repeated exposure with still exhibiting stable CsA concentrations for both applied concentrations. Separate analyses of compartments, i.e. cells, medium and plastic, revealed that CsA distribution reached rapidly a chemical equilibrium. These findings led to the hypothesis that major intracellular uptake of CsA is not via passive diffusion. Although transporter experiments support the hypothesis, it will become clearer when a transport system has been identified. The convenience of separate compartment analyses was verified by transporter experiments. CsA was recovered mainly in plastic and membrane, while active transporters were not present. Further, experiments performed on RPTEC/TERT1 cells revealed specific apical to basolateral cisplatinum transport, which would have been missed by pooling apical and basolateral medium samples. Furthermore, the low, but evident, intracellular uptake of cisplatinum as well as ADV and consequent ADV extrusion/biotransformation would not have been covered by avoiding the analyses of cell lysate samples apart from medium.

Finally, plastic adsorption turned out to be apparent and should be considered by modeling approaches leading to estimation of cellular processes *in vitro*, which can be used for subsequent scaling to *in vivo*. The CsA amount adsorbed to plastic was different for each system. This might be an effect of different plastic devices, but seems to be more affected by cells. Blank experiments showed that CsA is almost completely adsorbed to plastic, when cells are absent, while plastic adsorption was significantly lower in the presence of Caco-2 cells presumably due to plastic surface covered by cell monolayers. Further for HepaRG cells, CsA adsorption to plastic was high at the start of treatment and decreased within 24 hours due to efficient biotransformation and consequently shifting the concentration gradient.

Comparison of *in vitro* kinetic parameters with *in vivo*, revealed for PHH and HepaRG cells good correlation regarding scaled clearances, which has to be proven by similar experiments performed with other compounds. The same is true for PRH and RPTEC/TERT1 cells. The determined aberrations to the *in vivo* situation such as the overestimation of clearances for CsA treated PRH, low intracellular cisplatinum concentrations in RPTEC/TERT1 cells, higher tolerated cisplatinum concentrations by RPTEC/TERT1 cells, does not exclude these systems. Intra- and extracellular compound concentrations should be extrapolated by physiologically-based pharmacokinetic

modeling to get better estimates of the *in vivo* situation. Furthermore, possible aberration between *in vitro* and in *vivo* should be confirmed to be constant across similar compounds, in order to establish specific scaling factors. However, performed experiments with ADVd pointed out potential pitfalls by *in vitro* approaches. ADVd-induced nephrotoxicity would be underestimated or even categorized as not relevant for *in vivo* without considering that ADV is not taken up by this *in vitro* approach, which is not in accordance with the *in vivo* scenario. The issues of a compound's stability as well as its intracellular uptake *in vivo* have to be addressed, when *in vitro* data are interpreted.

Taken all together, this new experimental design displays reasonable potential. However, it has to be considered that well-studied compounds were used. Hence, a lot of information was present regarding biotransformation, intracellular uptake as well as extrusion processes, excretion route and target organs for adverse effects. In order to predict potential adverse effects *in vivo* caused by drugs in the developmental phase, a lot of research has to be included such as compound stability, potential uptake route and biotransformation (detoxification or toxification). Besides, *in vitro* systems account for one (rarely more) part(s) of an organ, while toxicity might be facilitated by the interaction of the whole organism. In the next future, this long-term *in vitro* experimental set-up can be applied on co-culture systems or organs-on-chips and be combined with physiologically-based pharmacokinetic modeling as well as system biology to understand and extrapolate the obtained data resulting in a reduction of animal testing for repeated dose toxicity studies.

5. References

Adler, S., Basketter, D., Creton, S., Pelkonen, O., Van Benthem, J., Zuang, V., Andersen, K.E., Angers-Loustau, A., Aptula, A., Bal-Price, A., 2011. Alternative (non-animal) methods for cosmetics testing: current status and future prospects—2010. Archives of toxicology **85**, 367-485.

Aktories, K., Förstermann, U., Hofmann, F.B., Starke, K., 2013. Allgemeine und spezielle Pharmakologie und Toxikologie: Begründet von W. Forth, D. Henschler, W. Rummel. Elsevier Health Sciences Germany.

Alexandre, E., Baze, A., Parmentier, C., Desbans, C., Pekthong, D., Gerin, B., Wack, C., Bachellier, P., Heyd, B., Weber, J.C., Richert, L., 2012. Plateable cryopreserved human hepatocytes for the assessment of cytochrome P450 inducibility: experimental condition-related variables affecting their response to inducers. Xenobiotica; the fate of foreign compounds in biological systems **42**, 968-979.

Amundsen, R., Asberg, A., Ohm, I.K., Christensen, H., 2012. Cyclosporine A- and tacrolimus-mediated inhibition of CYP3A4 and CYP3A5 in vitro. Drug metabolism and disposition: the biological fate of chemicals **40**, 655-661.

Aoki, M., Okudaira, K., Haga, M., Nishigaki, R., Hayashi, M., 2010. Contribution of rat pulmonary metabolism to the elimination of lidocaine, midazolam, and nifedipine. Drug Metabolism and Disposition **38**, 1183-1188.

Arany, I., Safirstein, R.L., 2003. Cisplatin nephrotoxicity, Seminars in nephrology. Elsevier, pp. 460-464.

Arrowsmith, J., Miller, P., 2013. Phase II and Phase III attrition rates 2011-2012. Nature Reviews Drug Discovery **12**, 568-568.

Atkinson, K., Biggs, J., Dodds, A., Concannon, A., 1983. Cyclosporine-associated hepatotoxicity after allogeneic marrow transplantation in man: Differentiation from other causes of posttransplant liver disease, Conference: Transplantation Proceedings, pp.

Atkinson, K., Biggs, J.C., Britton, K., 1982. Distribution and Persistence of Cyclosporin in Human-Tissues. Lancet **2**, 1165-1165.

Augustijns, P.F., Bradshaw, T.P., Gan, L.-S.L., Hendren, R.W., Thakker, D.R., 1993. Evidence for a polarized efflux system in Caco-2 cells capable of modulating cyclosporine A transport. Biochemical and biophysical research communications **197**, 360-365.

Bailer, A.J., Piegorsch, W.W., 1990. Estimating integrals using quadrature methods with an application in pharmacokinetics. Biometrics, 1201-1211.

Baldrick, P., 2003. Toxicokinetics in preclinical evaluation. Drug Discovery Today **8**, 127-133.

Barditch-Crovo, P., Toole, J., Hendrix, C.W., Cundy, K.C., Ebeling, D., Jaffe, H.S., Lietman, P.S., 1997. Anti-human immunodeficiency virus (HIV) activity, safety, and pharmacokinetics of adefovir dipivoxil (9-[2-(bis-pivaloyloxymethyl)-phosphonylmethoxyethyl]adenine) in HIV-infected patients. J Infect Dis **176**, 406-413.

Beauchesne, P.R., Chung, N.S., Wasan, K.M., 2007. Cyclosporine A: a review of current oral and intravenous delivery systems. Drug development and industrial pharmacy **33**, 211-220.

Bellwon, P., Culot, M., Wilmes, A., Schmidt, T., Zurich, M.G., Schultz, L., Gramowski-Voss, A., Weiss, D.G., Jennings, P., Bal-Price, A., Testai, E., Dekant, W., 2015 DOI: 10.1016/j.tiv.2015.01.003. Cyclosporine A kinetics in brain cell culture and its potential of crossing the blood-brain barrier. Toxicology in Vitro, in this issue.

Benet, L.Z., Cummins, C.L., 2001. The drug efflux-metabolism alliance: biochemical aspects. Adv Drug Deliv Rev **50 Suppl 1**, S3-11.

Bennett, W.M., Pulliam, J.P., 1983. Cyclosporine nephrotoxicity. Annals of internal medicine **99**, 851-854.

Bernareggi, A., Rowland, M., 1991. Physiologic modeling of cyclosporin kinetics in rat and man. J Pharmacokinet Biopharm **19**, 21-50.

Bessems, J.G., Geraets, L., 2013. Proper knowledge on toxicokinetics improves human hazard testing and subsequent health risk characterisation. A case study approach. Regulatory Toxicology and Pharmacology **67**, 325-334.

Bessems, J.G., Loizou, G., Krishnan, K., Clewell III, H.J., Bernasconi, C., Bois, F., Coecke, S., Collnot, E.-M., Diembeck, W., Farcal, L.R., 2014. PBTK modelling platforms and parameter estimation tools to enable animal-free risk assessment: Recommendations from a joint EPAA–EURL ECVAM ADME workshop. Regulatory Toxicology and Pharmacology **68**, 119-139.

Bi, H.c., Zhong, G.p., Zhou, S., Chen, X., Huang, M., 2005. Determination of adefovir in human plasma by liquid chromatography/tandem mass spectrometry: application to a pharmacokinetic study. Rapid communications in mass spectrometry **19**, 2911-2917.

Blaauboer, B.J., 2010. Biokinetic modeling and in vitro–in vivo extrapolations. Journal of Toxicology and Environmental Health, Part B **13**, 242-252.

Blaauboer, B.J., Boekelheide, K., Clewell, H.J., Daneshian, M., Dingemans, M.M., Goldberg, A.M., Heneweer, M., Jaworska, J., Kramer, N.I., Leist, M., 2012. t4 workshop report:-The use of biomarkers of toxicity for integrating in vitro hazard estimates into risk assessment for humans. ALTEX-Alternatives to Animal Experimentation **29**, 411.

Boland, J., Atkinson, K., Britton, K., Darveniza, P., Johnson, S., Biggs, J., 1984. Tissue distribution and toxicity of cyclosporin A in the mouse. Pathology **16**, 117-123.

Bouvier, d.Y.M., Prieto, P., Blaauboer, B., Bois, F., Boobis, A., Brochot, C., Coecke, S., Freidig, A., Gundert-Remy, U., Hartung, T., 2007. Physiologically-based Kinetic Modelling (PBK Modelling): meeting the 3Rs agenda. The report and recommendations of ECVAM Workshop 63. Alternatives to laboratory animals: ATLA **35**, 661.

Broeders, J.J.W., van Eijkeren, J.C.H., Blaauboer, B.J., Hermens, J.L.M., 2012. Transport of Chlorpromazine in the Caco-2 Cell Permeability Assay: A Kinetic Study. Chemical Research in Toxicology **25**, 1442-1451.

Brunner, D., Frank, J., Appl, H., Schoffl, H., Pfaller, W., Gstraunthaler, G., 2010. Serum-free cell culture: the serum-free media interactive online database. ALTEX **27**, 53-62.

Calne, R., Rolles, K., Thiru, S., McMaster, P., Craddock, G., Aziz, S., White, D., Evans, D., Dunn, D., Henderson, R., 1979. Cyclosporin A initially as the only immunosuppressant in 34 recipients of cadaveric organs: 32 kidneys, 2 pancreases, and 2 livers. The Lancet **314**, 1033-1036.

Cefalu, W.T., Pardridge, W.M., 1985. Restrictive transport of a lipid-soluble peptide (cyclosporin) through the blood-brain barrier. J Neurochem **45**, 1954-1956.

Christians, U., Sewing, K.-F., 1993. Cyclosporin metabolism in transplant patients. Pharmacology & therapeutics **57**, 291-345.

Chung, N.S., Wasan, K.M., 2004. Potential role of the low-density lipoprotein receptor family as mediators of cellular drug uptake. Advanced drug delivery reviews **56**, 1315-1334.

Ciarimboli, G., Ludwig, T., Lang, D., Pavenstädt, H., Koepsell, H., Piechota, H.-J., Haier, J., Jaehde, U., Zisowsky, J., Schlatter, E., 2005. Cisplatin nephrotoxicity is critically mediated via the human organic cation transporter 2. The American journal of pathology **167**, 1477-1484.

Cihlar, T., Lin, D.C., Pritchard, J.B., Fuller, M.D., Mendel, D.B., Sweet, D.H., 1999. The antiviral nucleotide analogs cidofovir and adefovir are novel substrates for human and rat renal organic anion transporter 1. Molecular pharmacology **56**, 570-580.

Coecke, S., Pelkonen, O., Leite, S.B., Bernauer, U., Bessems, J.G., Bois, F.Y., Gundert-Remy, U., Loizou, G., Testai, E., Zaldívar, J.-M., 2013. Toxicokinetics as a key to the integrated toxicity risk assessment based primarily on non-animal approaches. Toxicology in Vitro **27**, 1570-1577.

Combalbert, J., Fabre, I., Fabre, G., Dalet, I., Derancourt, J., Cano, J.P., Maurel, P., 1989. Metabolism of cyclosporin A. IV. Purification and identification of the rifampicin-inducible human liver cytochrome P-450 (cyclosporin A oxidase) as a product of P450IIIA gene subfamily. Drug metabolism and disposition: the biological fate of chemicals **17**, 197-207.

Cordon-Cardo, C., O'Brien, J.P., Boccia, J., Casals, D., Bertino, J.R., Melamed, M.R., 1990. Expression of the multidrug resistance gene product (P-glycoprotein) in human normal and tumor tissues. The journal of histochemistry and cytochemistry : official journal of the Histochemistry Society **38**, 1277-1287.

Cundy, K.C., Barditch-Crovo, P., Walker, R.E., Collier, A.C., Ebeling, D., Toole, J., Jaffe, H.S., 1995. Clinical pharmacokinetics of adefovir in human immunodeficiency virus type 1-infected patients. Antimicrob Agents Chemother **39**, 2401-2405.

Cundy, K.C., Fishback, J.A., Shaw, J.-P., Lee, M.L., Soike, K.F., Visor, G.C., Lee, W.A., 1994. Oral bioavailability of the antiretroviral agent 9-(2-phosphonylmethoxyethyl) adenine (PMEA) from three formulations of the prodrug bis (pivaloyloxymethyl)-PMEA in fasted male cynomolgus monkeys. Pharmaceut Res **11**, 839-843.

Cunningham, C., Burke, M.D., Wheatley, D.N., Thomson, A.W., Simpson, J.G., Whiting, P.H., 1985. Amelioration of Cyclosporin-Induced Nephrotoxicity in Rats by Induction of Hepatic Drug-Metabolism. Biochemical pharmacology **34**, 573-578.

Danta, M., Dusheiko, G., 2004. Adefovir dipivoxil: review of a novel acyclic nucleoside analogue. Int J Clin Pract **58**, 877-886.

de Arriba, G., Calvino, M., Benito, S., Parra, T., 2013. Cyclosporine A-induced apoptosis in renal tubular cells is related to oxidative damage and mitochondrial fission. Toxicology letters **218**, 30-38.

De Ceuninck, F., Allain, F., Caliez, A., Spik, G., Vanhoutte, P.M., 2003. High binding capacity of cyclophilin B to chondrocyte heparan sulfate proteoglycans and its release from the cell surface by matrix metalloproteinases: possible role as a proinflammatory mediator in arthritis. Arthritis and rheumatism **48**, 2197-2206.

DeConti, R.C., Toftness, B.R., Lange, R.C., Creasey, W.A., 1973. Clinical and pharmacological studies with cis-diamminedichloroplatinum (II). Cancer Research **33**, 1310-1315.

Dekant, W., Vamvakas, S., 2005. Toxikologie: eine Einführung für Chemiker, Biologen und Pharmazeuten. Elsevier-Spektrum Akademischer Verlag.

Diehl, K.H., Hull, R., Morton, D., Pfister, R., Rabemampianina, Y., Smith, D., Vidal, J.M., Vorstenbosch, C.V.D., 2001. A good practice guide to the administration of substances and removal of blood, including routes and volumes. Journal of Applied Toxicology **21**, 15-23.

DiMasi, J.A., Feldman, L., Seckler, A., Wilson, A., 2010. Trends in Risks Associated With New Drug Development: Success Rates for Investigational Drugs. Clinical Pharmacology & Therapeutics **87**, 272-277.

Directive, C., 1986. 86/609/EEC of 24 November 1986 on the approximation of laws, regulations and administrative provisions of the Member States regarding the

protection of animals used for experimental and other scientific purposes. Off. J. Eur. Commun **29**, L358.

Ducharme, M.P., Warbasse, L.H., Edwards, D.J., 1995. Disposition of intravenous and oral cyclosporine after administration with grapefruit juice. Clinical pharmacology and therapeutics **57**, 485-491.

Ekins, S., Vandenbranden, M., Ring, B.J., Gillespie, J.S., Yang, T.J., Gelboin, H.V., Wrighton, S.A., 1998. Further characterization of the expression in liver and catalytic activity of CYP2B6. Journal of Pharmacology and Experimental Therapeutics **286**, 1253-1259.

Englund, G., Lundquist, P., Skogastierna, C., Johansson, J., Hoogstraate, J., Afzelius, L., Andersson, T.B., Projean, D., 2014. Cytochrome P450 Inhibitory Properties of Common Efflux Transporter Inhibitors. Drug Metabolism and Disposition **42**, 441-447.

European Commission, 2006. Regulation (EU) no. 1907/2006 of the European Parliament and of the Council of 18 December 2006 concerning the registration, evaluation, authorization and restriction of chemicals (REACH), establishing a European Chemicals Agency, amending Directive 1999/45/EC and repealing Council Regulation (EEC) no. 793/93 and Commission Regulation (EC) no. 1488/94, as well as Council Directive 76/769/EEC and commission Directives 91/155/EEC, 93/67/EEC, 93/105/CE and 2000/21/EC. Off J Eur Union L **396**, 1-849.

European Commission, 2009. Regulation (EU) No 1223/2009 of the European Parliament and of the Council of 30 November 2009 on cosmetic products. Off J Eur Union L **342**, 59-209.

European Commission, 2010. Directive 2010/63/EU of the European Parliament and of the Council of 22 September 2010 on the protection of animals used for scientific purposes. Off J Eur Union L **276**, 33-76.

Fabulas-da Costa, A., Aijjou, R., Hachani, J., Landry, C., Cecchelli, R., Culot, M., 2013. In vitro blood-brain barrier model adapted to repeated-dose toxicological screening. Toxicol In Vitro **27**, 1944-1953.

Fahr, A., 1993. Cyclosporin clinical pharmacokinetics. Clinical pharmacokinetics **24**, 472-495.

Fearon, P., Lonsdale-Eccles, A.A., Ross, O.K., Todd, C., Sinha, A., Allain, F., Reynolds, N.J., 2011. Keratinocyte secretion of cyclophilin B via the constitutive pathway is regulated through its cyclosporin-binding site. J Invest Dermatol **131**, 1085-1094.

Fichtl, B., Marquardt, H., Schafer, G., MaClellan, R., Welsch, F., 1999. Principles of toxicokinetics.

Filov, V., 1973. Mathematical Aspects of Pharmacokinetics and Toxicokinetics. Farmakologiya. Khimioterapevticheskiye sredstva. Toksikologiya. Problemy Farmakologii **5**, 9-80.

Fok, B.S., Gardner, S., Piscitelli, S., Chen, S., Chu, T.T., Chan, J., Tomlinson, B., 2013. Pharmacokinetic Properties of Single-Dose Lamivudine/Adefovir Dipivoxil Fixed-Dose Combination in Healthy Chinese Male Volunteers. Clinical therapeutics **35**, 68-76.

Follath, F., Wen, M., Vozeh, S., Thiel, G., Brunner, F., Loertscher, R., Lemaire, M., Nussbaumer, K., Niederberger, W., Wood, A., 1983. Intravenous cyclosporine kinetics in renal failure. Clinical Pharmacology & Therapeutics **34**, 638-643.

Fossler, M.J., Collins, D.A., Thompson, M.M., Nino, A., Bianco, J.J., Chetty, D., 2014. Pharmacokinetic Bioequivalence Studies of a Fixed-Dose Combination of Tamsulosin and Dutasteride in Healthy Volunteers. Clinical drug investigation **34**, 335-349.

Fracasso, P.M., Goldstein, L.J., de Alwis, D.P., Rader, J.S., Arquette, M.A., Goodner, S.A., Wright, L.P., Fears, C.L., Gazak, R.J., Andre, V.A., 2004. Phase I study of docetaxel in

combination with the P-glycoprotein inhibitor, zosuquidar, in resistant malignancies. Clinical cancer research **10**, 7220-7228.

Fricker, G., Drewe, J., Huwyler, J., Gutmann, H., Beglinger, C., 1996. Relevance of p-glycoprotein for the enteral absorption of cyclosporin A: in vitro-in vivo correlation. British journal of pharmacology **118**, 1841-1847.

Fricker, G., Fahr, A., 1997. Mechanisms of hepatic transport of cyclosporin A: an explanation for its cholestatic action? The Yale journal of biology and medicine **70**, 379.

Gan, L.S., Moseley, M.A., Khosla, B., Augustijns, P.F., Bradshaw, T.P., Hendren, R.W., Thakker, D.R., 1996. CYP3A-like cytochrome P450-mediated metabolism and polarized efflux of cyclosporin A in Caco-2 cells. Drug metabolism and disposition: the biological fate of chemicals **24**, 344-349.

Ghose, A.K., Viswanadhan, V.N., Wendoloski, J.J., 1999. A knowledge-based approach in designing combinatorial or medicinal chemistry libraries for drug discovery. 1. A qualitative and quantitative characterization of known drug databases. Journal of combinatorial chemistry **1**, 55-68.

Giacomini, K.M., Huang, S.M., Tweedie, D.J., Benet, L.Z., Brouwer, K.L.R., Chu, X.Y., Dahlin, A., Evers, R., Fischer, V., Hillgren, K.M., Hoffmaster, K.A., Ishikawa, T., Keppler, D., Kim, R.B., Lee, C.A., Niemi, M., Polli, J.W., Sugiyama, Y., Swaan, P.W., Ware, J.A., Wright, S.H., Yee, S.W., Zamek-Gliszczynski, M.J., Zhang, L., Transporter, I., 2010. Membrane transporters in drug development. Nature Reviews Drug Discovery **9**, 215-236.

Gijtenbeek, J., Van den Bent, M., Vecht, C.J., 1999. Cyclosporine neurotoxicity: a review. Journal of neurology **246**, 339-346.

Go, R.S., Adjei, A.A., 1999. Review of the comparative pharmacology and clinical activity of cisplatin and carboplatin. Journal of Clinical Oncology **17**, 409-409.

Gramowski, A., Jugelt, K., Stuwe, S., Schulze, R., McGregor, G.P., Wartenberg-Demand, A., Loock, J., Schroder, O., Weiss, D.G., 2006. Functional screening of traditional antidepressants with primary cortical neuronal networks grown on multielectrode neurochips. The European journal of neuroscience **24**, 455-465.

Gstraunthaler, G., 2003. Alternatives to the use of fetal bovine serum: serum-free cell culture. Altex **20**, 275-281.

Guengerich, F.P., 2001. Common and uncommon cytochrome P450 reactions related to metabolism and chemical toxicity. Chemical research in toxicology **14**, 611-650.

Gupta, S., Legg, B., Solomon, L., Johnson, R., Rowland, M., 1987. Pharmacokinetics of cyclosporin: influence of rate of constant intravenous infusion in renal transplant patients. British journal of clinical pharmacology **24**, 519-526.

Ha, N.B., Ha, N.B., Garcia, R.T., Trinh, H.N., Vu, A.A., Nguyen, H.A., Nguyen, K.K., Levitt, B.S., Nguyen, M.H., 2009. Renal dysfunction in chronic hepatitis B patients treated with adefovir dipivoxil. Hepatology **50**, 727-734.

Hamaoka, N., Oda, Y., Hase, I., Asada, A., 2001. Cytochrome P4502B6 and 2C9 do not metabolize midazolam: kinetic analysis and inhibition study with monoclonal antibodies. British journal of anaesthesia **86**, 540-544.

Hendrikse, N.H., Schinkel, A.H., de Vries, E.G., Fluks, E., Van der Graaf, W.T., Willemsen, A.T., Vaalburg, W., Franssen, E.J., 1998. Complete in vivo reversal of P-glycoprotein pump function in the blood-brain barrier visualized with positron emission tomography. British journal of pharmacology **124**, 1413-1418.

Himmelstein, K.J., Patton, T.F., Belt, R.J., Taylor, S., Repta, A., Sternson, L.A., 1981. Clinical kinetics of intact cisplatin and some related species. Clinical Pharmacology & Therapeutics **29**, 658-664.

Hincal, A.A., Long, D., Repta, A.-J., 1978. Cis-platin stability in aqueous parenteral vehicles. Journal of the Parenteral Drug Association **33**, 107-116.

Hitchcock, M., Lacy, S., 1994. Bis-pivaloyloxymethyl PMEA as an oral prodrug of PMEA: pilot toxicity evaluation in rats, abstr. 567, Program and abstracts of the First National Conference on Human Retroviruses. American Society for Microbiology, Washington, DC, pp.

Ho, E.S., Lin, D.C., Mendel, D.B., Cihlar, T., 2000. Cytotoxicity of antiviral nucleotides adefovir and cidofovir is induced by the expression of human renal organic anion transporter 1. J Am Soc Nephrol **11**, 383-393.

Honegger, P., Defaux, A., Monnet-Tschudi, F., Zurich, M.G., 2011. Preparation, maintenance, and use of serum-free aggregating brain cell cultures. Methods Mol Biol **758**, 81-97.

Hsiao, P., Sasongko, L., Link, J.M., Mankoff, D.A., Muzi, M., Collier, A.C., Unadkat, J.D., 2006. Verapamil P-glycoprotein transport across the rat blood-brain barrier: cyclosporine, a concentration inhibition analysis, and comparison with human data. The Journal of pharmacology and experimental therapeutics **317**, 704-710.

Hu, C.-y., Liu, Y.-m., Liu, Y., Chen, Q., Wang, W., Wu, K., Dong, J., Li, J., Jia, J.-y., Lu, C., 2013. Pharmacokinetics and Tolerability of Tenofovir Disoproxil Fumarate 300 mg Once Daily: An Open-Label, Single-and Multiple-Dose Study in Healthy Chinese Subjects. Clinical therapeutics **35**, 1884-1889.

Huettner, J.E., Baughman, R.W., 1986. Primary culture of identified neurons from the visual cortex of postnatal rats. The Journal of neuroscience : the official journal of the Society for Neuroscience **6**, 3044-3060.

ICH S3A Guideline, Toxicokinetics: A Guidance for Assessing Systemic Exposure in Toxicity Studies., Center for Drug Evaluation, pp.

Ihde, D.C., Mulshine, J.L., Kramer, B.S., Steinberg, S.M., Linnoila, R.I., Gazdar, A.F., Edison, M., Phelps, R.M., Lesar, M., Phares, J.C., 1994. Prospective randomized comparison of high-dose and standard-dose etoposide and cisplatin chemotherapy in patients with extensive-stage small-cell lung cancer. Journal of clinical oncology **12**, 2022-2034.

Ito, S., 2014. Biotransformation. Clinical Pharmacology & Therapeutics **96**, 281-283.

Iwamoto, K., Watanabe, J., Aoyama, Y., 1987. High capacity for pulmonary first-pass elimination of propranolol in rats. Journal of pharmacy and pharmacology **39**, 1049-1051.

Izzedine, H., Launay-Vacher, V., Deray, G., 2005. Antiviral drug-induced nephrotoxicity. American journal of kidney diseases **45**, 804-817.

Jamei, M., Bajot, F., Neuhoff, S., Barter, Z., Yang, J., Rostami-Hodjegan, A., Rowland-Yeo, K., 2014. A mechanistic framework for in vitro-in vivo extrapolation of liver membrane transporters: prediction of drug-drug interaction between rosuvastatin and cyclosporine. Clin Pharmacokinet **53**, 73-87.

Josse, R., Aninat, C., Glaise, D., Dumont, J., Fessard, V., Morel, F., Poul, J.M., Guguen-Guillouzo, C., Guillouzo, A., 2008. Long-term functional stability of human HepaRG hepatocytes and use for chronic toxicity and genotoxicity studies. Drug metabolism and disposition: the biological fate of chemicals **36**, 1111-1118.

Kahn, J., Lagakos, S., Wulfsohn, M., Cherng, D., Miller, M., Cherrington, J., Hardy, D., Beall, G., Cooper, R., Murphy, R., 1999. Efficacy and safety of adefovir dipivoxil with antiretroviral therapy: a randomized controlled trial. Jama **282**, 2305-2312.

Kandárová, H., Letašiová, S., 2011. Alternative methods in toxicology: pre-validated and validated methods. Interdisciplinary toxicology **4**, 107-113.

Kansy, M., Senner, F., Gubernator, K., 1998. Physicochemical high throughput screening: parallel artificial membrane permeation assay in the description of passive absorption processes. J Med Chem **41**, 1007-1010.

Kato, R., Case, D.E., Hakusui, H., Noda, K., Sagami, F., Horii, I., Mayahara, H., Cayen, M.N., Marriott, T.B., Igarashi, T., 1993. Toxicokinetics: its significance and practical problems. The Journal of toxicological sciences **18**, 211-238.

Kawai, R., Mathew, D., Tanaka, C., Rowland, M., 1998. Physiologically based pharmacokinetics of cyclosporine A: extension to tissue distribution kinetics in rats and scale-up to human. The Journal of pharmacology and experimental therapeutics **287**, 457-468.

Kelly, P., Kahan, B.D., 2002. Review: metabolism of immunosuppressant drugs. Current drug metabolism **3**, 275-287.

Kemper, E.M., van Zandbergen, A.E., Cleypool, C., Mos, H.A., Boogerd, W., Beijnen, J.H., van Tellingen, O., 2003. Increased penetration of paclitaxel into the brain by inhibition of P-Glycoprotein. Clinical cancer research : an official journal of the American Association for Cancer Research **9**, 2849-2855.

Kerns, E.H., Di, L., Petusky, S., Farris, M., Ley, R., Jupp, P., 2004. Combined application of parallel artificial membrane permeability assay and Caco-2 permeability assays in drug discovery. J Pharm Sci-Us **93**, 1440-1453.

Kilford, P.J., Gertz, M., Houston, J.B., Galetin, A., 2008. Hepatocellular binding of drugs: correction for unbound fraction in hepatocyte incubations using microsomal binding or drug lipophilicity data. Drug Metabolism and Disposition **36**, 1194-1197.

Klintmalm, G., Säwe, J., Ringdén, O., von Bahr, C., Magnusson, A., 1985. Cyclosporine plasma levels in renal transplant patients: association with renal toxicity and allograft rejection. Transplantation **39**, 132-137.

Klintmalm, G.B., Iwatsuki, S., Starzl, T.E., 1981. Cyclosporin A hepatotoxicity in 66 renal allograft recipients. Transplantation **32**, 488.

Kola, I., Landis, J., 2004. Can the pharmaceutical industry reduce attrition rates? Nature Reviews Drug Discovery **3**, 711-715.

Kuipers, J.A., Boer, F., Olieman, W., Burm, A.G., Bovill, J.G., 1999. First-pass lung uptake and pulmonary clearance of propofol: assessment with a recirculatory indocyanine green pharmacokinetic model. Anesthesiology **91**, 1780.

Law, S.t., Li, K., Ho, Y., 2012. Nephrotoxicity, including acquired Fanconi's syndrome, caused by adefovir dipivoxil–is there a safe dose? Journal of clinical pharmacy and therapeutics **37**, 128-131.

Lecluyse, E.L., Alexandre, E., 2010. Isolation and culture of primary hepatocytes from resected human liver tissue. Methods Mol Biol **640**, 57-82.

LeCluyse, E.L., Witek, R.P., Andersen, M.E., Powers, M.J., 2012. Organotypic liver culture models: meeting current challenges in toxicity testing. Critical reviews in toxicology **42**, 501-548.

Lensmeyer, G.L., Wiebe, D.A., Carlson, I.H., Subramanian, R., 1991. Concentrations of cyclosporin A and its metabolites in human tissues postmortem. J Anal Toxicol **15**, 110-115.

Lewis, D.F., 2000. Structural characteristics of human P450s involved in drug metabolism: QSARs and lipophilicity profiles. Toxicology **144**, 197-203.

Li, A.P., 2001. Screening for human ADME/Tox drug properties in drug discovery. Drug discovery today **6**, 357-366.

Lilienblum, W., Dekant, W., Foth, H., Gebel, T., Hengstler, J., Kahl, R., Kramer, P.-J., Schweinfurth, H., Wollin, K.-M., 2008. Alternative methods to safety studies in experimental animals: role in the risk assessment of chemicals under the new European Chemicals Legislation (REACH). Archives of toxicology **82**, 211-236.

Lipinski, C.A., Lombardo, F., Dominy, B.W., Feeney, P.J., 1997. Experimental and computational approaches to estimate solubility and permeability in drug discovery and development settings. Advanced drug delivery reviews **23**, 3-25.

Liu, H.L., Sabus, C., Carter, G.T., Du, C., Avdeef, A., Tischler, M., 2003. In vitro permeability of poorly aqueous soluble compounds using different solubilizers in the PAMPA assay with liquid chromatography/mass spectrometry detection. Pharmaceut Res **20**, 1820-1826.

Lohmann, C., Huwel, S., Galla, H.J., 2002. Predicting blood-brain barrier permeability of drugs: evaluation of different in vitro assays. Journal of drug targeting **10**, 263-276.

Long, D., Repta, A., 1981. Review article cisplatin: Chemistry, distribution and biotransformation. Biopharmaceutics & drug disposition **2**, 1-16.

Lu, C., Li, P., Gallegos, R., Uttamsingh, V., Xia, C.Q., Miwa, G.T., Balani, S.K., Gan, L.-S., 2006. Comparison of intrinsic clearance in liver microsomes and hepatocytes from rats and humans: evaluation of free fraction and uptake in hepatocytes. Drug metabolism and disposition **34**, 1600-1605.

Lu, S.K., Callahan, S.A., Jin, R.Y., Brunner, L.J., 2004. Cyclosporine and bromocriptine-induced suppressions of CYP3A1/2 and CYP2C11 are not mediated by prolactin. European journal of pharmacology **501**, 215-224.

Maeng, H.-J., Chapy, H., Zaman, S., Sandy Pang, K., 2012. Effects of 1α, 25-dihydroxyvitamin D< sub> 3</sub> on transport and metabolism of adefovir dipivoxil and its metabolites in Caco-2 cells. European Journal of Pharmaceutical Sciences **46**, 149-166.

Mariller, C., Allain, F., Kouach, M., Spik, G., 1996. Evidence that human milk isolated cyclophilin B corresponds to a truncated form. Biochimica et biophysica acta **1293**, 31-38.

Marques-Santos, L.F., Bernardo, R.R., de Paula, E.F., Rumjanek, V.M., 1999. Cyclosporin A and Trifluoperazine, Two Resistance-Modulating Agents, Increase Ivermectin Neurotoxicity in Mice. Pharmacology & Toxicology **84**, 125-129.

Martinez, M.N., Jackson, A.J., 1991. Suitability of Various Noninfinity Area Under the Plasma Concentration–Time Curve (AUC) Estimates for Use in Bioequivalence Determinations: Relationship to AUC from Zero to Time Infinity (AUCO–INF). Pharmaceut Res **8**, 512-517.

Matthews, J., Altman, D.G., Campbell, M., Royston, P., 1990. Analysis of serial measurements in medical research. BMJ: British Medical Journal **300**, 230.

Miller, R.P., Tadagavadi, R.K., Ramesh, G., Reeves, W.B., 2010. Mechanisms of cisplatin nephrotoxicity. Toxins **2**, 2490-2518.

Min, D.I., Lee, M., Ku, Y.M., Flanigan, M., 2000. Gender-dependent racial difference in disposition of cyclosporine among healthy African American and white volunteers. Clinical pharmacology and therapeutics **68**, 478-486.

Ming, X., Thakker, D.R., 2010. Role of basolateral efflux transporter MRP4 in the intestinal absorption of the antiviral drug adefovir dipivoxil. Biochemical pharmacology **79**, 455-462.

Moran, D., De Buitrago, J.M., Fernandez, E., Galan, A.I., Munoz, M.E., Jimenez, R., 1998. Inhibition of biliary glutathione secretion by cyclosporine A in the rat: possible

mechanisms and role in the cholestasis induced by the drug. Journal of hepatology **29**, 68-77.

Nagai, N., Kinoshita, M., Ogata, H., Tsujino, D., Wada, Y., Someya, K., Ohno, T., Masuhara, K., Tanaka, Y., Kato, K., 1996. Relationship between pharmacokinetics of unchanged cisplatin and nephrotoxicity after intravenous infusions of cisplatin to cancer patients. Cancer chemotherapy and pharmacology **39**, 131-137.

Nakamura, T., Yonezawa, A., Hashimoto, S., Katsura, T., Inui, K.-i., 2010. Disruption of multidrug and toxin extrusion MATE1 potentiates cisplatin-induced nephrotoxicity. Biochemical pharmacology **80**, 1762-1767.

Nakata, K., TANAKA, Y., Nakano, T., Adachi, T., TANAKA, H., KAMINUMA, T., ISHIKAWA, T., 2006. Nuclear receptor-mediated transcriptional regulation in Phase I, II, and III xenobiotic metabolizing systems. Drug metabolism and pharmacokinetics **21**, 437-457.

Niederberger, W., Lemaire, M., Maurer, G., Nussbaumer, K., Wagner, O., 1983. Distribution and binding of cyclosporine in blood and tissues, Transplantation Proceedings. ELSEVIER SCIENCE INC 655 AVENUE OF THE AMERICAS, NEW YORK, NY 10010, pp. 2419-2421.

OECD No. 129, 2010. Series on testing and assessment, No. 129. Guidance Document on Using Cytotoxicity Tests to Estimate Starting Doses for Acute Oral Systemic Toxicity.

OECD Test Guideline No. 417, Test No. 417: Toxicokinetics. OECD Publishing.

OECD Test No. 428, Skin Absorption: In Vitro Method. OECD Publishing.

OECD Test No. 430, In Vitro Skin Corrosion: Transcutaneous Electrical Resistance Test (TER). OECD Publishing.

OECD Test No. 431, In Vitro Skin Corrosion: Human Skin Model Test. OECD Publishing.

OECD Test No. 432, In Vitro 3T3 NRU Phototoxicity Test. OECD Publishing.

OECD Test No. 435, In Vitro Membrane Barrier Test Method for Skin Corrosion. OECD Publishing.

OECD Test No. 439, In Vitro Skin Irritation - Reconstructed Human Epidermis Test Method. OECD Publishing.

OECD Test No. 471, Bacterial Reverse Mutation Test. OECD Publishing.

OECD Test No. 473, In vitro Mammalian Chromosome Aberration Test. OECD Publishing.

OECD Test No. 476, In vitro Mammalian Cell Gene Mutation Test. OECD Publishing.

Oto, T., Okazaki, M., Takata, K., Egi, M., Yamane, M., Toyooka, S., Sano, Y., Snell, G.I., Goto, K., Miyoshi, S., 2010. Calcineurin inhibitor-related cholestasis complicating lung transplantation. The Annals of thoracic surgery **89**, 1664-1665.

Pabla, N., Dong, Z., 2008. Cisplatin nephrotoxicity: mechanisms and renoprotective strategies. Kidney international **73**, 994-1007.

Pabla, N., Murphy, R.F., Liu, K., Dong, Z., 2009. The copper transporter Ctr1 contributes to cisplatin uptake by renal tubular cells during cisplatin nephrotoxicity. American Journal of Physiology-Renal Physiology **296**, F505-F511.

Palestine, A.G., Nussenblatt, R.B., Chan, C.-C., 1984. Side effects of systemic cyclosporine in patients not undergoing transplantation. The American journal of medicine **77**, 652-656.

Pammolli, F., Magazzini, L., Riccaboni, M., 2011. The productivity crisis in pharmaceutical R&D. Nature Reviews Drug Discovery **10**, 428-438.

Pardridge, W.M., Triguero, D., Yang, J., Cancilla, P.A., 1990. Comparison of in vitro and in vivo models of drug transcytosis through the blood-brain barrier. The Journal of pharmacology and experimental therapeutics **253**, 884-891.

Parke, D.V., 1987. Activation mechanisms to chemical toxicity. Archives of toxicology **60**, 5-15.

Ploemen, J.-P.H., Kramer, H., Krajnc, E.I., Martin, I., 2007. The use of toxicokinetic data in preclinical safety assessment: a toxicologic pathologist perspective. Toxicologic pathology **35**, 834-837.

Pond, S.M., Tozer, T.N., 1984. First-pass elimination basic concepts and clinical consequences. Clinical pharmacokinetics **9**, 1-25.

Poulin, P., Theil, F.P., 2002. Prediction of pharmacokinetics prior to in vivo studies. 1. Mechanism-based prediction of volume of distribution. J Pharm Sci-Us **91**, 129-156.

Prestayko, A., d'Aoust, J., Issell, B., Crooke, S., 1979. Cisplatin (< i> cis</i>-diamminedichloroplatinum II). Cancer treatment reviews **6**, 17-39.

Price, E.R., Jin, M., Lim, D., Pati, S., Walsh, C.T., McKeon, F.D., 1994. Cyclophilin B trafficking through the secretory pathway is altered by binding of cyclosporin A. Proc Natl Acad Sci U S A **91**, 3931-3935.

Purves, R.D., 1992. Optimum numerical integration methods for estimation of area-under-the-curve (AUC) and area-under-the-moment-curve (AUMC). Journal of pharmacokinetics and biopharmaceutics **20**, 211-226.

Qaqish, R.B., Mattes, K.A., Ritchie, D.J., 2003. Adefovir dipivoxil: a new antiviral agent for the treatment of hepatitis B virus infection. Clinical therapeutics **25**, 3084-3099.

Ransom, B.R., Neale, E., Henkart, M., Bullock, P.N., Nelson, P.G., 1977. Mouse spinal cord in cell culture. I. Morphology and intrinsic neuronal electrophysiologic properties. Journal of neurophysiology **40**, 1132-1150.

Renwick, A.G., 2001. Toxicokinetics-pharmacokinetics in toxicology. Principles and methods of toxicology, 101-147.

Rezzani, R., 2006. Exploring cyclosporine A-side effects and the protective role-played by antioxidants: the morphological and immunohistochemical studies.

Rosenberg, B., Van Camp, L., Krigas, T., 1965. Inhibition of cell division in Escherichia coli by electrolysis products from a platinum electrode. Nature **205**, 698-699.

Russell, W., Burch, R., 1959. The principles of humane experimental techniqueMethuen. London, UK.

Saeki, T., Ueda, K., Tanigawara, Y., Hori, R., Komano, T., 1993. Human P-glycoprotein transports cyclosporin A and FK506. The Journal of biological chemistry **268**, 6077-6080.

Sanghvi, A., Warty, V.S., Diven, W.F., Starzl, T., 1989. Receptor-mediated cellular uptake of cyclosporine, Transplantation proceedings. NIH Public Access, pp. 858.

Schultz, L., Culot, M., da Costa, A., Landry, C., Bellwon, P., Kristl, T., Ruzek, S., Gosselet, F., Cecchelli, R., Zurich, M.G., Schroeder, O.H.-U., Gramowski-Voss, A., Weiss, D.G., Bal-Price, A., 2015, submitted. Evaluation of drug-induced neurotoxicity based on metabolomics, proteomics and electrical activity measurements in complementary neuronal in vitro models. Toxicology in Vitro.

Seglen, P.O., 1976. Preparation of isolated rat liver cells. Methods Cell Biol **13**, 29-83.

Serkova, N.J., Christians, U., Benet, L.Z., 2004. Biochemical mechanisms of cyclosporine neurotoxicity. Mol Interv **4**, 97-107.

Sharanek, A., Bachour-El Azzi, P., Al-Attrache, H., Savary, C.C., Humbert, L., Rainteau, D., Guguen-Guillouzo, C., Guillouzo, A., 2014. Different Dose-Dependent Mechanisms Are Involved in Early Cyclosporine A-Induced Cholestatic Effects in HepaRG Cells. Toxicological Sciences **141**, 244-253.

Shaw, J.P., Louie, M.S., Krishnamurthy, V.V., Arimilli, M.N., Jones, R.J., Bidgood, A.M., Lee, W.A., Cundy, K.C., 1997. Pharmacokinetics and metabolism of selected prodrugs of PMEA in rats. Drug metabolism and disposition: the biological fate of chemicals **25**, 362-366.

Shen, G., Kong, A.N., 2009. Nrf2 plays an important role in coordinated regulation of Phase II drug metabolism enzymes and Phase III drug transporters. Biopharmaceutics & drug disposition **30**, 345-355.

Siddik, Z.H., 2003. Cisplatin: mode of cytotoxic action and molecular basis of resistance. Oncogene **22**, 7265-7279.

Soldatow, V.Y., LeCluyse, E.L., Griffith, L.G., Rusyn, I., 2013. In vitro models for liver toxicity testing. Toxicology research **2**, 23-39.

Spik, G., Haendler, B., Delmas, O., Mariller, C., Chamoux, M., Maes, P., Tartar, A., Montreuil, J., Stedman, K., Kocher, H.P., et al., 1991. A novel secreted cyclophilin-like protein (SCYLP). The Journal of biological chemistry **266**, 10735-10738.

Stewart, D.J., Benjamin, R.S., Luna, M., Feun, L., Caprioli, R., Seifert, W., Loo, T.L., 1982. Human tissue distribution of platinum after cis-diamminedichloroplatinum. Cancer chemotherapy and pharmacology **10**, 51-54.

Stewart, D.J., Mikhael, N., Nanji, A., Nair, R., Kacew, S., Howard, K., Hirte, W., Maroun, J., 1985. Renal and hepatic concentrations of platinum: relationship to cisplatin time, dose, and nephrotoxicity. Journal of Clinical Oncology **3**, 1251-1256.

Sun, D.q., Wang, H.s., Ni, M.y., Wang, B.j., Guo, R.c., 2007. Pharmacokinetics, safety and tolerance of single-and multiple-dose adefovir dipivoxil in healthy Chinese subjects. British journal of clinical pharmacology **63**, 15-23.

Takayama, A., Okazaki, Y., Fukuda, K., Takano, M., Inui, K., Hori, R., 1991. Transport of Cyclosporine-a in Kidney Epithelial-Cell Line (Llc-Pk1). Journal of Pharmacology and Experimental Therapeutics **257**, 200-204.

Takeguchi, N., Ichimura, K., Koike, M., Matsui, W., Kashiwagura, T., Kawahara, K., 1993. Inhibition of the multidrug efflux pump in isolated hepatocyte couplets by immunosuppressants FK506 and cyclosporine. Transplantation **55**, 646-650.

Tanji, N., Tanji, K., Kambham, N., Markowitz, G.S., Bell, A., D'Agati, V.D., 2001. Adefovir nephrotoxicity: possible role of mitochondrial DNA depletion. Human pathology **32**, 734-740.

Townsend, D.M., Deng, M., Zhang, L., Lapus, M.G., Hanigan, M.H., 2003. Metabolism of cisplatin to a nephrotoxin in proximal tubule cells. Journal of the American Society of Nephrology **14**, 1-10.

Tsuji, A., Tamai, I., Sakata, A., Tenda, Y., Terasaki, T., 1993. Restricted transport of cyclosporin A across the blood-brain barrier by a multidrug transporter, P-glycoprotein. Biochemical pharmacology **46**, 1096-1099.

Turpeinen, M., Jouko, U., Jorma, J., Olavi, P., 2005. Multiple P450 substrates in a single run: rapid and comprehensive in vitro interaction assay. European journal of pharmaceutical sciences **24**, 123-132.

Tuschl, G., Hrach, J., Walter, Y., Hewitt, P.G., Mueller, S.O., 2009. Serum-free collagen sandwich cultures of adult rat hepatocytes maintain liver-like properties long term: a valuable model for in vitro toxicity and drug-drug interaction studies. Chem Biol Interact **181**, 124-137.

Uwai, Y., Ida, H., Tsuji, Y., Katsura, T., Inui, K.-i., 2007. Renal transport of adefovir, cidofovir, and tenofovir by SLC22A family members (hOAT1, hOAT3, and hOCT2). Pharmaceut Res **24**, 811-815.

Wagner, O., Schreier, E., Heitz, F., Maurer, G., 1987. Tissue distribution, disposition, and metabolism of cyclosporine in rats. Drug metabolism and disposition: the biological fate of chemicals **15**, 377-383.

Wang, D., Lippard, S.J., 2005. Cellular processing of platinum anticancer drugs. Nature reviews Drug discovery **4**, 307-320.

Wang, P., Heitman, J., 2005. The cyclophilins. Genome biology **6**, 226.

Wason, S., Digiacinto, J.L., Davis, M.W., 2012. Effect of cyclosporine on the pharmacokinetics of colchicine in healthy subjects. Postgraduate medicine **124**, 189-196.

Watkins, P.B., 1997. The barrier function of CYP3A4 and P-glycoprotein in the small bowel. Adv Drug Deliv Rev **27**, 161-170.

Watkins, P.B., 2011. Drug Safety Sciences and the Bottleneck in Drug Development. Clinical Pharmacology & Therapeutics **89**, 788-790.

Wen, X., Buckley, B., McCandlish, E., Goedken, M.J., Syed, S., Pelis, R., Manautou, J.E., Aleksunes, L.M., 2014. Transgenic Expression of the Human MRP2 Transporter Reduces Cisplatin Accumulation and Nephrotoxicity in< i> Mrp2</i>-Null Mice. The American journal of pathology **184**, 1299-1308.

Wieser, M., Stadler, G., Jennings, P., Streubel, B., Pfaller, W., Ambros, P., Riedl, C., Katinger, H., Grillari, J., Grillari-Voglauer, R., 2008. hTERT alone immortalizes epithelial cells of renal proximal tubules without changing their functional characteristics. American Journal of Physiology-Renal Physiology **295**, F1365-F1375.

Wilmes, A., Bielow, C., Ranninger, C., Bellwon, P., Aschauer, L., Limonciel, A., Chassaigne, H., Kristl, T., Aiche, S., Huber, C.G., 2014. Mechanism of cisplatin proximal tubule toxicity revealed by integrating transcriptomics, proteomics, metabolomics and biokinetics. Toxicology in Vitro.

Wilmes, A., Limonciel, A., Aschauer, L., Moenks, K., Bielow, C., Leonard, M.O., Hamon, J., Carpi, D., Ruzek, S., Handler, A., Schmal, O., Herrgen, K., Bellwon, P., Burek, C., Truisi, G.L., Hewitt, P., Di Consiglio, E., Testai, E., Blaauboer, B.J., Guillou, C., Huber, C.G., Lukas, A., Pfaller, W., Mueller, S.O., Bois, F.Y., Dekant, W., Jennings, P., 2013. Application of integrated transcriptomic, proteomic and metabolomic profiling for the delineation of mechanisms of drug induced cell stress. J Proteomics **79**, 180-194.

Worth, A., Barroso, J., Bremer, S., Burton, J., Casati, S., Coecke, S., Corvi, R., Desprez, B., Dumont, C., Gouliarmou, V., 2014. Alternative methods for regulatory toxicology–a state-of-the-art review. Alternative methods for regulatory toxicology–a state-of-the-art review **5**, 457.

Xu, C., Li, C.Y.-T., Kong, A.-N.T., 2005. Induction of phase I, II and III drug metabolism/transport by xenobiotics. Archives of pharmacal research **28**, 249-268.

Yeh, K., Kwan, K., 1978. A comparison of numerical integrating algorithms by trapezoidal, Lagrange, and spline approximation. Journal of pharmacokinetics and biopharmaceutics **6**, 79-98.

Zanelli, U., Caradonna, N.P., Hallifax, D., Turlizzi, E., Houston, J.B., 2012. Comparison of cryopreserved HepaRG cells with cryopreserved human hepatocytes for prediction of clearance for 26 drugs. Drug metabolism and disposition: the biological fate of chemicals **40**, 104-110.

Ziegler, K., Polzin, G., Frimmer, M., 1988. Hepatocellular uptake of cyclosporin A by simple diffusion. Biochimica et Biophysica Acta (BBA)-Biomembranes **938**, 44-50.

Zuber, R., Anzenbacherova, E., Anzenbacher, P., 2002. Cytochromes P450 and experimental models of drug metabolism. J Cell Mol Med **6**, 189-198.

6. Appendix

6.1. Publications

Bellwon P., Culot M., Wilmes A., Schmidt T., Zurich M.G., Schultz L., Schmal O., Gramowski-Voss A., Weiss D.G., Jennings P., Bal-Price A., Testai E., Dekant W. 2015 Cyclosporine A kinetics in brain cell culture and its potential of crossing the blood-brain barrier. Toxicology in Vitro (doi: 10.1016/j.tiv.2015.01.003)

Crean D., Bellwon P., Aschauer L., Limonciel A., Moenks K., Hewitt P., Schmidt T., Herrgen K., Dekant W., Lukas A., Bois F., Wilmes A., Jennings P., Leonard M. 2014 Development of an in vitro renal epithelial disease state model for xenobiotic toxicity testing. Toxicology in Vitro (doi: 10.1016/j.tiv.2014.11.015)

Wilmes A., Bielow C., Ranninger C., Bellwon P., Aschauer L., Limonciel A., Chassaigne H., Kristl T., Aiche S., Huber C.G., Guillou C., Hewitt P., Leonard M., Dekant W., Bois F., Jennings P. 2014 Mechanism of cisplatin proximal tubule toxicity revealed by integrating transcriptomics, proteomics, metabolomics and biokinetics. Toxicology in Vitro (doi: 10.1016/j.tiv.2014.10.006)

Wilmes A., Limonciel A., Aschauer L., Moenks K., Bielow C., Leonard M.O., Hamon J., Carpi D., Ruzek S., Handler A., Schmal O., Herrgen, K., Bellwon P., Burek C., Truisi G.L., Hewitt P., Di Consiglio E., Testai E., Blaauboer B.J., Guillou C., Huber C.G., Lukas A., Pfaller W., Mueller S.O., Bois F.Y., Dekant W., Jennings P., 2013 Application of integrated transcriptomic, proteomic and metabolomic profiling for the delineation of mechanisms of drug induced cell stress. Journal of Proteomics **79**: 180-194 (doi: 10.1016/j.jprot.2012.11.022)

6.2. Affidavit

I hereby confirm that my thesis entitled “Kinetic assessment by *in vitro* approaches - A contribution to reduce animals in toxicity testing” is the result of my own work. I did not receive any help or support from commercial consultants. All sources and/or materials applied are listed and specified in this thesis.

Furthermore, I confirm that this thesis has not yet been as part of another examination process neither in identical nor in similar form.

_____ _____

Ort, Datum Patricia Bellwon

6.3. Eidesstattliche Erklärung

Hiermit erkläre ich an Eides statt, die Dissertation „Kinetic assessment by *in vitro* approaches - A contribution to reduce animals in toxicity testing” eigenständig, d.h. insbesondere selbstständig und ohne Hilfe eines kommerziellen Promotionsberaters, angefertigt und keine anderen als die von mir angegebenen Quellen und Hilfsmittel verwendet zu haben.

Ich erkläre außerdem, dass die Dissertation weder in gleicher noch in ähnlicher Form bereits in einem anderen Prüfungsverfahren vorgelegen hat.

_____ _____

Ort, Datum Patricia Bellwon